Wayne State University Dissertations

January 2019

Novel Insights Into The Use Of Ercc1 As A Biomarker For Response To Platinum-Based Chemotherapy In Lung Cancer

Joshua Ryan Heyza
Wayne State University, joshua.heyza@gmail.com

Follow this and additional works at: https://digitalcommons.wayne.edu/oa_dissertations

Part of the Molecular Biology Commons, and the Oncology Commons

**NOVEL INSIGHTS INTO THE USE OF ERCC1 AS A BIOMARKER FOR RESPONSE
TO PLATINUM-BASED CHEMOTHERAPY IN LUNG CANCER**

by

JOSHUA R. HEYZA

DISSERTATION

Submitted to the Graduate School

of Wayne State University,

Detroit, Michigan

in partial fulfillment of the requirements

for the degree of

DOCTOR OF PHILOSOPHY

2019

MAJOR: CANCER BIOLOGY

Approved By:

_____
Advisor   Date

_____

_____

_____

DEDICATION

To Michael who has given unwavering love and support.

To my Mom and Dad who have always supported me in my academic endeavors.

ACKNOWLEDGMENTS

First of all, I would like to thank my mentor, Dr. Steve Patrick, for his guidance and training over the past four and a half years. I am extremely grateful for the opportunity to study under Dr. Patrick and the training I have received has undoubtedly prepared me for the next step in my academic career as I begin a postdoctoral fellowship.

I would also like to thank a previous lab member, Dr. Akshada Sawant, for all of her time providing training when I entered the lab. I would like to thank former lab members who provided technical assistance and always made the Patrick lab an enjoyable environment, including Dr. Ashley Floyd, Dr. Akshada Sawant, Wen Lei, Ellen Zhang, Kayla Conner, and Natalie Snider.

I am also grateful for those who provided resources that made this entire project possible. For the A549 ERCC1 knockout cells used in this study, I would like to thank Dr. Jean-Charles Soria, Dr. Ken Olaussen, and Dr. Luc Friboulet. For the OV2008 and C13 cells, I would like to thank Dr. Stephen B. Howell.

I also want to thank my dissertation committee members, Dr. Manohar Ratnam, Dr. George Brush, and Dr. Lori Pile for their support, constructive criticism, and insightful comments that helped to propel this project forward. Also, this work would not have been possible without the support of Dr. Gerold Bepler who was instrumental in providing knowledgeable clinical insight and substantial scientific input. I would also like to acknowledge Dr. Ann G. Schwartz and Donovan Watza without whom the patient analysis would not have been possible.

I thank Jean Guerin and Nadia Daniel for the administrative help provided during my time in the Cancer Biology Graduate Program. Their assistance with processing

TABLE OF CONTENTS

vii

LIST OF TABLES

LIST OF FIGURES

x

xi

ABBREVIATIONS

7-AAD   7-aminoactinomycin D

ANOVA   Analysis of variance

ATCC   American type culture collection

ATM   Ataxia telangiectasia mutated

ATR   Ataxia telangiectasia and rad3-related

ATRi   ATR inhibitor

BER   Base excision repair

BRCA1   Breast cancer gene 1

BRCA2   Breast cancer gene 2

CAPS   N-cyclohexyl-3-aminopropanesulfonic acid

Cas9   CRISPR associated protein 9

CDDP   Cis-diamminedichloroplatinum(II)

CDK4   Cyclin-dependent kinase 4

CDK6   Cyclin-dependent kinase 6

CDKN1A   Cyclin-dependent kinase inhibitor 1A

cDNA   Complementary DNA

cGAS   Cyclic GMP-AMP synthase

Chek1   Checkpoint kinase 1

Chk1   See Chek1

Cis   See CDDP

CO_2   Carbon dioxide

CRISPR   Clustered regularly interspaced short palindromic repeats

crRNA	CRISPR RNA
CTLA4	Cytotoxic T-lymphocyte associate protein 4
Δ	Deletion or knockout
DAPI	4′,6-Diamidino-2-phenylindole dihydrochloride
DBF4	Dumbbell former 4
DDK	DBF4-dependent kinase
DMEM	Dulbecco's modified eagle's medium
DMSO	Dimethyl sulfoxide
DNA	Deoxyribonucleic acid
DNA-PK	DNA-dependent protein kinase
DNA-PKcs	DNA-dependent protein kinase catalytic subunit
DSB	Double-strand break
dsDNA	Double-stranded DNA
ECL	Enhanced chemiluminescence
EdU	5-Ethynyl-2'-deoxyuridine
EGFR	Epidermal growth factor receptor
ERCC1	Excision repair cross-complementation group 1
ERCC4	Excision repair cross-complementation group 4
FA	Fanconi anemia
FBS	Fetal bovine serum
FDA	Food and Drug Administration
GG-NER	Global Genomic Nucleotide Excision Repair
γH2AX	Phosphorylated Histone H2A.X at S139
hBRCA2	Human BRCA2

hRad52	Human Rad52
HEPES	2-[4-(2-hydroxyethyl)piperazin-1-yl]ethanesulfonic acid
HR	Homologous recombination
HRR	Homologous recombination repair
IC_{50}	50 percent inhibitory concentration
ICL	Interstrand crosslink
ICL-R	Interstrand crosslink repair
IFN	Interferon
IgG	Immunoglobulin G
IHC	Immunohistochemistry
ISA	Instrastrand adduct
KCl	Potassium chloride
kDa	Kilodalton
KRAS	KRAS proto-oncogene, GTPase
K-ras	See KRAS
MEM	Minimum essential medium
MMC	Mitomycin C
MMEJ	Microhomology mediated end joining
mRNA	Messenger RNA
Mus81	Mus81 structure-specific endonuclease subunit
NaCl	Sodium chloride
NaOH	Sodium hydroxide
NER	Nucleotide excision repair
NHEJ	Non-homologous end joining

NS	Not statistically significant
NSCLC	Non-small cell lung cancer
OS	Overall survival
p21	See CDKN1A
p53	See TP53
PARP	Poly (ADP-ribose) polymerase
PBS	Phosphate-buffered saline
PCR	Polymerase chain reaction
PD-L1	Programmed death-ligand 1
PE	Phosphatidylethanolamine
PI	Propidium iodide
PMSF	Phenylmethylsulfonyl fluoride
PVDF	Polyvinylidene difluoride
QCMG	Queensland centre for medical genomics
qRT-PCR	Quantitative real-time polymerase chain reaction
RNA	Ribonucleic acid
RNase	Ribonuclease
RPA	Replication protein A
rpm	Revolutions per minute
RPMI	Roswell park memorial institute
SD	Standard deviation
SDS	Sodium dodecyl sulfate
SEM	Standard error of the mean
shRNA	Short hairpin RNA

SSA	Single strand annealing
ssDNA	Single stranded DNA
STING	Stimulator of interferon genes
TBS	Tris-buffered saline
TCGA	The cancer genome atlas
TP53	Tumor protein 53
tracrRNA	Trans-activating crRNA
UV	Ultraviolet
UV-C	Ultraviolet C
Wee1	Wee1 G_2 checkpoint kinase
WT	Wild-type
XPA	Xeroderma pigmentosum group A
XPF	Xeroderma pigmentosum group F

CHAPTER 1- INTRODUCTION TO ERCC1 IN DNA REPAIR AND ITS POTENTIAL UTILITY IN PREDICTING RESPONSE TO PLATINUM-BASED CHEMOTHERAPY IN LUNG CANCER

1.1 THE ERCC1 GENE AND GENE PRODUCTS

A variety of human diseases can be attributed to defects in proteins that are involved in DNA repair and genome maintenance. These diseases can generally be segregated into three categories, 1. Diseases associated with developmental or neurological deficits; 2. Diseases associated with premature aging, 3. Diseases related to cancer susceptibility. Some of these diseases related to mutations in DNA repair genes include Xeroderma Pigmentosum, Ataxia Telangiectasia, Fanconi Anemia, Cockayne Syndrome, Cerebro-Oculo-Facial Syndrome, Bloom Syndrome, as well as a variety of cancer predispositions (1-5). In general, the genetic mutations associated with these diseases lead to loss of function or decreased functionality of the gene products that contributes to the accumulation of DNA damage, mutation, or telomere shortening and together these effects lead to anemias, premature aging, neurological deficits, and/or cancer.

Efforts to understand the underlying mechanisms contributing to these diseases with functional loss of various DNA repair pathways could lead to new therapies for treating these rare diseases as well as contribute to possible new treatments for cancer. A hallmark of cancer is increased genome instability which allows cells to actively adapt to various pressures (including immune, tumor-microenvironment, and drug-induced pressures) thereby supporting tumor cell growth (6). In support of the hypothesis that mutations in DNA repair genes may support these processes, a large number of tumors harbor defects in DNA repair genes or factors that indirectly influence DNA repair, including ERCC1, BRCA1, BRCA2, ATM, among many others. By some estimates, up to

50% of all lung cancers harbor mutations in DNA repair genes conferring phenotypes similar to BRCA1/2 mutations supporting the importance of studying the role of functional loss of DNA repair and genome stability in promoting tumor formation, growth, drug resistance, as well as for novel drug development and biomarker-driven clinical trial design (7). Because of this weakness in tumor cells, substantial scientific effort is being made to understand the mechanistic basis underlying these tumor-specific DNA repair deficiencies and to find novel ways to exploit these DNA repair deficiencies selectively in tumors while sparing normal cells.

One critical DNA repair factor that is often altered at the mRNA and protein levels in lung and ovarian tumors is the protein Excision Repair Cross Complementation Group 1 (ERCC1). ERCC1 forms a constitutive heterodimer with its protein partner, Xeroderma Pigmentosum Group F (XPF) (8). Together these proteins form a structure-specific 5' – 3' endonuclease which plays multiple critical roles in a number of DNA repair pathways including Nucleotide Excision Repair (NER), Interstrand Crosslink Repair (ICL-R), Homologous Recombination (HR), and Single Strand Annealing (SSA) as well as a number of specialized cellular functions including in gene imprinting (8-11). ERCC1 was first functionally identified in 1984 in complementation experiments in a UV-sensitive Chinese hamster ovary cell line where expression of ERCC1 could complement the UV sensitivity observed indicating that ERCC1 was involved in repair of UV-induced DNA damage, including thymine dimers and cyclobutane dimers, and ultimately provided evidence that mutations in ERCC1 could be associated with the disease Xeroderma Pigmentosum (12). The ERCC1 gene is located on chromosome 19 at the cytogenetic band 19q13.32. The ERCC1 gene is composed of 9 coding exons and the predominant splice variant of ERCC1 consists of 297 amino acids (Figure 1.1) (13). Many important
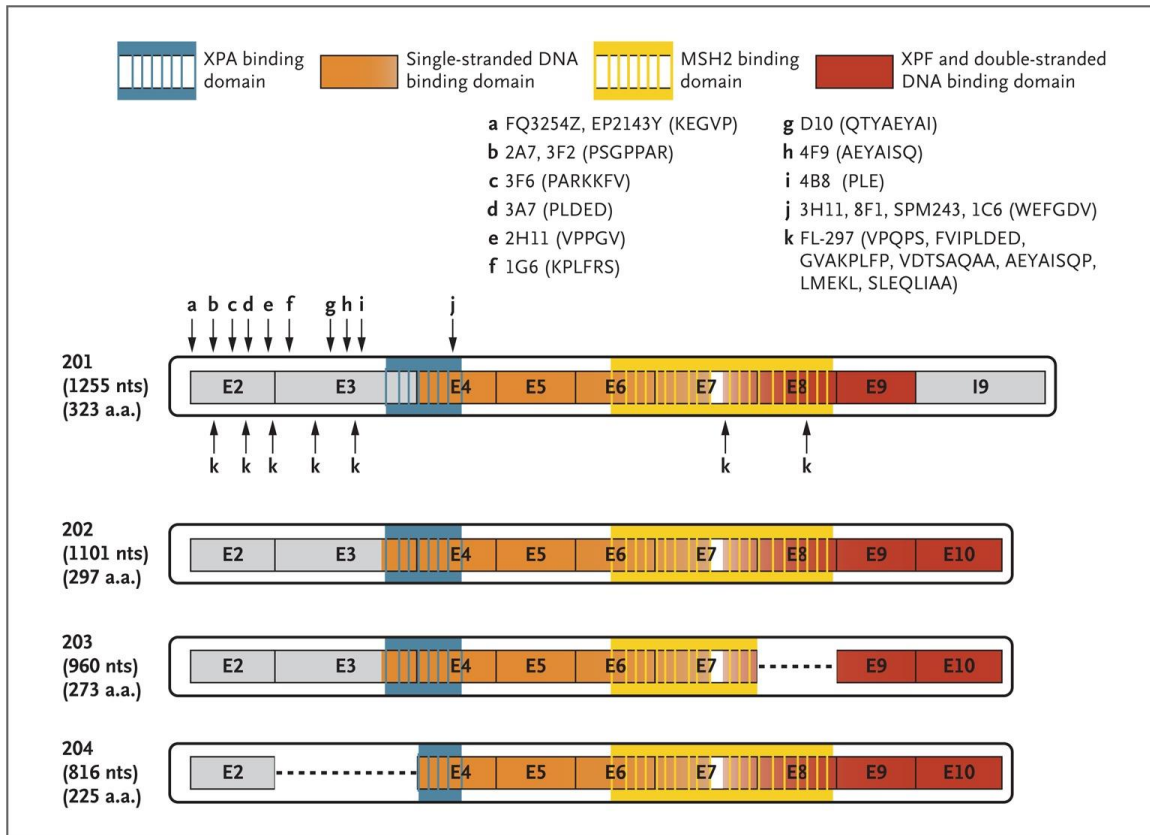
Figure 1.1 Structure of ERCC1 isoforms and protein-protein interaction domains. Cartoon illustrates the gene structure of ERCC1 isoforms and currently available antibodies for detection of ERCC1. Reproduced with permission from Friboulet *et al.* New England Journal of Medicine, 2013 (13), © Copyright Massachusetts Medical Society.

interaction domains have subsequently been identified in ERCC1 that are associated with its cellular functions. Some of these key interaction domains include important interactions with XPF, XPA, single strand DNA binding domain, and double strand DNA binding domain (Figure 1.1) (13-15). These important functional domains will be discussed further in 1.3.

Alternative splicing of the ERCC1 gene was first discovered in the mid-1990s and there are currently four known protein-coding splice variants of ERCC1 in human cells which are denoted as ERCC1-202, ERCC1-201, ERCC1-203, and ERCC1-204 (Figure 1.1) (13, 16). It is currently thought that ERCC1-202 is the only functional splice variant involved in DNA repair. Each splice variant differs from ERCC1-202 by single exon exclusion or intron inclusion (Figure 1.1). ERCC1-201 excludes exon 10 in favor of inclusion of intron 9. ERCC1-203 excludes exon 8 and ERCC1-204 excludes exon 3. The mechanistic basis for alternative splicing of ERCC1 remains undefined although a report identified alternative splicing of ERCC1 can be controlled by certain types of DNA damage that induce hyperphosphorylation of RNA Polymerase II (e.g. topoisomerase I poisons) which theoretically leads to inclusion or exclusion of specific RNA splicing factors (17).

While ERCC1-202's roles in DNA repair are well known, functions for the other three splice variants remain unknown. A previous report provided evidence that ERCC1-203 mRNA levels were negatively associated with activity in Nucleotide Excision Repair (16). Thus, it was postulated that ERCC1-203 could be dominant-negative to ERCC1-202 activity. However, the evidence for this hypothesis is conflicting as work by Friboulet *et al.* did not identify any differences in sensitivity to the DNA crosslinking agent cisplatin between A549 ERCC1 knockout cells re-expressing ERCC1-202 and dual ectopic e-

expression of ERCC1-202 with ERCC1-201, -203, or -204 (18). The authors only observed rescue from cisplatin sensitivity with re-expression of ERCC1-202, suggesting that ERCC1-202 is the only variant functional in DNA repair (18). However, this does not entirely rule out the possibility that ERCC1-203 could negatively regulate ERCC1-202 function by means independent of ectopic re-expression of ERCC1-202. Importantly, Friboulet *et al.* discovered that only ERCC1-202 was capable of interaction with its protein partner XPF, indicating that alternative splicing of ERCC1 may impact protein folding in such a way as to block the interaction of ERCC1 splice variants with XPF (18). Very little is currently known about ERCC1-201 function in cells. Currently available information suggests that it is non-functional in Nucleotide Excision Repair and Interstrand Crosslink Repair (13, 18). Furthermore, it is incapable of interaction with XPF as well as with another NER factor, XPA (18). Until recently, it was thought that ERCC1-204 was also completely non-functional in DNA repair and that it could not interact with XPF as described in Friboulet *et al.* (18). In the development of antibodies specific to the ERCC1/XPF heterodimer and subsequent co-immunoprecipitation experiments, it was identified that ERCC1-204 (which retains the entire XPF binding domain) could interact with XPF, which may suggest it has roles in promoting DNA repair or preserving genome stability (19). The lack of effect of ERCC1-204 on sensitivity to DNA crosslinking agents may support the idea that ERCC1-204/XPF has more specialized, non-essential roles in DNA processing and there is evidence that XPF endonuclease activity is involved in some specialized DNA processing events (20). Subsequent studies focused on identifying functions for ERCC1-204 in genome stability would benefit from exploring potential functions independent of ERCC1's canonical roles in NER and ICL-R.

1.2 CRITICAL PHYSICAL INTERACTION BETWEEN ERCC1 AND XPF

Key to ERCC1's functions in DNA repair is its heterodimeric interaction with the protein XPF (8, 21, 22). This constitutive interaction is not only critical for XPF's nuclease activity during DNA repair but is also essential for ERCC1 and XPF protein stability (22). Similar to the yeast homologues of ERCC1/XPF, Rad1 and Rad10 (21, 23), this protein heterodimer forms a 5'-3' structure specific endonuclease (8, 24). After ERCC1's discovery in 1984, it was discovered that Rad1 and Rad10 formed a heterodimer and possessed intrinsic endonuclease activity (23, 25-27). Shortly thereafter ERCC1's heterodimer was definitively identified as the Xeroderma Pigmentosum protein XPF (8, 28). This early work also showed clearly that activity of purified ERCC1/XPF activity was similar to Rad1/Rad10 in terms of DNA cleavage of a specific *in vitro* DNA substrate (8, 24). ERCC1 and XPF interact through their C terminal HhH_2 domain and it is generally thought that this interaction leads to proper protein folding which is required for stability (15, 29). While it is thought that ERCC1 and XPF require each other for protein stability and/or proper protein folding, the effects on stability of XPF with loss of ERCC1 may be more severe than the effects on ERCC1 stability with loss of XPF (30-32). Thus, it is still unclear whether ERCC1 absolutely requires XPF for protein folding in all circumstances or whether its folding/stability is only partly reduced when XPF is depleted. In addition, it was recently observed that in some instances XPF can self-dimerize and stabilize itself in biochemical assays, however it is unclear whether these XPF homodimers are actively formed *in vivo* and whether they possess any functionality (33).

1.3 THE ROLE OF ERCC1 IN DNA REPAIR

1.3.1 NUCLEOTIDE EXCISION REPAIR

Nucleotide Excision Repair (NER) is a DNA repair pathway tasked with removing bulky ssDNA adducts from DNA. These bulky lesions are all similar in that they distort the DNA helix, although different lesions vary in the extent of helical distortion. As a result, this pathway contributes to the removal of a wide range of DNA adducts. In general, these types of lesions include those caused by UV light, endogenous reactive aldehydes, lesions induced by various environmental exposures (including metals), and a subset of those caused by various chemotherapy agents including cisplatin and mitomycin C. While NER as a DNA repair pathway is conserved from prokaryotes to humans, eukaryotic NER (i.e. from yeast to humans) is quite distinct from prokaryotic NER with limited homology between prokaryotic and eukaryotic NER factors (34, 35). The bacterial NER system is rather simple with a requirement for very few proteins including UvrA, UvrB, UvrC (the endonuclease component, which has a distinct catalytic domain from the eukaryotic NER endonuclease XPF) and DNA helicase II (35). On the other hand, eukaryotic NER requires a larger set of factors including those involved in DNA damage recognition, repair scaffolding proteins, and DNA endonucleases (34). The increased complexity of eukaryotic NER is likely due to evolutionary changes in eukaryotic genomes including substantial increases in genome size (including heterochromatic and euchromatic regions), limited genome copy number, more complex genome structure and architecture, as well as a dramatically longer cell cycle. A number of proteins are involved in NER in humans including, XPA, XPB, XPC, XPD, XPF, XPG, ERCC1, DDB1, DDB2, CSA, CSB, RPA1, RPA2, CETN2, LIG1, MMS19, RAD23A, RAD23B, TFIIH complex, and XAB2 (although this is not an exhaustive list of all accessory proteins involved in human NER) (34).

Two general pathways for NER exist in yeast and mammalian NER including Global-Genomic NER (GG-NER) and Transcription-Coupled NER (TC-NER) (34). The main difference between these two NER pathways is whether the DNA damage is encountered in the presence or absence of the transcriptional machinery (Figure 1.2). In GG-NER, damage is initially recognized by the protein XPC in conjunction with the factors CETN2 and RAD23B (36, 37). Depending on the extent of the helical distortion induced by the lesion, XPC-DNA binding may also require involvement of the damage recognition complex UV-DDB (containing DDB1 and DDB2) which promotes the binding of XPC to the DNA (38, 39). For lesions inducing small distortions, UV-DDB is generally involved in GG-NER. For lesions that cause greater helical distortions, XPC can directly bind to the DNA but this process may also involve UV-DDB in some cases. Binding of XPC to the DNA promotes recruitment of the TFIIH complex (including XPB and XPD) where the complex's helicase activity is essential for creating a DNA bubble composed of two ssDNA regions flanked by dsDNA regions on the 5' and 3' side (40, 41). While one strand of the ssDNA is bound by TFIIH complex, the complementary strand of ssDNA is bound by the ssDNA binding protein RPA (42). Once the DNA bubble is formed the DNA is primed for incision by the 5'- 3' DNA endonuclease ERCC1/XPF and the 3'-5' endonuclease XPG. This process is influenced by the presence of RPA as well as the scaffolding protein XPA which help to recruit ERCC1/XPF and coordinate/stimulate nucleolytic incisions by ERCC1/XPF (through direct interaction with ERCC1) and XPG (42-45). After two incisions, one by ERCC1/XPF and a second by XPG, a short, excised DNA is produced that is generally ~17-32 nucleotides in length (46). DNA replication across the ssDNA gap occurs following incision by ERCC1/XPF and involves PCNA, Replication Factor C, as well as a DNA polymerase (34). DNA
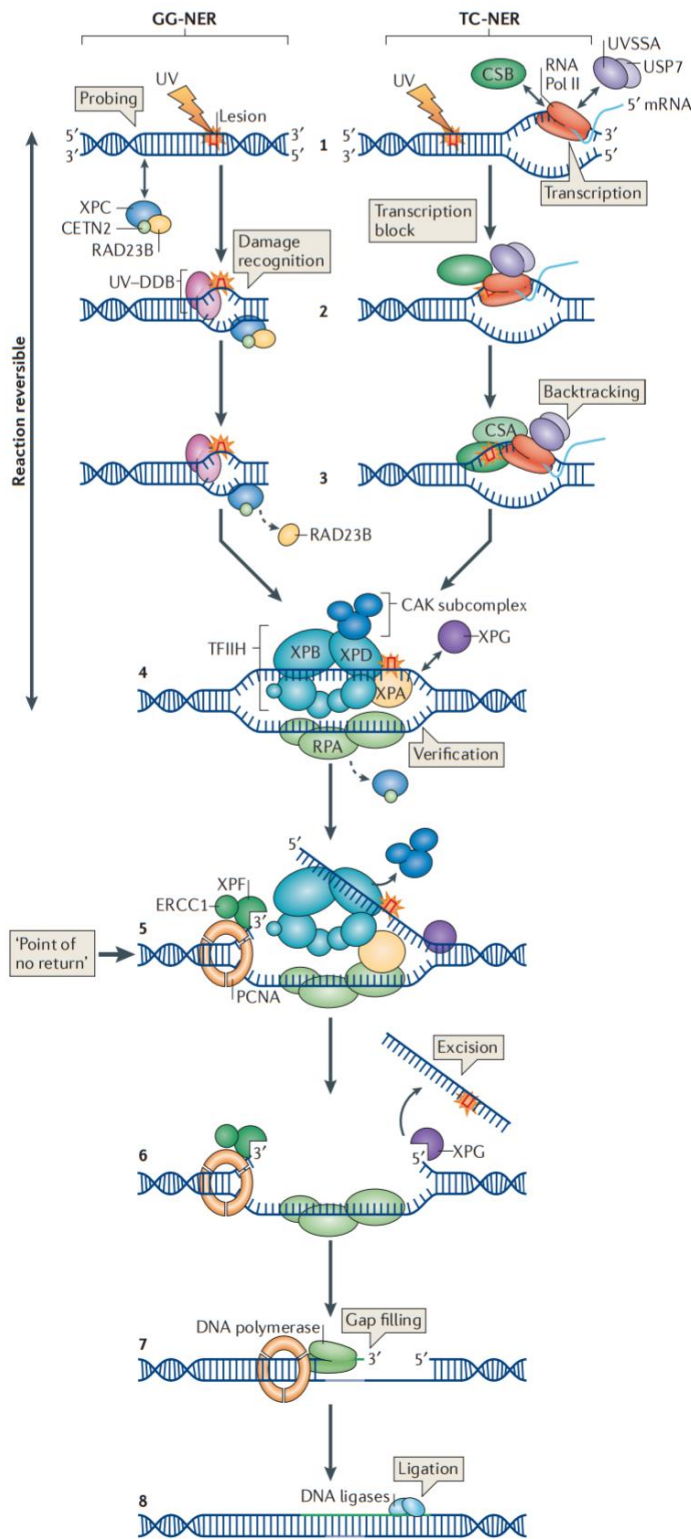
Figure 1.2 Model of Global Genomic and Transcription-Coupled Nucleotide Excision Repair. Reprinted with permission from Springer Nature. Marteijn *et al.* Understanding Nucleotide Excision Repair and its roles in cancer and aging. Nature Reviews Molecular Cell Biology. 2014. © Springer Nature.

replication is ultimately followed by DNA ligation stimulated by DNA Ligase I or XRCC1-DNA Ligase 3 (34).

TC-NER differs from GG-NER in that it is coupled to the transcriptional machinery. TC-NER may be critical for less distorting DNA lesions that may possess slow kinetics of removal from the DNA. When a bulky single-stranded lesion interferes with normal transcription, TC-NER is activated by stalled RNA Polymerase II (47). Stalling leads to recruitment of two key factors, CSA and CSB (48, 49). Additionally, the initial factors involved in TC-NER, CSA and CSB, likely aid in the removal of other types of DNA damage not generally repaired by NER including oxidative base damage (Reviewed in (34)). Thus, TC-NER is likely more complex in terms of DNA repair pathway choice, however, the mechanisms for CSA- and CSB-mediated repair and repair pathway choice is incompletely understood. In other words, the TC-NER pathway is likely not a process specifically devoted to NER, but rather a broader, transcription-linked DNA repair pathway that possesses inherent flexibility in terms of which downstream DNA repair pathway undergoes subsequent activation. Recruitment of these factors is critical for further recruitment of the NER machinery. Because RNA Polymerase II is a large complex of proteins, movement of RNA Polymerase II can be essential for physical exposure of the bulky adduct for efficient processing by TC-NER. One way that movement of the polymerase can be accomplished in order to facilitate repair is via physical reversal of theRNA polymerase on the DNA, although the specific mechanism for reversal of the RNA polymerase on the DNA is not fully understood (50). Upon recruitment of CSA and CSB to the site of the bulky DNA lesion and physical reversal of the RNA polymerase II, TC-NER converges with GG-NER by leading to the

recruitment of the core NER factors described above, including the DNA endonuclease ERCC1/XPF.

1.3.2 INTERSTRAND CROSSLINK REPAIR

Interstrand crosslinks (ICL) constitute a specific type of DNA lesion which involves linkages between nucleotides in opposing strands of DNA. ICLs can be induced by a variety of endogenous and exogenous chemicals, including reactive aldehyde species and various types of chemotherapies. In fact, ICL-inducing agents have been widely utilized for cancer therapy since the 1940s and these agents include nitrogen mustards, platinum-based compounds, and mitomycin C. While often initially effective, toxicity and resistance remain substantial clinical limitations to the long-term success of ICL-inducing agents. ICLs distort the DNA helix to different extents depending upon the agent and the DNA sequence at which binding occurs and this helical distortion can aid in detection of ICLs (51). Additionally, if left unrepaired these lesions can block replication and transcription, induce replication fork collapse, and activate cellular pathways involved in cell cycle arrest and apoptosis (52).

ICLs require several DNA repair pathways for ultimate removal and repair of the DNA damage. Also, the specific repair pathways responsible for interstrand crosslink repair differ by the cell cycle phase in which the lesions are encountered. In G_1 phase, it is generally thought that NER is the major pathway involved in removal and repair of ICLs, although a Mismatch Repair-mediated ICL repair mechanism was recently described in extracts from *Xenopus laevis* (53). The major difference between NER in removal of single strand adducts vs. ICLs is that a second set of incisions mediated by ERCC1/XPF and XPG must occur to fully remove the ICL from both strands of DNA
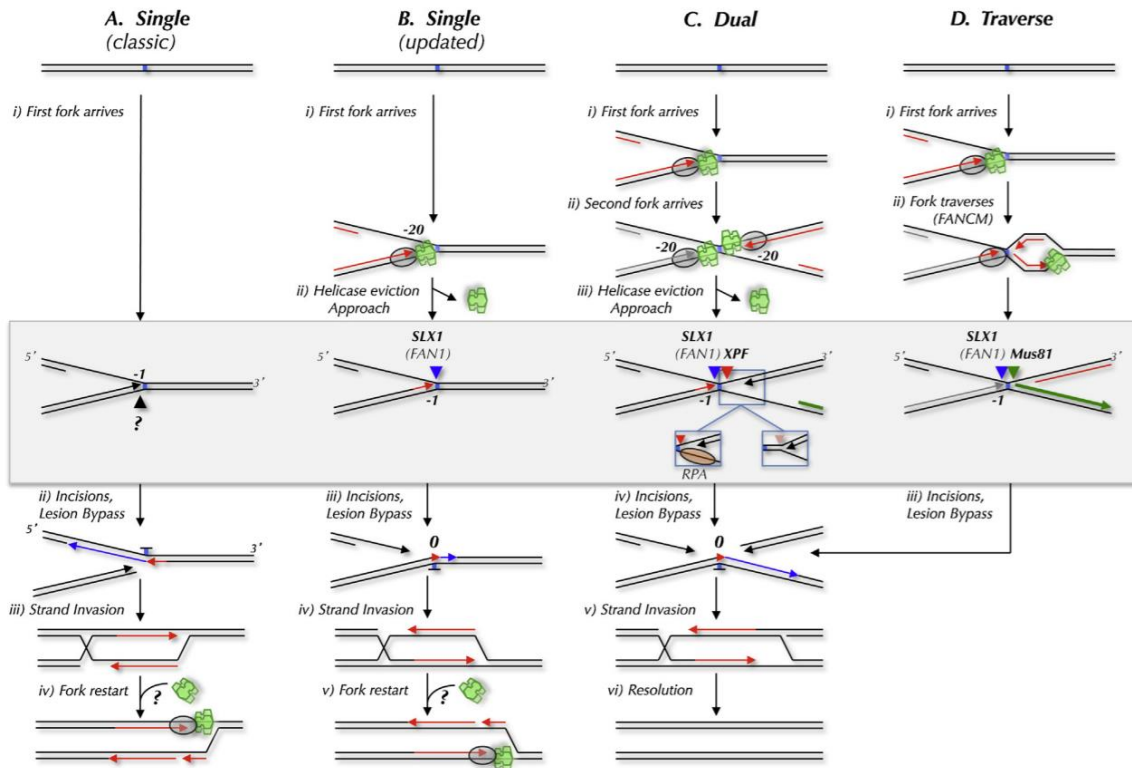
Figure 1.3 Models of Replication-Coupled Interstrand Crosslink Repair. Reprinted from "Mechanism and regulation of incisions during DNA inter-strand crosslink repair," *DNA Repair,* Vol 19, Zhang and Walter, pp. 135-142, © Copyright 2014, with permission from Elsevier.

(54). In G$_1$ phase where this mechanism would be relied upon, there is general consensus that there exist no known endonucleases capable of compensating for loss of ERCC1/XPF ultimately implying that ERCC1/XPF activity is absolutely essential for ICL repair in G$_1$ phase.

While ICLs can be repaired during G$_1$ phase, it is generally thought that most ICLs are encountered during S phase (55). During S phase, ICL-R is much more complex where ICL-R involves several nucleolytic incisions and DNA repair pathways including the Fanconi Anemia (FA) and HR machineries (56). In general, the initial processing of the ICL (i.e. double strand break formation) depends on the type of replication fork that stalls (57). Depending on the state of the replicated DNA at the fork and whether the fork has a replisome on one or both sides of the ICL, this creates varying structures capable of being nucleolytically cleaved by endonucleases to produce a DNA double strand break (57). There are currently three models for incisions at an ICL that depend on the nature of the replication fork: a single fork model, convergent fork model and replication traverse model (Figure 1.3) (57). The earliest model is the single fork model, the next model to be postulated was the convergent or dual fork model, and the most recently described model is the replication traverse model. All these models likely represent actual structures encountered during S phase in living cells. Recent evidence suggests that the single fork model accounts for approximately 20% of all ICLs encountered (58). The dual-fork model accounts for approximately 15% of all ICLs encountered (58). Finally, and somewhat surprisingly, replication traverse represents approximately 55% of all replication events at ICLs (58). This was surprising because ICLs were thought to act as complete replication blocks because there was no known mechanism for replication bypass of ICLs which would require either lesion bypass by

the DNA polymerase or unloading and reloading of the replicative CMG helicase. Furthermore, replication is tightly controlled in cells and so it is unclear how the CMG helicase could be reloaded onto the DNA in order to allow DNA replication to continue.

Despite the gaps in knowledge, what is unique to each model is the type of DNA structure formed. Five nucleases have been described to play roles in interstrand crosslink repair, including ERCC1/XPF, EME1/Mus81, SLX1/SLX4, Fan1, and SNM1A. Elegant studies in *Xenopus* extracts showed in a dual-fork model that ERCC1/XPF activity was critical for incision of an ICL substrate (59). It was also discovered that ERCC1/XPF acted in conjunction with the scaffolding protein SLX4 to facilitate incision at an ICL (59). SLX4 is an important master regulator of endonuclease recruitment during replication coupled ICL repair and is known to interact with the endonucleases ERCC1/XPF, EME1/Mus81, and SLX1 (57). Furthermore, ERCC1/XPF activity is linked to activation of the FA pathway where localization of ERCC1/XPF and SLX4 to the site of the ICL in a dual fork model is dependent upon the FA core factor, FANCD2 (59). As another layer of complexity, it was recently shown that ERCC1/XPF incision at the site of an ICL in living cells may require RPA loading which is similar to the requirement for RPA to stimulate XPF incision during NER (60). In this model, RPA loading adjacent to the ICL activates ERCC1/XPF activity which in turn leads to recruitment of the SNM1A nuclease which can physically digest past the ICL (60).

Initial observations were made in NER mutant cells that ERCC1/XPF defective cells were more sensitive to ICL-inducing agents than cells that harbored mutations in other NER factors. This suggested that ERCC1/XPF could have additional roles in the repair of ICLs independent of NER (61-63). Work from Kuraoka *et al.* was the first to clearly show that ERCC1/XPF was indeed involved in ICL-R independently of its NER

function, where ERCC1/XPF was capable of incising near an ICL in a synthetic ICL-containing DNA substrate *in vitro* (10). To this day, the regulation of which DNA endonucleases cleave which substrate and at what time remains incompletely understood. For example, work from Niedernhofer *et al.* showed that double-strand break formation during ICL-R was independent of ERCC1/XPF and that resolution of these double strand breaks required ERCC1/XPF activity (55). That observation at first seem incompatible with a requirement of ERCC1/XPF activity for the initial incision steps at ICLs. However, considering the number of potential ICL repair models, it is possible that in the absence of ERCC1, the bulk of ICLs are incised by other endonucleases including Mus81 whose preferred substrate is formed during replication fork traverse and Slx1 and Fan which might prefer those structures formed at single fork structures (57).

The recent discovery that replication fork traverse may be the predominant model for replication at ICLs combined with the understanding that the structures formed during this process are ideal for cleavage by Mus81 appear to support the idea that ERCC1/XPF activity is likely important for multiple steps during ICL-R including the initial incision steps and during resolution of HR intermediate structures since the cleavage product produced via Mus81 cleavage would produce a structure that would likely require ERCC1/XPF 5' endonuclease activity to facilitate HR completion (55, 64). This hypothesis would better support the observation that ERCC1/XPF deficient cells are more sensitive to ICL-inducing agents than other ICL-R endonucleases. In 2008, Bergstrahl and Sekelesky boldly postulated that ERCC1/XPF activity was not required for ICL unhooking and that its most important roles during ICL-R occurred downstream of the initial processing events (65). The evidence appears to support this idea: if dual fork models of ICL-R (ideal substrates for ERCC1/XPF activity) only account for

approximately 15% of all ICLs encountered in replicating cells, this would be inconsistent with hypersensitivity to ICLs beyond other endonucleases, particularly Mus81 which may provide the initial cleavage step at up to 60% of ICLs *in vitro*. Thus, the role of ERCC1/XPF in resolving complex ICL repair intermediate structures during HR may be critical for supporting cell viability after exposure to ICL-inducing agents. Indeed, recent work has shown that Mus81-mediated cleavage at sites of DNA harboring secondary structures such as G quadruplexes or AT-rich stem loops requires ERCC1/XPF activity to cleave the 3' overhangs to facilitate HR (64). It is interesting to speculate whether processing of a platinum-DNA adduct during ICL-R would create a structure in which ERCC1/XPF activity is essential for cleaving 5' to the ICL in order to allow HR to be completed. In line with this hypothesis, ERCC1/XPF is known to interact with Slx4 which is known to be involved in binding to branched DNA structures formed during HR such as the one that would be formed during HR of a substrate containing an (partially) unhooked platinum-DNA adduct.

Once initial processing occurs at ICLs, it is generally thought that there is activation of the HR machinery to facilitate repair of the DNA DSB that is produced by ICL unhooking. This process would entail the traditional components of HRR including displacement of RPA coated ssDNA by Rad51 which is mediated by BRCA2, strand invasion, DNA polymerization, followed by ligation (Reviewed in (66)). Additionally, HR repair of ICL-induced DNA damage likely requires at least three additional nucleolytic events at multiple steps beyond ICL unhooking: one incision would be required to completely unhook the ICL from one strand of DNA (3' flap structures containing bulky DNA damage), two additional incisions would be required to remove the ICL from the complementary strand of DNA (mediated by NER?), and additional incision steps may

be necessary to resolve intermediate structures during HR. However, these intermediate structures have been difficult to define and thus, the roles of ERCC1/XPF in downstream processing of HR repair intermediates are unclear except to state that ERCC1/XPF activity appears to have essential, significant roles in processing of HR intermediates (resolution of Holliday junctions/cleavage of 3' flaps) during HR-mediated repair of ICLs (64, 67).

1.3.3 SINGLE STRAND ANNEALING

Aside from the role of ERCC1/XPF activity in NER and ICL-R, ERCC1/XPF has essential roles in error-prone mechanisms of double strand break repair, including clearly defined roles in Single Strand Annealing (SSA) independent of any clearly defined roles in Microhomology Mediated End Joining (MMEJ) (i.e. Alternative End-Joining) which is another error-prone pathway for DNA DSB repair (9, 68, 69). SSA is an error-prone double strand break repair pathway that is conserved from yeast to mammals (70). In general, it relies upon sequences containing greater than 100 base pairs of homology near a double strand break to promote repair with a non-homologous sequence of DNA (i.e. a sequence different than that found on the sister chromatid) which ultimately promotes ligation, resolution of the double strand break, and loss of genetic information (70). A DNA double strand break can be shuffled into Homology Directed Repair during S and G2 phase or into Non-Homologous End Joining (NHEJ) in any phase of the cell cycle. However, under some contexts which remain unclear, double strand breaks can be repaired via the SSA repair pathway. It is likely that under certain circumstances there may be DSBs that are not compatible with HRR or NHEJ and so SSA plays an important role in limiting the persistence of DNA DSBs. Alternatively, SSA may be a backup repair pathway that functions when an otherwise

HRR- or NHEJ-compatible DSB is not repaired via these pathways. Unique from DSBs repaired via NHEJ where Ku70/Ku80 proteins limit end resection in an attempt to limit genomic instability, SSA relies on DNA end resection to expose homologous sequences adjacent to the DNA DSB that can be utilized for annealing to a short, homologous sequence in a generally unrelated region of DNA (70). Upon annealing of the short, homologous sequence, the non-homologous 3' tail of DNA is cleaved by endonucleases (ERCC1/XPF), a DNA polymerase synthesizes DNA across the gap, and ligation occurs to ultimate resolve the DSB (70).

SSA annealing relies upon a conserved set of proteins including phosphorylated CtIP and the absence of recruitment of factors that limit DNA end resection including 53BP1 (68, 71, 72). The necessity of CtIP for SSA suggests that this pathway is generally only active during S/G_2 phase of the cell cycle because CtIP phosphorylation is necessary for its roles in promoting DNA end resection and exposure of homologous DNA sequences and its phosphorylation which is controlled by cyclin-dependent kinases is generally limited to S/G_2 phase of the cell cycle (72-75). This is an important event because during S/G_2 phase where the sister chromatid is present, DNA end resection is an important aspect of HR. Conversely, during G_1 phase where the sister chromatid is not present, end resection could lead to dramatic losses in genetic information, thus for NHEJ-mediated repair of DNA DSBs, DNA end resection is not required and is actively suppressed (72). In this context, DNA end resection is not only critical for repair of DNA DSBs through HR, but also is important for SSA and MMEJ suggesting that these pathways may generally be most active during S/G_2 phases of the cell cycle. Upon resection and exposure of the homologous sequence, this substrate is capable of being annealed to the donor which is mediated by the protein Rad52 (76). After annealing, the

next step in repair is endonucleolytic cleavage of the 3' ssDNA overhangs formed during the annealing process. This process is mediated by ERCC1/XPF endonuclease activity which is stimulated by Rad52 (77). Finally, the resulting gaps are ligated by a DNA ligase. Further evidence for the role of Rad52 and ERCC1/XPF nuclease activity in SSA is supported by the observation that the yeast homologues of these factors, Rad52 (hBRCA2 and hRad52) and Rad1/Rad10, also play essential roles in SSA annealing in yeast (78).

There are several major differences between SSA and MMEJ. The first major difference is the length of the homologous sequence utilized for annealing. MMEJ can be performed with homologous sequences as short as 1-16 nucleotides while SSA usually has sequences of homology generally longer than 100 nucleotides (e.g. repetitive sequences of DNA in the genome) (79). A second major difference between MMEJ and SSA is the amount of DNA resection that occurs (70, 79). For MMEJ, this resection is rather limited while extensive resection generally occurs at breaks that undergo SSA (70, 79). This makes sense considering that less resection would be required to expose a homologous sequence of 1-16 nucleotides while more extensive resection would be required to expose a homologous region of greater than 100 nucleotides. One could also hypothesize that this might impact the recruitment of specific DNA repair factors and alter the specificity for cleavage of the 3' overhangs by endonucleases. A final major difference between these two pathways are the key DNA repair factors that mediate each repair pathway. While SSA strongly relies upon Rad52 function, Rad52 function is not required for MMEJ (68). Conversely, PARP and Polθ activity are essential for MMEJ repair, but not for SSA (80-85). Although the importance of these factors for MMEJ remains unclear, some have postulated that PARP may be

critical for recruiting Polθ to displace RPA, promote annealing likely in conjunction with Rad52, and promote extension of the DNA in order to stabilize the microhomologous DNA sequences which can be 1 - 16 nucleotides (79, 82). Together these data support a hypothesis in which SSA plays an important role in eukaryotic DNA repair leading to its being evolutionarily conserved from yeast to humans.

1.4 PLATINUM-BASED CHEMOTHERAPY

1.4.1 CISPLATIN

Platinum-based antineoplastic agents were first discovered in the 1960s by Barnett Rosenberg at Michigan State University. Rosenberg was investigating how magnetic and electrical fields impacted cellular division in bacteria. While investigating how electrical fields impact cell division, *E. coli* were grown in medium with platinum-containing electrodes and subsequently exposed to an electrical current (86). The results from these experiments showed that the bacteria were incapable of dividing until after the electrical current was removed. However, subsequent work identified platinum-containing compounds that leached from the platinum electrodes as being responsible for inhibiting cell division (87). It was out of these follow-up studies that the compound cisplatin (*cis*-diamminedichloroplatinum(II)) was first discovered (87). Further work investigated the potential of utilizing cisplatin to inhibit tumor growth utilizing a murine sarcoma model (88). These early *in vivo* studies showed that cisplatin was capable of inhibiting tumor growth and could even be curative against murine sarcoma. Eventually, cisplatin entered clinical trials and was subsequently FDA approved in 1978 (52).

Platinum-based chemotherapy remains a mainstay for cancer treatment over 50 years since its original discovery and is often given as first-line treatment in combination
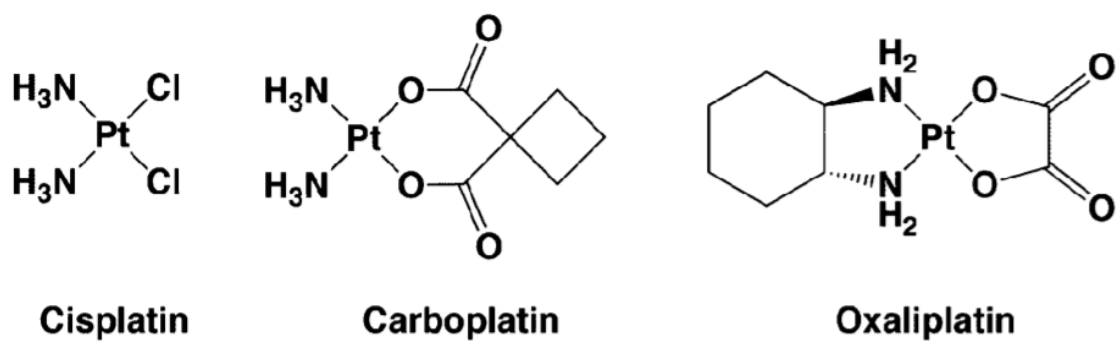
Figure 1.4 Structure of platinum-based antineoplastic agents. Reproduced from (91) (Todd and Lippard. Metallomics. 2009) with permission from The Royal Society of Chemistry

with a second cytotoxic agent or in combination with immunotherapy. It remains widely used for the treatment of a variety of human cancers including lung, ovarian, head and neck, testicular, bladder and cervical cancers and nearly 50% of all cancer patients will receive a platinum-based agent during the course of treatment (89). Platinum-based therapy even has curative potential when given in combination with other cytotoxic agents in testicular germ cell tumors which until the advent of cisplatin remained a devastating disease with few treatment options (90).

Cisplatin is structurally a very simple compound containing a platinum atom with two *cis* NH_3 groups and two *cis* chloride groups bound to the platinum (Figure 1.4) (91). In the blood stream where chloride concentrations remain high (~100 mM), these chloride molecules remain intact and cisplatin remains inert (92, 93). However, upon entry into the cell where chloride concentrations are much lower (~3 – 20 mM), cisplatin undergoes two aquation reactions where two water molecules displace the chloride atoms to form a monoaquated platinum and subsequently a diaquated platinum molecule (92-94). Upon the aquation reactions, cisplatin becomes a biologically active molecule (94). Platinum-based drugs inhibit tumor cell growth by inducing DNA, RNA, and protein damage, but it is generally accepted that the main cause of its antitumor effects is via its binding to DNA (52, 95, 96). Cisplatin is capable of binding at multiple sites on purines in the DNA, but it's up to four orders of magnitude more reactive for guanine than for adenine (97). Together this means that platinums mainly function by binding to guanines in the DNA, specifically to the N7 position of guanine (97).
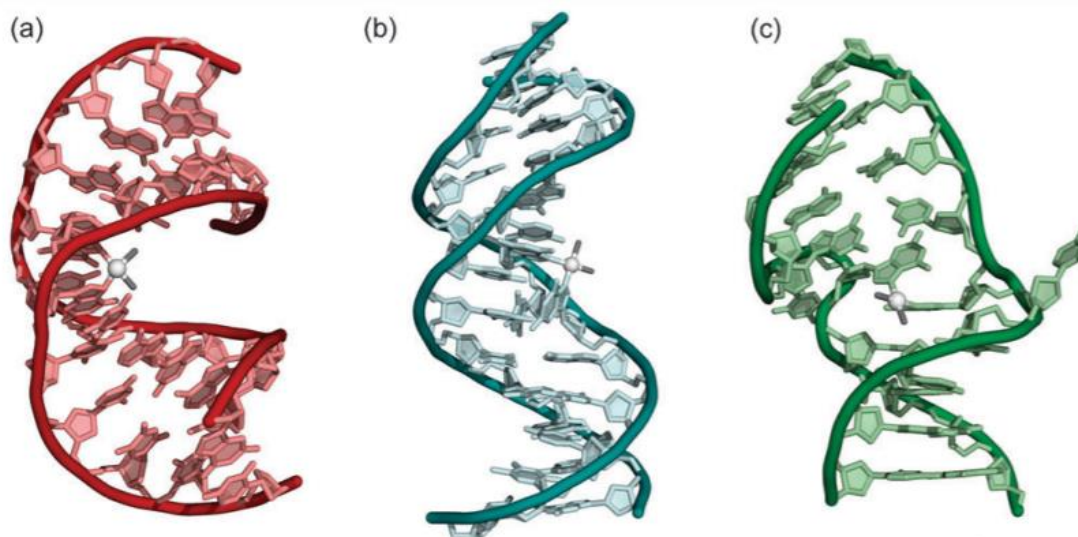
Figure 1.5 Structure of platinum-DNA complexes. A. Structure of a cisplatin 1,2 d(pGpG) adduct. B. Structure of a cisplatin 1,3 d(pGpTpG) adduct. C. Structure of a cisplatin interstrand crosslink. Reproduced from (91) (Todd and Lippard. Metallomics. 2009) with permission from The Royal Society of Chemistry

Cisplatin can form three distinct types of lesions on the DNA including monoadducts (platinum bound to a single base on a single strand of DNA), ISAs (platinum bound to two bases on a single strand of DNA), and ICLs (platinum bound to two bases on opposing strands of DNA). Monoadducts are generally formed in low abundance after cisplatin treatment (<5%) and evidence suggests that monoadducts do not inhibit DNA synthesis which might suggest that monoadducts in low abundance have limited toxicity (91, 98, 99). ISAs are the most abundant type of cisplatin-DNA lesion formed and they can constitute up to 90% of all lesions formed (92, 100, 101). These lesions are generally of three types including d(pGpG), d(pGpXpG) (where X represents adenine, thymine, or cytosine), and d(pApG). Formation of d(pGpG) adducts represents approximately 65% of all adducts formed by cisplatin, while the d(pGpXpG) and d(pApG) adducts represent approximately 25% and 5-10% respectively (91). These ISAs are bulky lesions that distort the DNA helix in different ways and are capable of blocking DNA synthesis and inhibiting transcription even if the lesion is located on the non-coding strand of DNA (91, 98, 102). For example, a d(pGpTpG) adduct induces localized unwinding of the DNA double helix and bends the duplex DNA ~ 30°, while a d(pGpG) adduct leads to a more substantial bending of the duplex DNA at 60-70° (Figure 1.5 A and B) (91). Finally, formation of G-G ICLs crosslinks is a relatively rare event and these lesions constitute 1-8% of all platinum-DNA lesions (91, 103). The structures induced by platinum-DNA ICLs are unique from those induced by ISAs. ICLs formed by cisplatin induce bending of the DNA helix by ~47° and induce localized unwinding which leads to adjacent cytosines (cytosine that were initially paired with the guanines that became crosslinked to the platinum) being extrahelically flipped from the DNA helix (Figure 1.5 C) (91, 104, 105). Due to the relative abundance of ISAs relative to ICLs, some have

speculated that the ISAs are the likely abundant source of toxicity induced by cisplatin (reviewed in (93)). While this hypothesis makes sense, there is still debate in the field as to what the general contribution of ISAs vs. ICLs is to cytotoxicity as a whole.

Cisplatin is in opposition to transplatin which was also discovered in Rosenberg's initial experiments (87). Transplatin consists of two *trans* chloride groups and two *trans* NH$_3$ groups. Even though the chloride groups also undergo two aquation reactions, the structure of transplatin limits its ability to form intrastrand adducts (ISAs), while it can still form monoadducts (106). While these monoadducts can be converted to interstrand crosslinks in biochemical assays utilizing synthetic DNA substrates, the kinetics of this reaction are exceedingly slow (t$_{1/2}$ > 24 hours) and thus, transplatin has greatly reduced biological activity compared to cisplatin (106, 107). It is thought that the steric hinderance caused by the *trans* amine groups in transplatin likely limits the types of lesions that transplatin can form. While some have postulated that transplatin is capable of forming ISAs at d(pGpXpG) sites, other have postulated that in double stranded DNAs, these ISAs actually lead to formation of ICLs (106). Finally, other groups have suggested that transplatin forms no ICLs while only forming a minimal number of ISAs (106). The determination of what type of DNA lesions are formed by transplatin is likely an academic exercise as transplatin displays virtually no biological activity.

1.4.2 CARBOPLATIN

Cisplatin is a highly toxic drug with many patients experiencing nephrotoxicity, myelosuppression, and neuropathy. Due to this fact much effort has been made to develop new platinum-based drug analogues that are either more selective for tumor tissue or less toxic. This is especially important for patients who may be particularly susceptible to toxicities associated with cisplatin including those with comorbidities or in

older patients. Since the advent of cisplatin, a number of structural analogues have been developed preclinically and several entered into clinical trials in the United States and around the world with two of these platinum analogues receiving FDA approval, including carboplatin and oxaliplatin. The most widely used of these platinum analogues is carboplatin, which was FDA approved in 1986. Structurally, carboplatin has a cyclobutane dicarboxylate group in place of the two chloride groups found in cisplatin (Figure 1.4). While carboplatin is structurally distinct from cisplatin, upon aquation it becomes identical to the biologically active form of cisplatin as only the chemical leaving groups differ between the two. While both cisplatin and carboplatin form the same DNA lesions, carboplatin has been widely used due to its reduced toxicity profile. Although the DNA lesions induced by carboplatin are identical to cisplatin, the kinetics of DNA adduct formation differ slightly based upon the length of time that is required for removal of the cyclobutane dicarboxylate leaving group (94). Knox *et al.* were among the first to show that the chloride leaving groups of cisplatin are much more labile as compared to the cyclobutane dicarboxylate group on carboplatin meaning that aquation of cisplatin occurs with faster kinetics by nearly two orders of magnitude compared to carboplatin (94). This difference in reaction kinetics also means that DNA lesions are formed with faster kinetics in the presence of cisplatin compared to carboplatin (94).

1.4.3 OXALIPLATIN

A second platinum analogue known as oxaliplatin is also widely utilized in the clinic and was approved by the U.S. FDA in 2002. Its clinical appeal was that it had an even further reduced toxicity profile compared to cisplatin and carboplatin (108-110). Additionally, its use is generally restricted to older patients or those with comorbidities for whom the toxicities of cisplatin or carboplatin would be prohibitive. A number of studies

have consistently shown similar performance of cisplatin or carboplatin compared to oxaliplatin in a number clinical studies with beneficial toxicity profiles in the oxaliplatin treated arms of these studies (108-110). Subsequently, an oxaliplatin-containing regimen did become FDA approved for first-line treatment of metastatic colorectal cancer patients in 2004 and showed superiority to the previous standard of care, 5-Fluorouracil/Leucovorin (111, 112). However, in many other cancers oxaliplatin use still remains restricted to those not capable of tolerating cisplatin or carboplatin treatment. Oxaliplatin is structurally distinct from cisplatin even upon aquation and forms structurally distinct DNA lesions, although with lower efficiency than cisplatin (91, 113). While oxaliplatin induces fewer total lesions than cisplatin, some of these lesions may in fact be more cytotoxic than those induced by cisplatin as oxaliplatin was shown to be more effective than cisplatin at inhibiting DNA replication (113).

1.4.4 OTHER PLATINUM ANALOGUES

This subsequent section is by no means an exhaustive list of platinum-based compounds currently undergoing preclinical or clinical development which was reviewed in (114). However, several other platinum analogues and platinum formulations (including liposomal) have been developed which showed promise in preclinical studies. Satraplatin was first developed in 1993 and it is structurally distinct from cisplatin, carboplatin, and oxaliplatin in that it is based upon Pt^{4+} as opposed to Pt^{2+} (91, 115). Another major difference from the FDA approved platinum analogues which are all given intravenously is that satraplatin can be administered orally (115, 116). 17 clinical trials are listed for satraplatin in clinicaltrials.gov with 16 trials having been completed or terminated. The only current active clinical trial with satraplatin is based in China.

Satraplatin failed to meet its endpoint in Phase III clinical trials in castration-resistant prostate cancer and it appears that further clinical development has been halted.

Another platinum analogue known as picoplatin showed promising preclinical results (117). It is structurally similar to cisplatin, carboplatin, and oxaliplatin in that it is based upon Pt^{2+} (117). Like cisplatin it has two *cis* chloride molecules. While it also has a single amine group, it structurally differs from cisplatin by the addition of a 2-methylpyridine group (117). It was thought that the addition of this bulky ring structure helped the drug to avoid neutralization by thiol groups intracellularly (114). Additional preclinical studies showed that picoplatin was capable of overcoming resistance to cisplatin, carboplatin, and oxaliplatin in platinum-resistant cell line models (118, 119). Aside from *in vitro* studies, *in vivo* studies were also promising in ovarian tumor models (117). Picoplatin entered into Phase I and ultimately into Phase II clinical trials in several cancers including in non-small cell lung cancer as first-line therapy and in small-cell lung cancer as second-line therapy in patients previously treated with platinum-based chemotherapy (120). Picoplatin failed to meet its primary endpoint and had limited effects on inhibiting tumor progression (120). As such, picoplatin is not currently undergoing further therapeutic evaluation.

1.4.5 ROLE OF NER IN RESISTANCE TO PLATINUM-BASED CHEMOTHERAPY

A major limitation to the use of platinum-based agents in cancer therapy is the presence of intrinsic or acquired resistance. Platinum-based agents are often given as first-line therapy in a number of tumor types, including lung cancers. However, a subset of patients will not respond to treatment and these tumors are defined as intrinsically resistant. Alternatively, many patients whose tumor responds to platinum-based chemotherapy initially, will ultimately acquire resistance to these agents and no longer

respond. Many mechanisms of resistance to platinum-based chemotherapy have been described including increased NER, increased translesion synthesis, loss of mismatch or base excision repair (BER), decreased apoptotic potential, and increased platinum inactivation or reduced platinum accumulation which have been reviewed in (52, 92, 121, 122). Tumors generally display widespread clonal heterogeneity and it is likely that in most instances resistance does not occur on a global level, but rather treatment selects for clones that are intrinsically resistant to therapy.

Because the lesions induced by cisplatin are up to 90% intrastrand adducts which are repaired via the NER pathway, increased NER is thought to be a predominant mechanism of resistance to platinum-based chemotherapy. By increasing the rate of removal of platinum-DNA lesions, this would decrease the amount of time that intact lesions can activate the DNA damage response and stimulate cellular apoptotic pathways and ultimately reduce the therapeutic window for treatment. In support of this, there is a general inverse correlation between expression of NER factors and sensitivity to cisplatin both *in vitro* and in retrospective patient studies (123-128). NER as a mediator of platinum resistance has been widely studied in the context of *in vitro*, *in vivo*, and patient-based studies. One key NER factor that has been widely studied in the context of platinum resistance/sensitivity in multiple tumor types including non-small cell lung, ovarian, bladder, and head and neck cancer is ERCC1. In the studies referenced above, increased ERCC1 expression is generally associated with increased resistance to platinum-based chemotherapy. Conversely, low ERCC1 is associated with prolonged survival after platinum treatment. As part of the ERCC1/XPF endonuclease which is generally required for removal of platinum-DNA ISAs and ICLs, dysregulated ERCC1 expression is thought to be a biomarker for predicting responders and non-responders to

platinum-based treatment. Somewhat counterintuitively, high ERCC1 expression in early-stage lung cancers is associated with increased overall survival (129, 130). This may indicate that in early stage disease, high ERCC1 promotes genome stability and thus contributes to less aggressive disease, while in advanced disease which is associated with increased genomic instability and mutation burden high ERCC1 is associated with therapy resistance which in turns supports tumor growth. Due to this relationship between increased NER and resistance to platinum-based chemotherapy, various NER factors have become potential targets for therapeutic development, including XPA, ERCC/XPF, RPA (131-137). Some of these small molecule inhibitors of NER factors are currently undergoing further preclinical development.

1.5 ERCC1 AS A BIOMARKER FOR PLATINUM RESPONSE

The expression of ERCC1 and its correlation to sensitivity to DNA crosslinking agents aside from those formed by UV light began to emerge in the early 1990s. In patient tumors, initial evidence was provided in 1992 that ERCC1 mRNA expression was 2.6-fold higher in tumors from ovarian cancer patients who were resistant to platinum-based chemotherapy (138). This observation was confirmed in a later study from the same group utilizing ovarian cancer tissue (139). These data pointed to the possible role for ERCC1 expression in mediating response to platinum-based chemotherapy. *In vitro* evidence that ERCC1 expression may be associated with sensitivity to DNA crosslinking agents was published in 1991 in the context of nitrogen mustards, which at the time was a commonly used treatment for various types of leukemias (140). Additional evidence was published that ERCC1 was involved in mediating resistance to other DNA crosslinking agents commonly used in cancer therapy including mitomycin C and cyclophosphamide (63, 141, 142). In relation to ERCC1-mediated cisplatin resistance,

in 1993 and 1994 two papers were published directly implicating ERCC1 in mediating repair of cisplatin-induced DNA damage (143, 144). Early studies implicated ERCC1 expression as being potentially important for regulating cisplatin cytotoxicity in cell lines and patient tumors, and biochemical analyses showing ERCC1/XPF is physically involved in processing of cisplatin-DNA ISAs and psoralen ICLs were published in 1994, 1996, and 2000 (10, 145, 146). Furthermore, it was identified that after cisplatin treatment, ERCC1 expression increases due to increased stimulation of ERCC1 transcription (but not ERCC4/XPF transcription) mediated by c-Fos and c-Jun, downstream mediators of Ras/MAPK signaling (147). Indeed, the Ras/MAPK pathway has been associated with increased ERCC1 expression in cancer cell lines likely due to increased transcriptional activity via two AP-1 sites in the ERCC1 promoter (148-150). Since these first observations, data has continued to accumulate over the last 25 years establishing ERCC1 expression as a bona fide marker of cisplatin sensitivity/resistance.

The first clinical evaluation of the impact of ERCC1 tumoral expression on patient survival was published in 1998 in gastric cancer where patients with low ERCC1 mRNA expression responded better to combination fluorouracil/cisplatin than those with high ERCC1 mRNA expression (151). During the early 2000s, ERCC1 and its clinical potential for predicting response to platinum-based chemotherapy began to blossom. In 2001, a retrospective patient study once again identified ERCC1 mRNA expression as a predictor of overall survival in response to platinum-based chemotherapy in gastric cancer (152). In 2002, a subsequent study identified low ERCC1 mRNA expression was associated with increased overall survival in non-small cell lung cancer patients with advanced disease receiving a regimen of platinum and gemcitabine (153). Additional follow-up studies (including a Phase II clinical trial) in non-small cell lung cancer

validated these observations with ERCC1 mRNA expression as well as by protein expression as measured by immunohistochemistry (123, 154-156). However, these results showing low ERCC1 corresponds with better response to platinum-based chemotherapy were not always consistent between studies from different research groups (157, 158). While most clinical studies utilized ERCC1 mRNA expression as the means for quantifying ERCC1 expression, there were efforts to utilize immunohistochemistry-based approaches to quantify ERCC1 protein which was thought to be a better predictor of tumoral expression of ERCC1 than mRNA (123). However, subsequent studies proposed that the antibody utilized in that study was not appropriate for immunohistochemical detection of ERCC1 and actually bound a second antigen, namely CCTα (159, 160). A subsequent study showed that there were inherent problems with the antibody used in those clinical studies, specifically problems pertaining to batch-to-batch variability that ultimately impacted the predictive nature of IHC-based ERCC1 quantitation in terms of clinical response to platinum-based chemotherapy (13). A second problem with the IHC-based studies is the lack of specificity for the functional ERCC1 isoform (ERCC1-202). In other words, ERCC1 quantification via IHC could artificially inflate the number of ERCC1 positive tumors and impact patient stratification, although recent studies have confirmed that IHC-based quantification of ERCC1 is predictive of overall survival in ovarian cancers (13, 18, 127). While these issues have become well known, there have been efforts made to create antibodies specific for ERCC1/XPF heterodimer to circumvent problems with ERCC1 splice variant expression (19).

Use of ERCC1 as a potential first-in-class platinum response biomarker began to gain traction in the field of non-small lung cancer partly because of the limited efficacy of

this therapy. Thus, identifying a biomarker that would predict (non)responders to therapy could lead to the identification of patients that would be ideal responders (i.e. personalized/targeted therapy) and could aid in the development of novel therapies to treat those who do not respond to platinum-based chemotherapy (161, 162). While preclinical data showing that ERCC1 expression was promising in multiple studies, a prospective international, randomized Phase III clinical trial in non-small cell lung cancer failed to show benefit for patients with low ERCC1 who received a platinum agent (163).

1.6 CENTRAL HYPOTHESIS

Many *in vitro* preclinical studies investigating ERCC1-deficiency as a predictive marker for cisplatin sensitivity clearly showed that low ERCC1 is associated with better response to cisplatin. While many retrospective clinical studies also corroborated results from *in vitro* studies, an international, randomized Phase III study failed to show benefit for patients with low ERCC1 who received a platinum agent. Together, these data suggest that there remains an incomplete understanding regarding the biological relationship between ERCC1 expression and sensitivity to platinum-based chemotherapy in the patient setting. With this in mind, we hypothesized that confounding biological variables exist that may have impacted previous studies investigating ERCC1 as a platinum biomarker. Furthermore, we hypothesized that better understanding how ERCC1 expression is associated with sensitivity to DNA crosslinking agents could lead to an improved understanding as to how best to select for patients that would benefit specifically from a chemotherapy regimen containing a platinum agent. To address these hypotheses, this study investigated the following specific aims.

Aim 1: Investigate the role of p53 status in modulating sensitivity of ERCC1-deficient cell lines to DNA crosslinking agents.

Aim 2: Explore the potential of utilizing the ATR inhibitor, M6620, to overcome platinum tolerance in ERCC1-deficient cells.

CHAPTER 2- IDENTIFICATION AND CHARACTERIZATION OF SYNTHETIC VIABILITY WITH ERCC1 DEFICIENCY IN RESPONSE TO DNA CROSSLINKS IN LUNG CANCER

This chapter has been reprinted with modification from Heyza et al. Clinical Cancer Research. 2019 with permission from the American Association for Cancer Research © AACR 2019

2.1 Introduction

The structure-specific endonuclease excision repair cross-complementation group 1 (ERCC1)/xeroderma pigmentosum group F (XPF) plays key roles in nucleotide excision repair (NER), interstrand crosslink repair (ICL-R), homologous recombination (HR) repair, and single-strand annealing pathways. Although the role of ERCC1/XPF in NER is well established, the totality of its specific functions in the processing and repair of interstrand crosslinks (ICL) has remained unclear (see refs. (65, 164) for review). ICLs are produced upon exposure to agents that covalently link bases in opposing strands of DNA, and endonucleases are required for cleavage of the phosphodiester backbone adjacent to ICLs in order to initiate repair (54). Much recent evidence indicates ERCC1/XPF is required for ICL-unhooking, whereas other work highlights additional roles for this complex in ICL-R downstream of unhooking (55, 59, 62, 165).

Use of interstrand crosslinking agents, including cisplatin, remain a mainstay in the treatment of malignancies. Several mechanisms for resistance to platinum-based chemotherapy have been described, including loss of base excision repair and mismatch repair, decreased drug accumulation, increased sequestering by thiols, decreased apoptosis, and increased translesion synthesis (52, 166-168). Another proposed mechanism of resistance to cisplatin involves increased expression of ERCC1/XPF observed both *in vitro* with cisplatin-sensitive/resistant cell lines and in relation to survival

in patient samples (123, 153-155, 168-170). Work by our laboratory and others have shown that downregulation of ERCC1/XPF sensitizes cancer cells to cisplatin and that this sensitivity is related to a reduction in ICL and intrastrand adduct (ISA) repair (31). In addition, small molecule inhibitors of ERCC1/XPF can increase cisplatin sensitivity both *in vitro* and *in vivo*, indicating the potential of pharmacologically targeting ERCC1/XPF to enhance platinum efficacy (135, 137).

First identified as a potential biomarker for response to platinum-based chemotherapy in the late 1990s, low ERCC1 expression was observed in a relatively high amount of patient tumors including in non–small cell lung cancers, head and neck cancers, and ovarian serous adenocarcinomas. Although preclinical data were promising, many challenges faced the clinical implementation of ERCC1 as the first platinum biomarker including problems with antibody specificity, splice variant expression, and conflicting results from clinical and preclinical studies. However, it is possible that an incomplete understanding of basic biological factors controlling sensitivity to ICL-inducing agents in the absence of ERCC1 may also have contributed to the failure of the ERCC1 clinical trials. What has become clear over the past 10 years is that a DNA-repair deficiency does not necessarily predispose to sensitivity to a particular drug. This is most notably observed with BRCA1/2 deficiencies in the context of PARP inhibition where loss of subsequent secondary factors is capable of making BRCA1/2-mutant tumors resistant to PARP inhibition. In the context of ICL repair, recent evidence has shown that loss of p53, the deubiquitinase, USP48, or the BLM–RMI1–TOPIIIa signaling axis is capable of increasing resistance of Fanconi anemia (FA) deletion mutants to ICLs both *in vitro* and *in vivo* (171-173). In particular, these findings directly

implicate increased reliance on DNA repair pathways to deal with ICLs that would otherwise be unrepaired as a result of loss of canonical ICL-R.

In this study, we identified p53 status as at least a partial modifier of the sensitivity of ERCC1 knockout (Δ) cells to ICL-inducing agents. Here, we characterize a panel of ERCC1Δ lung cancer cell lines developed with CRISPR-Cas9. We describe a differential phenotype in sensitivity to cisplatin and mitomycin c (MMC) that appears to be correlated with p53 status where ERCC1Δ/p53WT cell lines exhibit hypersensitivity to ICL-inducing agents, but ERCC1Δ/p53$^{mutant/null}$ cells exhibit only mild sensitivity. Finally, we show evidence that tolerance to interstrand crosslinks with ERCC1 deficiency is supported by entry into S-phase and relies on BRCA1 and DNA-PKcs function. Together this evidence suggests that functional loss of p53 may allow for the uncovering of alternate repair mechanisms capable of at least partially overcoming the repair defects associated with loss of ERCC1/XPF activity thus leading to the identification of a new subset of cisplatin-tolerant, ERCC1-deficient tumors. These findings have direct clinical ramifications for future studies of ICL-repair in human tumors as well as impacting any attempts to implement biomarkers for sensitivity to ICL-inducing agents in the future.

2.2 Materials and Methods

2.2.1 Cell lines and cell culture

H1299, H460, H522, H1703, H1650, H358 were all obtained from the ATCC, were tested for mycoplasma, and authenticated by the BioBanking and Correlative Sciences Core Facility at Karmanos Cancer Institute. A549 WT and ERCC1Δ cells were obtained from Jean-Charles Soria, Ken Olaussen, and Luc Friboulet (Gustave Roussy Cancer Center). OV2008 and C13* cells were obtained from Stephen B. Howell (University of California San Diego). A549 and OV2008 cells were not further

authenticated or tested for mycoplasma. Cell lines were maintained for no greater than 15 passages during the course of experiments. H1703, H522, H460, OV2008, C13*, H1650, H358, and H1299 cells were cultured in RPMI1640 (Dharmacon) media supplemented with 10% FBS (Atlanta Biologicals) and 1% penicillin/streptomycin (Dharmacon) and grown at 37 °C in 5% CO_2. A549 cells were cultured in DMEM (Dharmacon) supplemented with 10% FBS, 1% penicillin/ streptomycin, 1% MEM, nonessential amino acids (Dharmacon), and 1% HEPES (Dharmacon).

2.2.2 CRISPR-Cas9–mediated gene knockout (*Method adapted from* (135))

Cas9-lentivirus was produced using the Lenticrispr V2, pVSVg, and psPAX2 plasmids (Addgene) in HEK293T cells. The day following seeding, cells were transduced for ~16-hours with Cas9 lentivirus. Cells were selected with puromycin and clones were selected using standard methods for ERCC1 knockout experiments. Cas9 expression in selected clones was assessed by western blot and a high-expressing Cas9 clone was chosen for ERCC1 knockout experiments. For all other knockout experiments, pooled Cas9-expressing cells were used for subsequent transfection steps. Synthetic tracrRNA and crRNA was purchased from Dharmacon. Transfection was performed as per the manufacturer's protocol. The day before transfection 150,000 - 300,000 cells were seeded in antibiotic-free RPMI media. The following day synthetic RNA was diluted to a 100 µM stock in a 10 mM Tris pH 7.4 buffer containing nuclease-free water. A final concentration of 50 nM was used for both tracrRNA and crRNA and was transfected with 3 µg/mL Dharmafect Duo Transfection Reagent (Dharmacon) in a total reaction volume of 2.4 mL in a six-well plate format. Cells were transfected for 48 hours after which complete media was added for 24 hours. Cells were seeded for clones and clones were selected using standard methods. Clones were initially screened for knockout by

western blot. Validation of genome editing was performed by PCR amplification of genomic DNA with Taq polymerase (NEB). PCR product was cloned into a linearized pCR4-TOPO vector and transformed into OneShot TOP10 *E. coli* using the TOPO-TA Cloning Kit for Sequencing (Thermofisher). Bacterial colonies were selected with ampicillin and plasmid was extracted using standard procedures. Plasmid was sequenced by GeneWiz using an M13R primer. Knockout clones were validated by Sanger sequencing excluding second ERCC1 knockout clones and the XPA knockout clones which were validated by western blot.

crRNA sequences:

ERCC1 #1: 5' AGGGACCUCAUCCUCGUCGA 3'

ERCC1 #2: 5' AUCACAAAUUUCUUCCUUGC 3'

ERCC4: 5' GCCAUGGCAAUCCGUCGAGC 3'

TP53: 5' CCGGUUCAUGCCGCCCAUGC 3'

XPA: 5' UGCUCUAAAGCCGCCGCCUC 3'

2.2.3 Colony survival assays

Colony survival assays were performed as previously described (166). Cells were treated with cisplatin (Sigma-Aldrich) or MMC (Selleckchem) for two hours or gemcitabine (Selleckchem), camptothecin (Selleckchem), or etoposide (Selleckchem) for four hours in serum-free medium. Cells were treated with Palbociclib (Selleckchem), Ribociclib (Selleckchem), DNA-PK inhibitor (NU-7441; Selleckchem), or XL-413 (DBF4-dependent kinase inhibitor; Tocris) for 24 hours in complete medium. For UV-C treatment, 2,000 cells were seeded in six-well plates and treated with the corresponding UV-C dose the following day. Plates were fixed and stained with crystal violet three days posttreatment and crystal violet was dissolved in 10% acetic acid and absorbance at 595

nm was measured using a SpectraMax M5 plate reader (Molecular Devices). IC_{50}s were estimated using SigmaPlot 10.0 Software.

2.2.4 Viability assays

A total of 12,000 cells were seeded in 24-well plates. Cells were treated with cisplatin for 24 hours and allowed to grow for an additional 24 hours. Live/dead cells were counted using Trypan Blue exclusion and ~100 cells were counted for each concentration.

2.2.5 Flow cytometry

Apoptosis was measured by flow cytometry using the PE Annexin V Apoptosis Detection Kit (BD Biosciences). Cell-cycle profiles were determined using the propidium iodide (PI) Flow Cytometry Kit (Abcam). For both assays, 5×10^5 cells were seeded in 10 cm plates. The following day cells were treated with 500 nmol/L cisplatin for two hours in serum-free medium and cells were allowed to grow for 48 hours (for apoptosis) or were collected at various time points (cell cycle). Flow cytometry was performed on a BD LSR II SORP Flow Cytometer (BD Biosciences). Data were analyzed using ModFit LT (Verity Software House) and FlowJo v10 (FlowJo, LLC).

2.2.6 Modified alkaline comet assay

Modified alkaline comet assays were performed essentially as previously described (135, 166, 174). Cells were seeded in six-well plates so that they would be 70% to 90% confluent at the time of harvesting. H522 and H1299 cells were treated with cisplatin for two hours. Control and cisplatin-treated cells were then treated with 100 μmol/L H_2O_2 (Fisher Scientific) for 15 minutes immediately prior to harvesting by trypsinization at 0, 24, and 48 hours post-cisplatin treatment. Cells were embedded in 0.5% low-melting agarose (Fisher Scientific; Catalog No. BP165-25) and spread on

slides coated with 1.5% Standard Low–mr Agarose (Bio-Rad; Catalog No. 162-0100) and allowed to solidify. After 10 minutes, slides were placed in 4 °C lysis buffer (2.5 M NaCl, 100 mmol/L EDTA, 10 mmol/L Tris base, 1% Triton X-100, pH 10) for one hour. Excess buffer was removed and slides were placed in the electrophoresis tank with 4 °C alkaline electrophoresis buffer (0.3 mol/L NaOH, 1 mmol/L EDTA) and incubated for 20 minutes. Slides were electrophoresed for 25 minutes at 300 mA (22–26 V). Slides were then incubated with 4 °C neutralization buffer (0.4 mol/L Tris Base, pH 7.5) for 10 minutes. Slides were fixed in 95% ethanol for 10 minutes and allowed to dry followed by incubation with SYBR-Gold (Invitrogen). Slides were imaged with a Nikon epifluorescence microscope. Approximately 50 cells were analyzed per slide with Komet Assay Software 5.5F (Kinetic Imaging). ICLs were measured as the ratio of the median tail moment of the treated compared with the untreated sample where the ratio at 0 hours post-cisplatin treatment was normalized to 100% for each isogenic cell line.

2.2.7 Patient survival analysis

The Cancer Genome Atlas (TCGA) provisional lung adenocarcinoma cohort was utilized to assess the relationship of *ERCC1* tumor expression and *TP53* mutational status on patient outcomes (175, 176). Tumor genomic and patient outcomes data were accessed for these TCGA patients on cBIOportal (176, 177). Genomic data were cleaned and normalized prior to release as described previously (175, 176). *ERCC1* expression was stratified into two groups, high and low, at the upper quartile of expression values. *TP53* mutation status was also stratified into two categories, mutated or wild-type (WT), based upon the presence or absence of nonsynonymous mutations in the coding region of the gene as detected by whole-exome sequencing. Patient overall survival (OS) was modeled in R (version 3.4.3) using the Kaplan–Meier method and log-

rank test. Because treatment data for the TCGA lung adenocarcinoma cohort is not publicly available, we also analyzed the 2017 TCGA ovarian cancer data set. Patients with stage 3 or 4 disease who received a platinum agent were included in the analysis. Patients were selected based upon the presence or absence of a *TP53* mutation and patients were stratified based upon *ERCC1* expression using the Affymetrix probe ID: 203720_s_at and the "auto select best cutoff" function. Data were analyzed using KMPlotter (kmplotter.org/ovar/; (178)).

2.2.8 Immunofluorescence

Cells were seeded on coverslips and treated with 500 nmol/L cisplatin for two hours. 48 hours posttreatment cells were fixed with 4% paraformaldehyde and permeabilized in 0.3% Triton-X in PBS. Cells were blocked in 10% FBS in 0.1% Triton-X in PBS for one hour and incubated with primary antibody for one hour and secondary antibody for 1.5 hours in 1% BSA/0.1% Triton-X. DNA was stained with 300 nmol/L DAPI for five minutes and coverslips mounted on slides with DakoCytomation Fluorescent Mounting Medium (Agilent) and sealed with nail polish. Slides were imaged with a Nikon epifluorescence microscope and images were analyzed using ImageJ software and the Find Maxima function. A minimum of 100 cells per group per experiment were analyzed. Antibodies are available in Table 2.1.

2.2.9 shRNA knockdowns and re-expression of p53 and ERCC1

BRCA1 and BRCA2 shRNAs were purchased as bacterial stocks from Sigma-Aldrich.

BRCA1 shRNA sequence: 5' CCGGGAGTATGCAAACAGCTATAATCTCGAGATTATAG CTGTTTGCATACTCTTTTG 3'

BRCA2 shRNA sequence: 5' CCGGTACAATGTACACATGTAACACCTCGAGGTGTTA

CATGTGTACATTGTATTTTTG 3'

ERCC1-202 cDNA was purchased from Genscript and was cloned into pCDH-puro lentiviral vector. shRNA lentivirus and *ERCC1*-202 lentivirus was produced and transductions were performed as previously described (179). *TP53* cDNA was purchased from Origene (Catalog No. R200003). Cells were transfected with 2.5 μg/DNA per well with a final concentration of 3 μg/well Lipofectamine for six hours. Cells were allowed to rest for 24 hours, after which geneticin sulfate was added. Approximately two weeks post-transfection, cells were harvested to assess p53 expression and experiments were performed. Knockdown of BRCA1 was validated by western blot. BRCA2 knockdown was validated by quantitative real time polymerase chain reaction (qRT-PCR) as described in Sawant *et al.* (174) using the following primers:

Forward Primer: 5' GTTGTGAAAAAAACAGGACTTG 3'

Reverse Primer: 5' CAGTCTTTAGTTGGGGTGGA 3'

2.2.10 Statistical analysis for cell line studies

Flow cytometry and modified alkaline comet assay data were analyzed by two-sample t test. Data comparing the dose effects of cisplatin or MMC on p53 status stratified by ERCC1 WT and knockout were analyzed by two-way ANOVA with interaction test. γH2AX foci data were analyzed by Wilcoxon rank-sum test. Drug response, apoptosis, and modified alkaline comet assay experiments were all performed at least three times, unless otherwise stated. Cell cycle and γH2AX foci formation experiments are presented as a representative result from two to three individual experiments.

2.2.11 Western blot analysis

Protein extraction and Western blot analysis were performed as previously described (174). Antibodies used for Western blot analysis are available in Table 2.1.

Table 2.1

Antibody	Identifier	Distributor	Dilution	Application
β-actin	A5441	Sigma-Aldrich	1:100,000	Western Blot
α-tubulin	T5168	Sigma-Aldrich	1:100,000	Western Blot
ERCC1	ab76236	Abcam	1:1,000	Western Blot
XPF	sc-136153	Santa Cruz	1:1,000	Western Blot
p53	OPO9	Calbiochem	1:1,000	Western Blot
CDKN1A/p21	GTX112898	GeneTex	1:1,000	Western Blot
XPA	Ab-1	Neomarkers	1:1,000	Western Blot
γH2AX	05-636	EMD Millipore	1:1,000 1:800	Western Blot Immunofluorescence
PARP-1	sc-1561	Santa Cruz	1:1,000	Western Blot
BRCA1	SAB2702136	Sigma-Aldrich	1:1,000	Western Blot
Goat anti-Mouse	172-1011	BioRad	1:2,000	Western Blot
Goat anti-Rabbit	172-1019	BioRad	1:2,000	Western Blot
Alexa Fluor 488 Goat anti-Mouse	A11029	Invitrogen	1:1,500	Immunofluorescence

2.3 Results

2.3.1 ERCC1Δ cells exhibit 2 distinct phenotypes upon cisplatin treatment

We developed a panel of ERCC1Δ cell lines using CRISPR-Cas9 to assess differences in sensitivity to ICL-inducing drugs (Fig. 2.1 A). ERCC1 has 4 known splice variants, which differ by single intron inclusion or single exon exclusion (13, 18), so in order to generate a clean background for our studies, we designed a crRNA targeting ERCC1 exon 2, which is shared by all ERCC1 splice variants. We utilized lung cancer cell lines that differed in p53, EGFR, and K-Ras status (Fig. 2.3 A). As expected, loss of
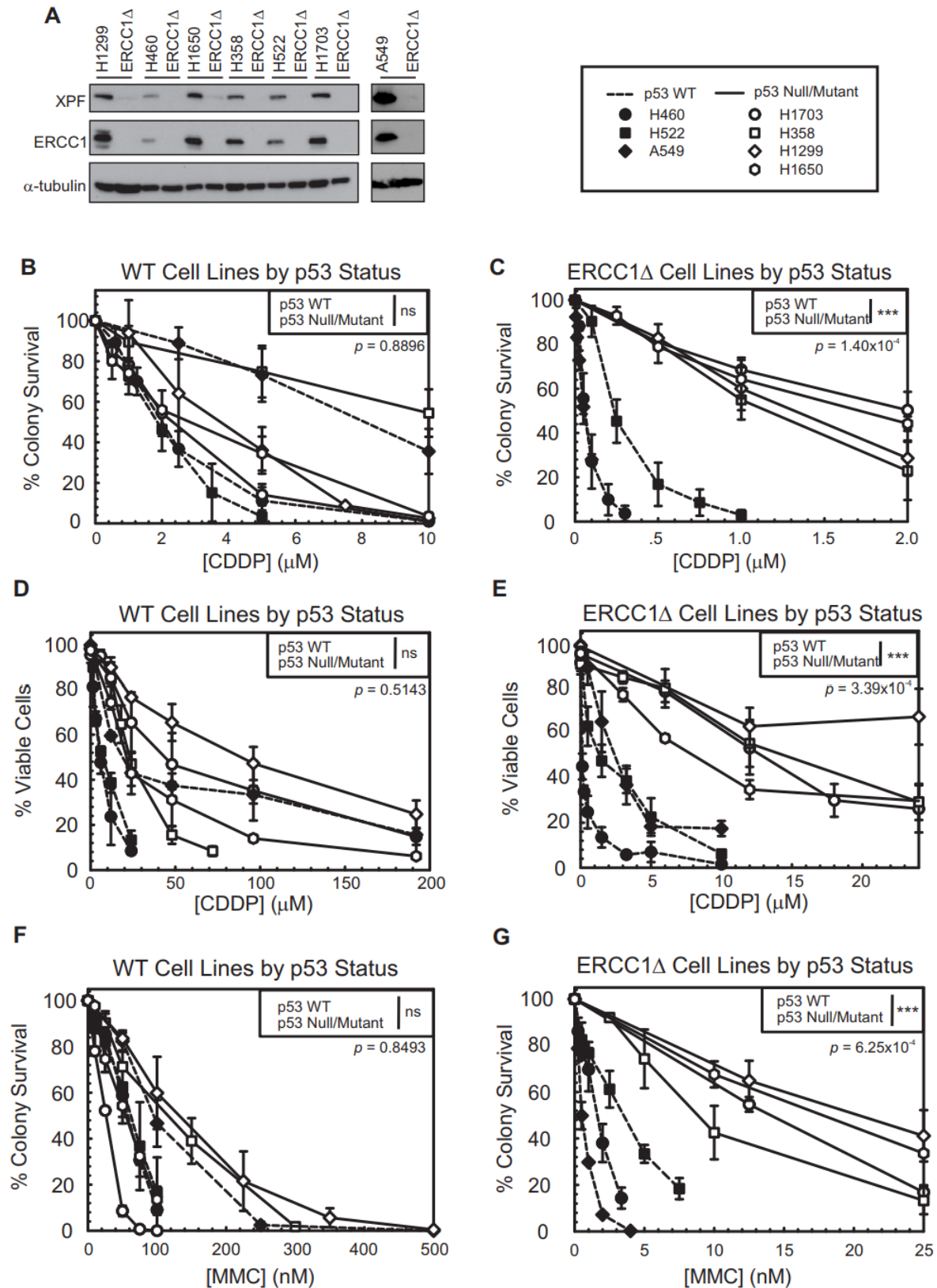
Figure 2.1. Cisplatin and mitomycin c sensitivity of a panel of ERCC1Δ lung cancer cell lines. A. Western blot depicting ERCC1 and XPF expression in the WT and ERCC1Δ cell lines generated by CRISPR-Cas9 and the A549 WT and ERCC1Δ cells. **B-C.** Clustering of cisplatin clonogenicity assays of ERCC1 WT and ERCC1Δ cells by p53 status. **D-E.** Clustering of cisplatin viability assays of ERCC1 WT and ERCC1Δ cells by p53 status. **F-G.** Clustering of MMC clonogenicity assays of ERCC1 WT and ERCC1Δ cells by p53 status. Data analyzed by two-way ANOVA. *** $p < 0.001$.
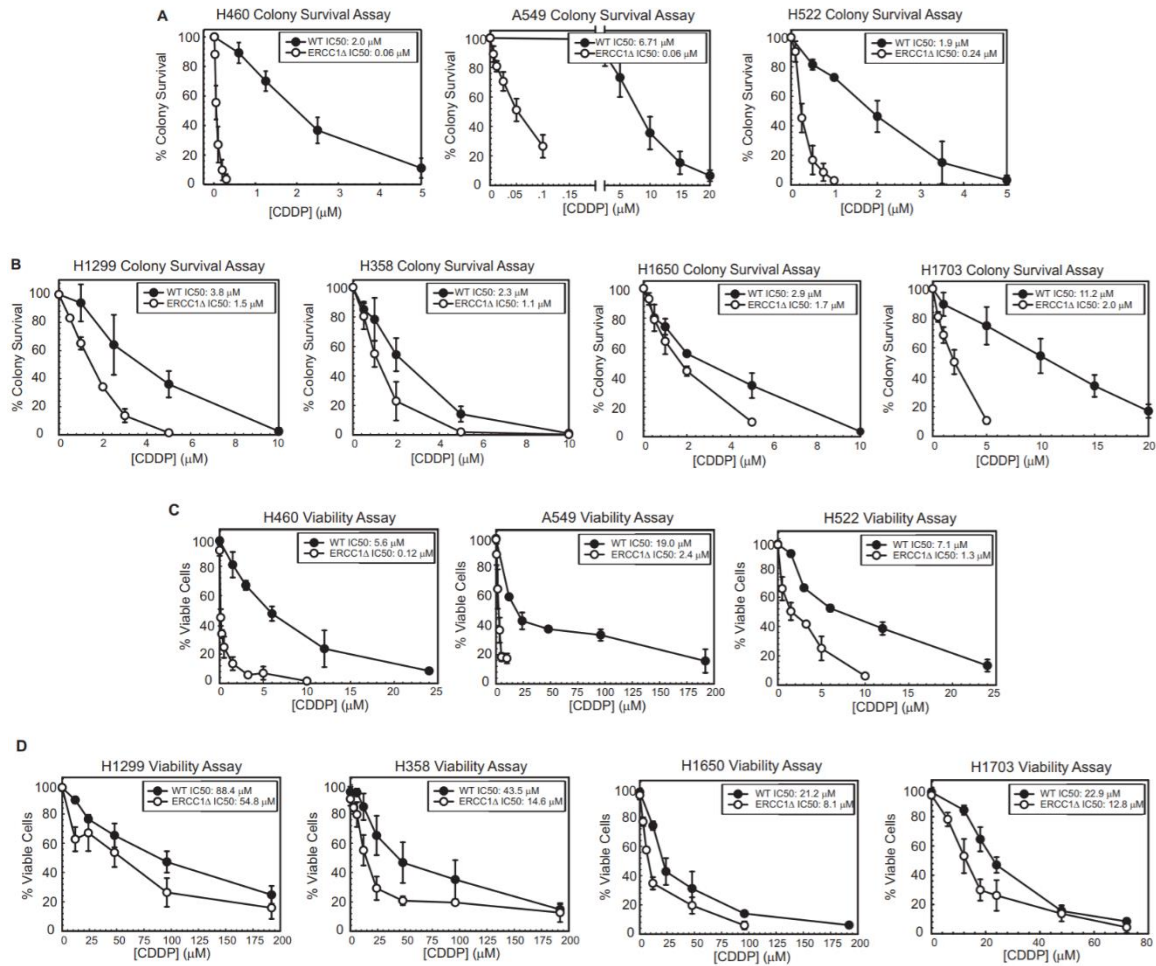
Figure 2.2 Clonogenic survival and viability after cisplatin treatment in ERCC1 wildtype and knockout cell lines. A. Clonogenic survival assays with cisplatin treatment in p53 WT cell lines ± ERCC1. **B.** Clonogenic survival assays with cisplatin treatment in p53-null and p53-mutant cell lines ± ERCC1. n = 3 independent experiments plated in triplicate for each cell line. Data plotted as average of at least three independent experiments ± SD. **C.** Viability assays with cisplatin treatment in p53 WT cell lines ± ERCC1. **D.** Viability assays with cisplatin treatment in p53-null and p53-mutant cell lines ± ERCC1. n = 3 independent experiments plated in triplicate for each cell line. Data plotted as average of at least three independent experiments ± SD.

A

Cell Line	p53 Status	EGFR Status	K-Ras Status
H460	WT/WT	WT	Q61H
H522	WT/WT	WT	WT
A549	WT/WT	WT	G12S
H1703	Mutant	WT	WT
H1650	Mutant	E746-A750del	WT
H1299	Null/Null	WT	WT
H358	Null/Null	WT	G12C

B

C H460 Colony Survival Assay
WT IC50: 2.0 µM
ERCC1Δ Clone #2 IC50: 0.06 µM

D H1299 Colony Survival Assay
WT IC50: 3.8 µM
ERCC1Δ Clone #2 IC50: 1.9 µM

E H1299 Colony Survival Assay
WT IC50: 3.6 µM
ERCC1Δ crRNA #2 IC50: 1.8 µM

F H1299 Colony Survival Assay
WT IC50: 3.8 µM
XPFΔ IC50: 1.3 µM

G H460 Colony Survival Assay
WT IC50: 2.1 µM
ERCC1Δ+202 IC50: 0.6 µM
ERCC1Δ IC50: 0.06 µM

H H1299 Colony Survival Assay
WT IC50: 4.8 µM
ERCC1Δ+202 IC50: 4.4 µM

Figure 2.3 Cell line characteristics, secondary knockout clones and re-expression of ERCC1-202. A. Cell lines utilized in the current study and status of p53, EGFR, and K-ras are listed. Mutation status was obtained from Cosmic Database (cancer.sanger.ac.uk) or cBIOportal (cbioportal.org) (except for H522 p53 status where Sanger sequencing did not identify the homozygous deletion that was previously reported. **B.** Western blot of additional ERCC1Δ clones in H460 and H1299 cells and the XPFΔ H1299 cells. Additional ERCC1Δ clones in this figure were validated by western blot and the XPFΔ clone was validated by sequencing. **C-F.** Colony survival assays of additional ERCC1Δ and XPFΔ clones. **G-H.** Western blot showing re-expression of ERCC1-202 in H460 and H1299 ERCC1Δ cells. Colony survival assay shows increased resistance to cisplatin with re-expression of ERCC1-202. n=3, plated in triplicate for each colony assay performed in this figure. Error bars represent SD of the averages of all experiments.

ERCC1 led to loss of XPF expression, because both factors generally require each other for loss of ERCC1 led to loss of XPF expression, because both factors generally require each other for stability. However, a self-dimerization–based mechanism for XPF stability in the absence of ERCC1 has been reported in biochemical studies and could explain why one H1299 ERCC1Δ clone did not have reduced XPF expression (Fig. 2.3 B; (33)). In addition, we received A549 ERCC1Δ cells for our investigations (Fig. 2.1 A).

Because ERCC1 is necessary for key aspects of NER, HR, and ICL-R, we expected that ERCC1 loss would hypersensitize cells to cisplatin and MMC. Interestingly, upon titration of cisplatin in clonogenic and viability assays, we saw two distinct phenotypes, hypersensitivity and modest tolerance. H522, A549, and H460 ERCC1Δ (p53^{WT}) cells were all very sensitive to cisplatin in both clonogenic (IC$_{50}$s ranging from 60 to 240 nmol/L) and viability assays (Fig. 2.2 A and C). These observations were validated in a second ERCC1Δ clone in H460 cells which showed the same hypersensitive phenotype (Fig. 2.3 B and C). Interestingly, loss of ERCC1 in H1650, H1703, H358, and H1299 cells (p53$^{null/mutant}$) only resulted in modest increased sensitivity to cisplatin in clonogenic (IC$_{50}$s ranging from 1.1 to 2.0 μmol/L) and viability assays (Fig. 2.2 B and D). These effects were validated with multiple ERCC1Δ clones developed with two crRNAs, and a XPFΔ clone in H1299 cells, suggesting this modest sensitivity is a true phenotype of loss of functional ERCC1/XPF (Fig. 2.3 B, D-F). We were able to fully restore resistance to cisplatin in H1299 ERCC1Δ cells and partially restore cisplatin resistance in H460 ERCC1Δ cells when ERCC1-202 was re-expressed (Fig. 2.3 G and H). We also observed this differential phenotype with MMC, a more potent inducer of interstrand crosslinks than cisplatin (Fig. 2.4 A and B). Conversely, we did not observe increased sensitivity of ERCC1Δ compared with ERCC1 WT cells with
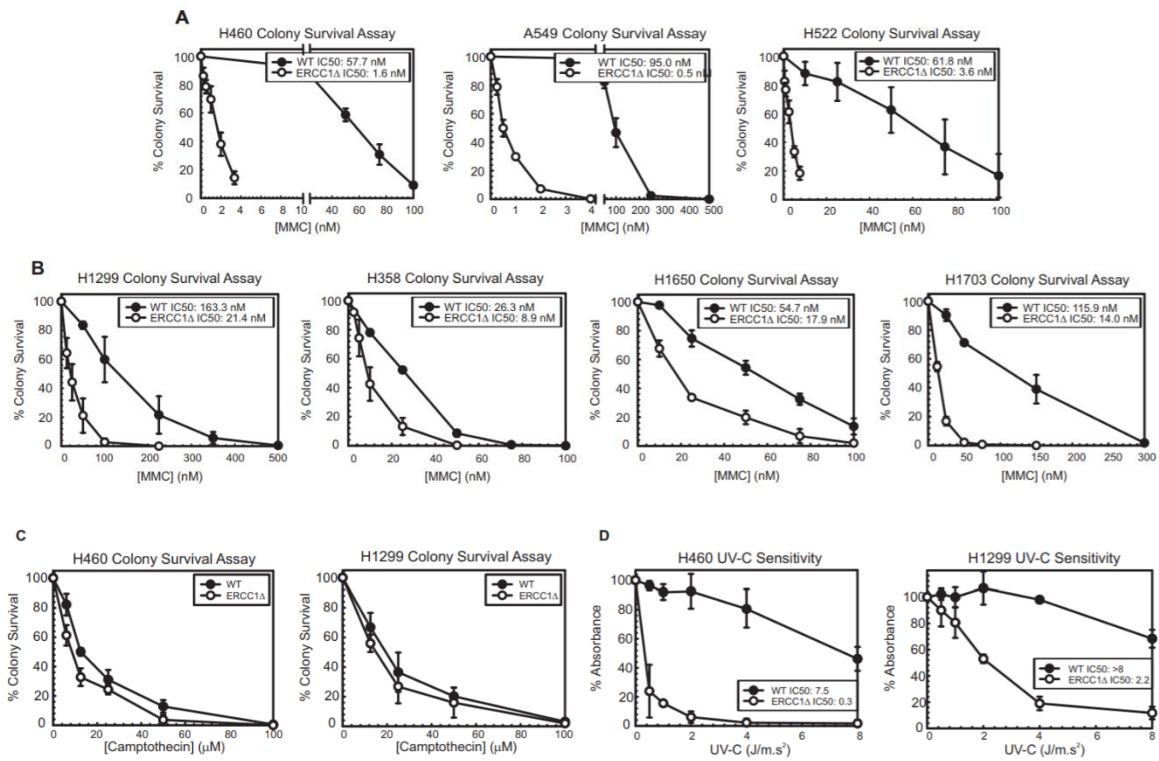
Figure 2.4. **Clonogenic survival after mitomycin C treatment in ERCC1 wildtype and knockout cell lines. A.** Clonogenic survival assays with MMC treatment in p53^{WT} cell lines ± ERCC1. **B.** Clonogenic survival assays with MMC treatment in p53-null and p53-mutant cell lines ± ERCC1. n=2, in triplicate for all colony survival assays with MMC treatment. Error bars represent ± SD. **C.** Clonogenic survival assays of H460 and H1299 WT and ERCC1Δ cells with camptothecin treatment. n=3, in triplicate. Error bars represent ± SD. **D.** UV-C sensitivity assays in H460 and H1299 WT and ERCC1Δ cells. n=2, in triplicate. Error bars represent ± SD.
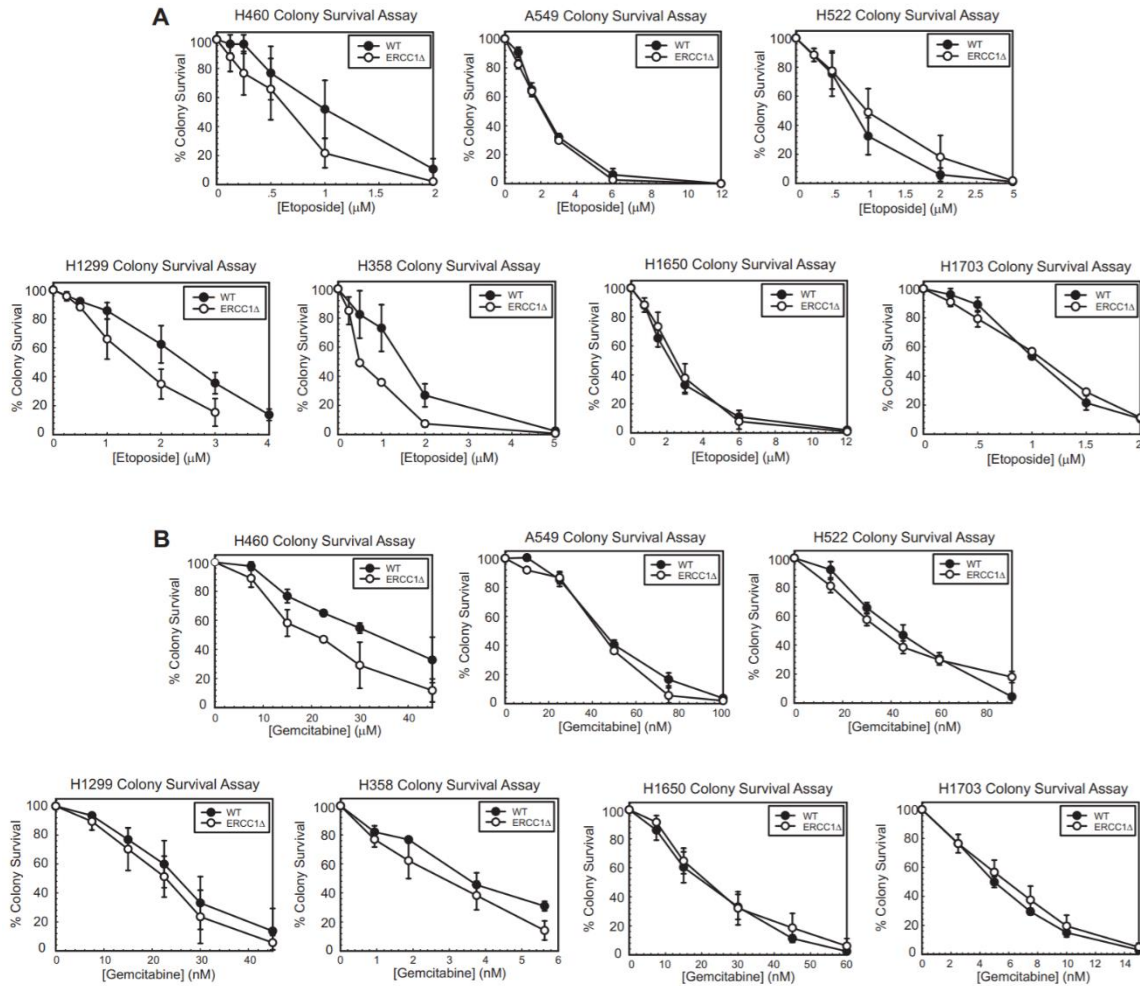
Figure 2.5 Clonogenic survival after etoposide or gemcitabine treatment in ERCC1 wildtype and knockout cell lines. A. Sensitivity of parental and ERCC1Δ cells to etoposide treatment in colony survival assays. n=2, plated in triplicate for each cell line. Error bars represent ± SD. **B.** Sensitivity of parental and ERCC1Δ cells to gemcitabine treatment in colony survival assays. n=2, plated in triplicate for each cell line. Error bars represent ± SD.

etoposide, gemcitabine or camptothecin in clonogenic assays, but both H460 and H1299 ERCC1Δ cells were sensitive to UV-C irradiation (Fig. 2.4 C and D; 2.5 A and B).

We observed that this differential phenotype appeared to be correlated with p53 status and so we performed clustering analysis based upon ERCC1 and p53 status. No differential clustering was observed in ERCC1 WT cells stratified by p53 status in the clonogenic survival or viability assays after cisplatin or MMC treatment (Fig. 2.1 B, D, and F). However, plotting all ERCC1Δ cell lines together displayed two distinct phenotypes that appeared to be correlated with p53 status, where p53^{WT}/ERCC1Δ cells were significantly more sensitive to cisplatin and MMC compared with p53$^{mutant/null}$/ERCC1Δ cells (Fig. 2.1 C, E, and G).

2.3.2 Altering p53 status alters the differential sensitivity of ERCC1Δ cells to cisplatin

The differential phenotype of ERCC1Δ cells to cisplatin and MMC appeared to be correlated with p53 status, and we hypothesized that altering p53 status could alter or reverse the observed phenotypes. To test this hypothesis, we overexpressed WT p53 in the p53-null H1299 cell line and assessed clonogenic potential after cisplatin treatment (Fig. 2.6 A; Fig. 2.7 A). We observed that expression of p53 in parental and ERCC1Δ cells increased sensitivity to cisplatin (WT: 4.4 μmol/L vs. 2.3 μmol/L and ERCC1Δ: 1.3 μmol/L vs. 0.4 μmol/L; Fig. 2.6 A). To address whether loss of p53 could increase tolerance of p53^{WT}/ERCC1Δ cells to cisplatin, we utilized CRISPR-Cas9 to disrupt the *TP53* gene in H460 and H522 parental and ERCC1Δ cells using a crRNA targeted to Exon 7 of *TP53*. Western blot analyses show loss of p53 in the H460 cell lines at steady-
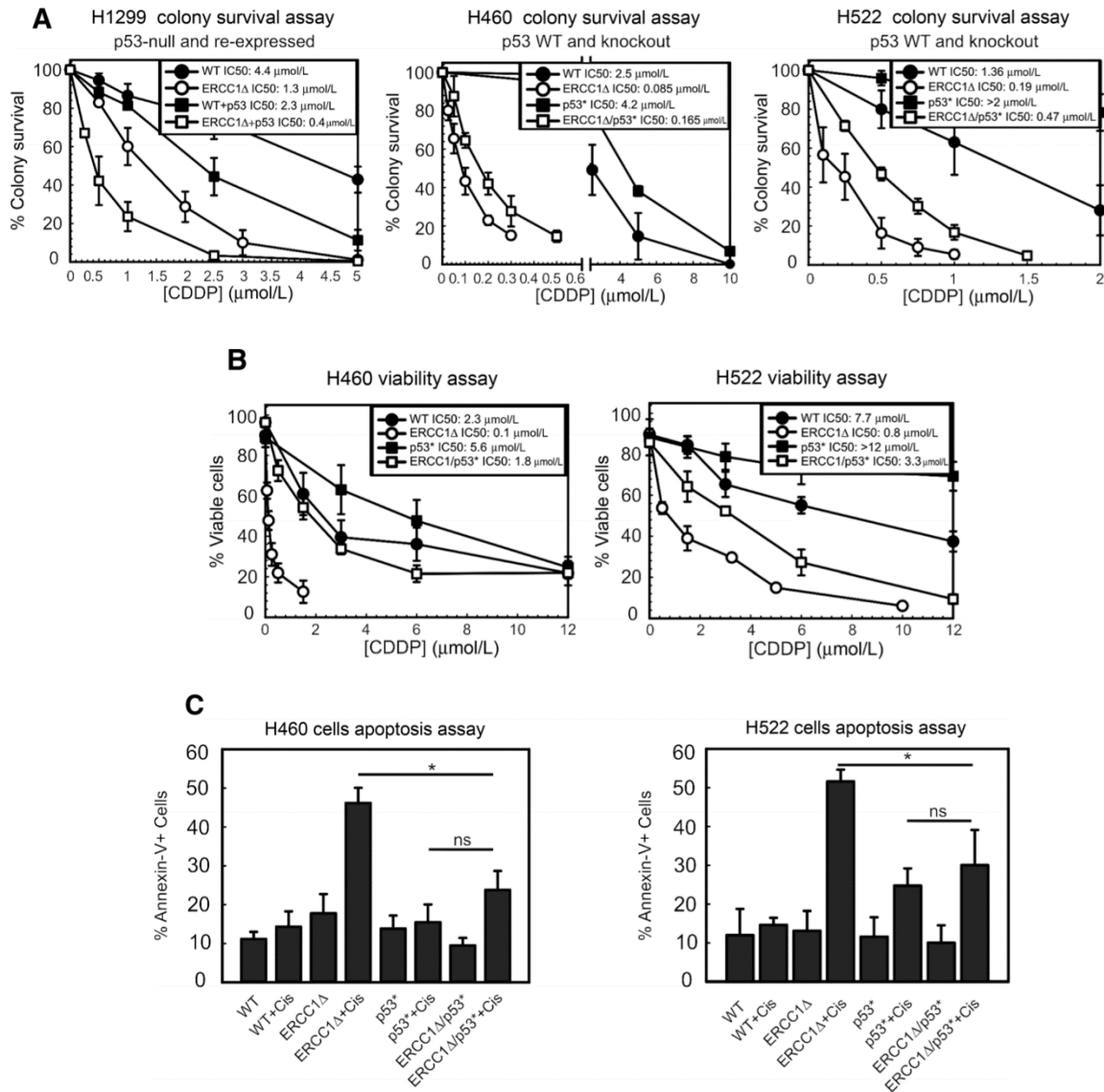
Figure 2.6 Effects of p53 on sensitivity of ERCC1Δ cells to cisplatin. A. Clonogenic survival after cisplatin treatment in H1299 (p53-null and p53 re-expressed), H460 (p53 WT and knockout), and H522 (p53 WT and knockout) isogenic cell lines differing by p53 and ERCC1 status. n = 3; data plotted as average of 3 independent experiments ± SD. **B.** Cisplatin viability assays of H460 and H522 isogenic cell lines treated with escalating doses of cisplatin., n = 3; data plotted as average ± SD. **C.** Compilation of data for H460 and H522 cells from 3 independent flow cytometry experiments representing % Annexin-V positive cells ± single-dose cisplatin treatment. Data represented as average % Annexin-V positive cells ± SD. *, p < 0.05 measured by 2-sided t test. NS, no significance, p > 0.05.

Figure 2.7 Western blots of p53 expression and sequencing results of p53 disruption by CRISPR-Cas9. A. p53 re-expression/disruption by CRISPR-Cas9 in H1299, H460, and H522 cells. **B.** Clonogenic assay of H460 ERCC1Δ and ERCC1Δ/p53* cells fixed at Day 6 and Day 12. **C.** p53 disruption by CRISPR-Cas9 in A549 cells. **D.** Clonogenic survival of A549 isogenic cells after treatment with cisplatin. n=3, plated in triplicate for each cell line. Error bars represent ± SD. **E.** Sequencing results of p53 editing in H460, H522, and A549 cells. **F.** Validation of ERCC1Δ in OV2008 and C13* cells by western blot. **G.** Induction of p53 after cisplatin treatment. **H.** Clonogenic survival of OV2008 and C13* cells after cisplatin treatment. n=2, plated in triplicate for each cell line. Error bars represent ± SD.

state levels and upon induction with Nutlin-3 (Fig. 2.7 A). In addition, we confirmed disruption of *TP53* by DNA sequencing (Fig. 2.7 E). In H460 ERCC1Δ/p53* cells, we observed modest increased clonogenicity (two-fold) after platinum treatment compared with ERCC1Δ alone in shorter-duration colony assays (Fig. 2.6 A). This fold difference could be dramatically enhanced (10-fold) by extending the length of the colony assay from 6 to 12 days (Fig. 2.7 B). Despite reports that H522 cells harbor a homozygous single-base deletion in codon 191 of the *TP53* gene, we were not able to detect this deletion when sequencing exons 5 and 6 of *TP53*. Therefore, for the purposes of this study, we considered the H522 cell line p53 WT. The p53-edited H522 cell lines were validated by sequencing which showed that the *TP53* alleles were disrupted by CRISPR-Cas9 in the H522 p53* cells, including an 8 amino acid in-frame deletion in 1 allele which would account for a slightly reduced molecular weight band near 50 kDa; we also observed the acquisition of a truncated p53 mutant near 25 kDa (Fig. 2.7 A and E). In H522 ERCC1Δ cells, *TP53* was partially disrupted (Fig. 2.7 E). This would be consistent with Western blot analysis results showing induction of p53 in the ERCC1Δ/p53* clone (Fig. 2.7 A). Partial *TP53* disruption in H522 cells also resulted in increased colony formation after cisplatin treatment in the ERCC1Δ cells (Fig. 2.6 A). Similar results were also observed in A549 WT and ERCC1Δ cells upon *TP53* disruption (Fig. 2.7 C-E).

We also assessed changes in viability of H460 and H522 isogenic cell lines with increasing doses of cisplatin by Trypan Blue live/dead assays. Strikingly, we saw that disruption of p53 in ERCC1Δ H460 cells increased the IC_{50} in viability assays >15-fold (100 nmol/L vs. 1.8 μmol/L; Fig. 2.6 B). In H522 cells, partial disruption of *TP53* in ERCC1Δ cells increased the IC_{50} in viability assays four-fold (0.8 μmol/L vs. 3.3 μmol/L; Fig. 2.6 B). We also performed flow cytometry-based analysis of apoptosis with H460

and H522 isogenic cells lines. All paired cell lines were treated for 24 hours with the IC$_{50}$ dose of the ERCC1Δ determined in the live/ dead assays and cells were allowed to grow for an additional 24 hours before proceeding with flow cytometry. In H460 and H522 ERCC1Δ cells, cisplatin treatment resulted in approximately 50% cell death as measured by the percent Annexin-V positive cells (Fig. 2.6 C). In ERCC1Δ/p53* cells, loss of p53 conferred significant protection from cisplatin-induced apoptosis (Fig. 2.6 C). In addition, the level of apoptosis observed in ERCC1Δ/p53* cells was not statistically different from p53* cells. These viability data appear to suggest that p53 loss is critical for limiting apoptosis in the presence of unrepaired ICLs with loss of ERCC1.

Next, we tested whether knockout of ERCC1 had differential effects on cisplatin sensitivity in the OV2008/C13* cell line model of cisplatin resistance. C13* cells exhibit increased levels of ERCC1 compared with OV2008 cells (Fig. 2.7 F). Although both cell lines possess WT p53, p53 induction in C13* cells is impaired and p53 is not stabilized upon platinum treatment (Fig. 2.7 G; (180, 181)). In clonogenic assays, we observe OV2008 ERCC1Δ cells are more sensitive to cisplatin than the C13* ERCC1Δ cells (Fig. 2.7 H). These data suggest that the differential phenotype may not be limited to p53 mutations but could be extended to include defects in p53 stability/induction.

2.3.3 Kinetics of the DNA damage response in ERCC1Δ cells

Our hypothesis regarding the role of p53 in this differential phenotype was that p53 predisposed repair-deficient cells to apoptosis and that loss of p53 promoted DNA damage tolerance. To assess general levels of DNA damage signaling in the ERCC1Δ cells, we performed a treatment time-course and measured levels of p53, CDKN1A (p21), PARP1 cleavage, and H2AX phosphorylation at various time points by Western blot analysis. In the cisplatin hypersensitive H460 and H522 ERCC1Δ cells, we saw

induction of PARP cleavage after treatment, consistent with the viability assays (Fig. 2.8 A). In addition, we saw induction of p53 and p21 over time which persisted (Fig. 2.8 A). Consistent with previously reported observations (55), we detected a large induction of γH2AX in the H460 and H522 ERCC1Δ cell lines which continued to the 48-hour time point indicating persistent, unrepaired DNA DSBs in the hypersensitive cells (Fig. 2.8 A). H1299 ERCC1Δ cells exhibited very little induction of cleaved PARP after treatment with cisplatin (Fig. 2.8 A). Unexpectedly, there was very little induction of γH2AX in H1299 ERCC1Δ cells compared with WT cells (Fig. 2.8 A), indicating either 1. DNA damage signaling is defective, or that 2. DSB repair is not defective in these cells. The former possibility is unlikely, considering cells defective in phosphorylation of H2AX are sensitized to DNA damaging agents such as ionizing radiation (182-184). This evidence suggests differential responses to DNA damage may contribute to the bimodal phenotype observed in our panel of ERCC1Δ cells.

We further confirmed γH2AX results from Western blot analysis by immunofluorescence. In H460 WT cells, cisplatin treatment did not result in increased γH2AX foci formation 48 hours post-cisplatin treatment, whereas in ERCC1Δ cells foci formation was dramatically increased (Fig. 2.8 B). These data would suggest that DSB formation during ICL-R is at least partially independent of ERCC1/XPF activity. This would be consistent with previous reports in ERCC1-deficient cells showing other endonucleases are capable of the initial incision steps of ICL-R including Mus81 and Fan1 (reviewed in (57)). In H460 ERCC1Δ/p53* cells, we observed a significant reduction in the number of γH2AX foci present 48 hours after treatment (Fig. 2.8 B). Conversely, in cisplatin-tolerant H1299 ERCC1Δ cells we observed very few γH2AX foci
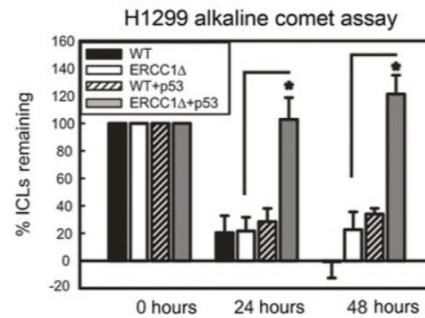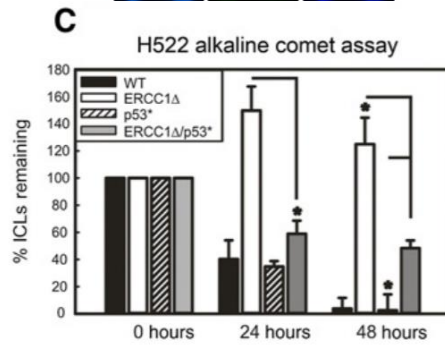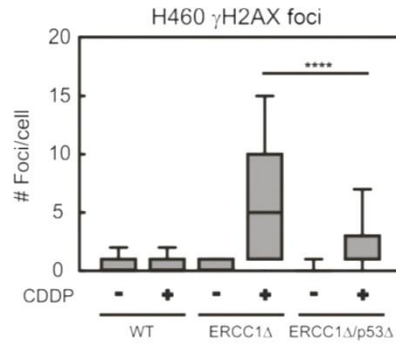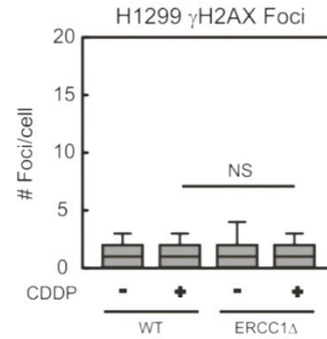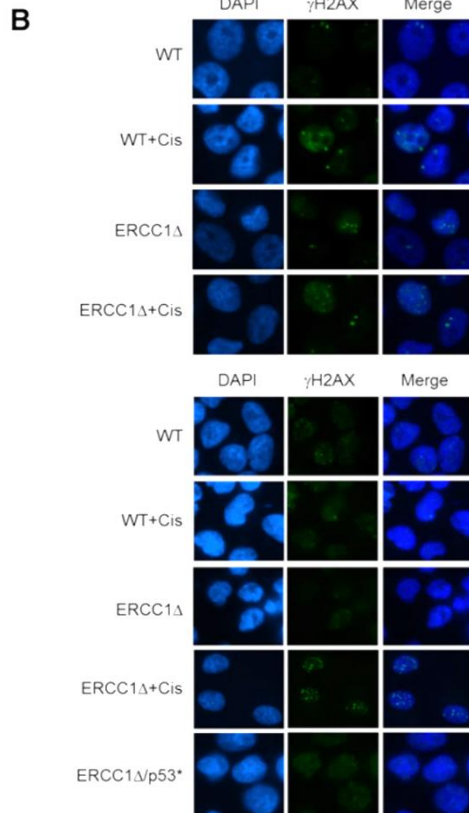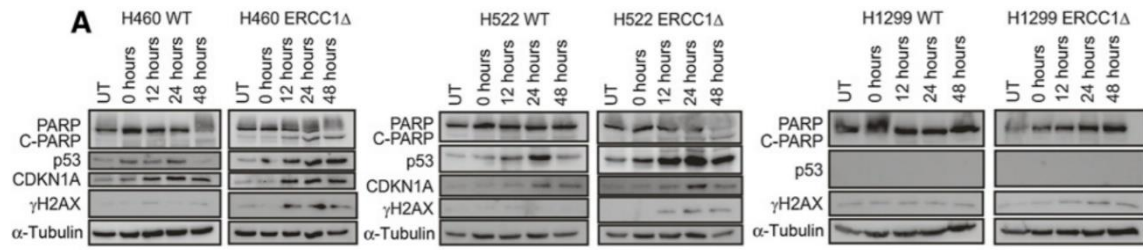
Figure 2.8 Differential DNA damage signaling and interstrand crosslink repair in ERCC1Δ cells. A. Western blot analysis of a cisplatin treatment time course measuring induction of cleaved PARP, γH2AX, p53, and p21 up to 48 hours in H460, H522, and H1299 WT and ERCC1Δ cells. **B.** Images and quantification of one representative experiment showing γH2AX foci formation in H1299 and H460 cells 48 hours post-cisplatin treatment. ****, $P < 0.0001$ as measured by Wilcoxon rank-sum test; experiments performed 3 times. **C.** Modified alkaline comet assay data indirectly measuring ICL-R in H522 and H1299 cells. Data presented as mean of 3 independent experiments. Error bars represent SEM. *, $p < 0.05$ as measured by Student t test.

at 48 hours post-cisplatin treatment likely suggesting that ICL-R is largely not defective in these cells (Fig. 2.8 B).

Cisplatin is a bifunctional drug, which induces ISAs between guanine residues on the same strand of DNA and these structures, which are repaired through NER, represent >90% of the damage caused by cisplatin whereas ICLs represent approximately 1% to 5% of total DNA adducts generated by cisplatin. We suspected that ISAs, which should persist in ERCC1Δ cells, may be less toxic than ICLs which can function as complete replication blocks. To tease apart whether the modest sensitivity we observe in H1299 ERCC1Δ cells in clonogenic assays is due to unrepaired ISAs, we generated XPAΔ clones in H1299 cells (Fig. 2.9 A and D). XPA's only described function is to act as a scaffolding protein during NER, and XPA-deficient cells are less sensitive to MMC than ERCC1-deficient cells (61). So, XPAΔ cells should display the relative contribution of unrepaired ISAs in H1299 cells. In clonogenic assays, XPAΔ cells display the same sensitivity to cisplatin as ERCC1- or XPF-deficient cells, strongly pointing to the modest sensitivity observed as the relative contribution of unrepaired ISAs (Fig. 2.9 B and E). We also measured sensitivity to MMC, which induces monoadducts and a higher level of ICLs than cisplatin. We observed a classic phenotype, where ERCC1 and XPF knockout cells were 2.5-fold more sensitive to MMC than XPAΔ cells (Fig. 2.9 C). We hypothesize that the relative amount of ICLs compared with the total amount of DNA damage may impact this differential phenotype with ERCC1 deficiency. To assess differences in ICL-R between our isogenic cell lines, we performed modified alkaline comet assays in the H522 and H1299 isogenic cell lines. Although this assay is an indirect measure of interstrand crosslinked DNA, it is commonly used to measure
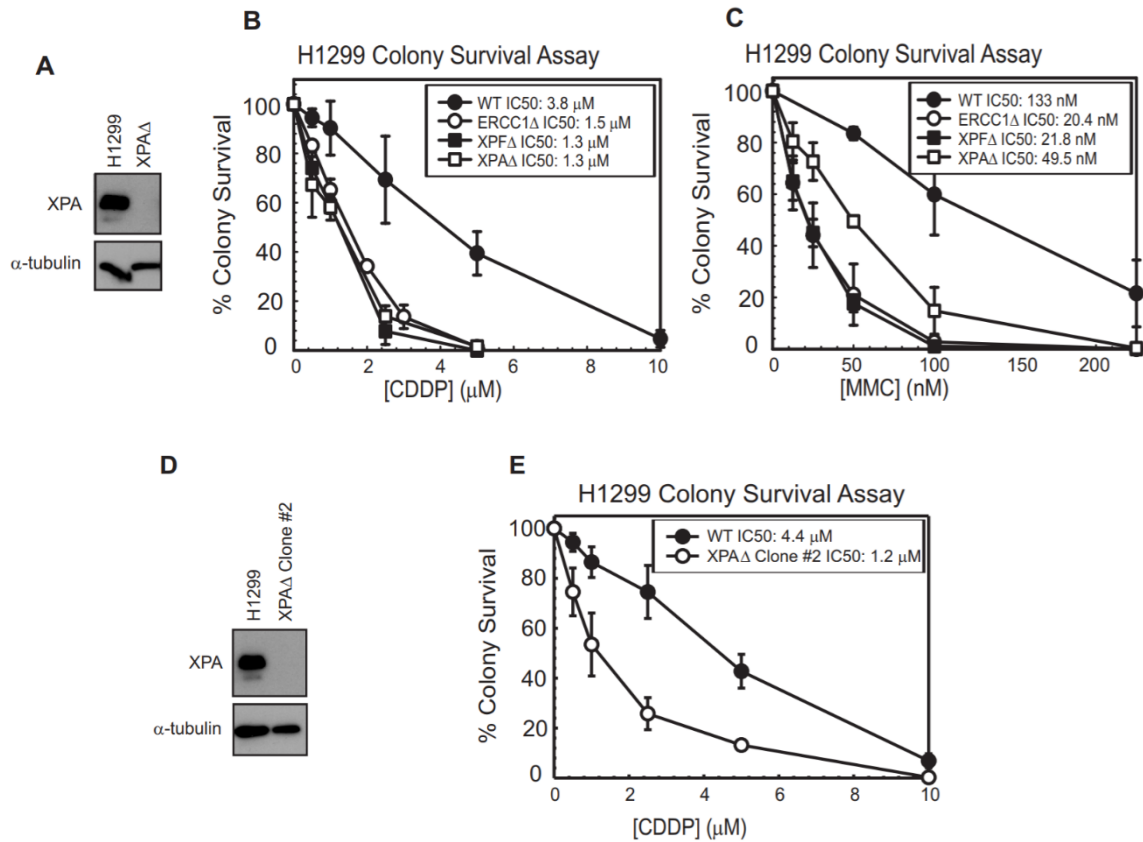
Figure 2.9 Sensitivity of XPA knockout cells to cisplatin and mitomycin C. A. Western blot validation of XPA knockout by CRISPR-Cas9. Colony survival assay of H1299 WT, ERCC1Δ, XPFΔ, and XPAΔ after **B.** cisplatin and **C.** MMC treatment. **D.** Validation of second XPAΔ clone by western blot. **E.** Colony survival assay of H1299 WT and second XPAΔ clone with cisplatin treatment.

platinum ICL-R. H1299 cells were treated with 5 µmol/L and H522 cells with 1.5 µmol/L cisplatin for two hours followed by measurements of ICL-R at the 0- (immediately after treatment), 24-, and 48-hour timepoints. Despite attempts to perform these analyses with H460 isogenic cell lines, the ERCC1Δ cells were too sensitive to cisplatin to observe significant differences between untreated and treated samples at the 0-hour time point when treated with 500 nmol/L cisplatin, making it impossible to accurately monitor ICL DNA repair via this assay. As we expected, H522 ERCC1Δ cells were not capable of ICL-R (Fig. 2.8 C). In H522 ERCC1Δ/p53* cells, ICL-R was at least partially rescued where there was no difference compared with WT or p53* cells at the 24-hour time point, but statistically greater amounts of ICL DNA damage remained at 48 hours posttreatment relative to p53* cells and less amounts of damage remained relative to ERCC1Δ cells (Fig. 2.8 C). This observation would be consistent with partial disruption of *TP53* in these cells. Consistent with the DNA damage signaling we observed in H1299 ERCC1Δ cells, no delay in ICL-R compared with H1299 WT cells was detectable (Fig. 2.8 C), however, re-expression of p53 in H1299 ERCC1Δ cells induced a near-complete block of ICL-R compared with parental cells (Fig. 2.8 C).

2.3.4 Cell-cycle arrest profiles differ in ERCC1Δ cells after cisplatin treatment

Many reports with ERCC1 knockout and knockdown cells have shown that after treatment with a crosslinking agent there is a potent G_2–M cell-cycle arrest which has been attributed to unrepaired DNA damage. To test whether p53 status affected cell-cycle arrest after treatment with cisplatin, we assessed cell-cycle profiles in a time course after treatment. Although the p53 null H1299 cells exhibited no distinct G_2–M arrest after platinum treatment, we consistently observed a slight increase in G_2–M arrest in the H1299 ERCC1Δ cells at the 24-hour time point, which resolved by the 48-

A

H1299 WT

H1299 ERCC1Δ

Untreated
24 hours
48 hours
72 hours

PI-A

B

H460 WT

H460 ERCC1Δ

H460 ERCC1Δ/p53*

PI-A

C

G₂–M quantification post-cisplatin treatment

% Cells in G_2–M

H1299 WT   H1299 ERCC1Δ   H460 WT   H460 ERCC1Δ   H460 ERCC1Δ/p53*
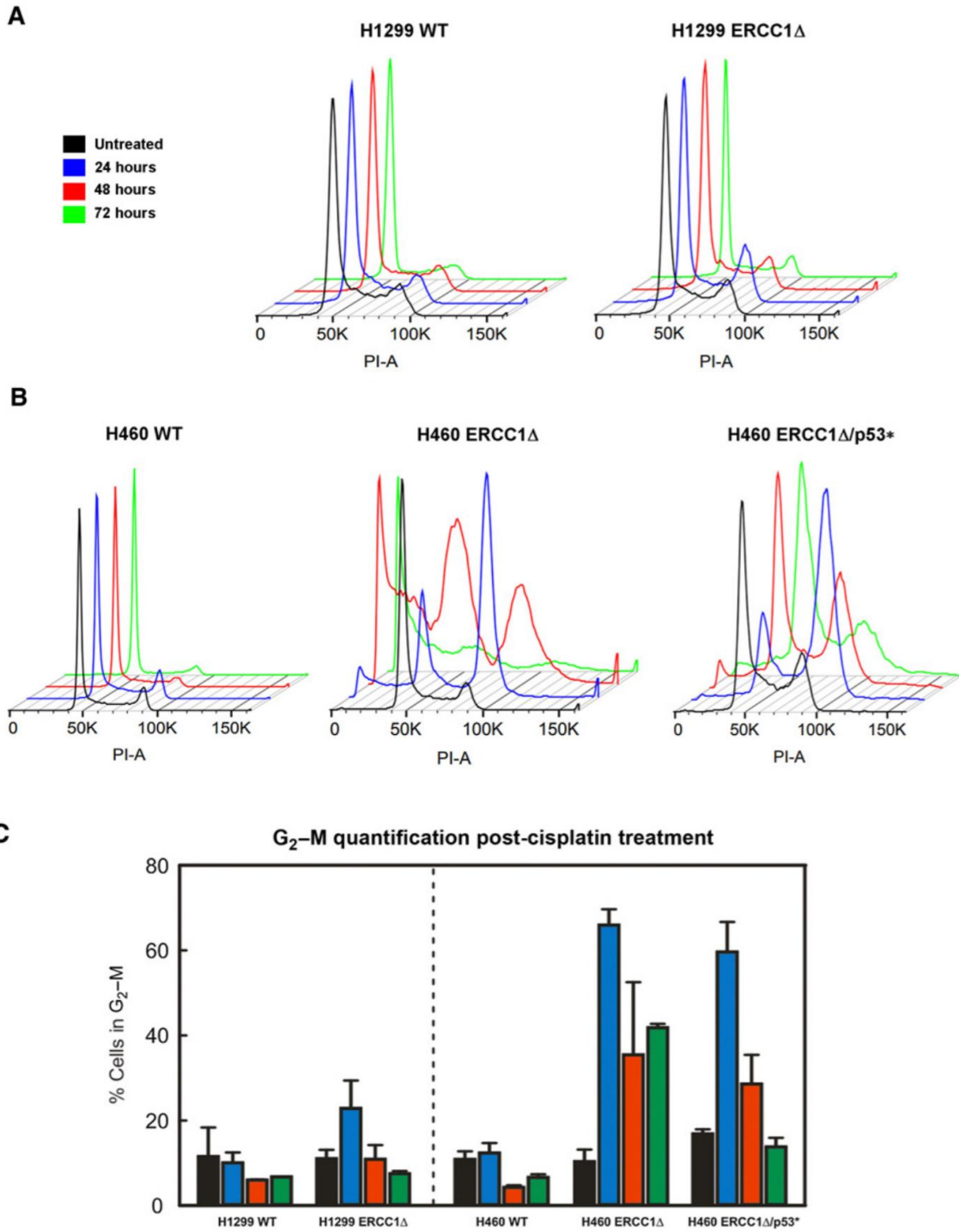
Figure 2.10 Cell-cycle profiles after cisplatin treatment in ERCC1Δ isogenic cell lines. Representative data from flow cytometry experiments measuring cell cycle profiles in **A.** H1299 and **B.** H460 isogenic cells at varying time points after cisplatin treatment (n = 2 for each sample). **C.** Quantification of the percent of cells in G_2–M phase following cisplatin treatment. Analysis excludes the sub-G_1 population of cells from the quantification.

hour time point (Fig. 2.10 A and C). Conversely, in H460 ERCC1Δ cells, we observed a potent G_2–M arrest 24 hours post-cisplatin treatment (Fig. 2.10 B and C). By 48 hours post-treatment, we detected a sharp increase in a sub-G_1 population consistent with an increase in cell death. In the H460 ERCC1Δ/p53* cells, we observed the same potent G_2–M arrest that we observed in H460 ERCC1Δ cells at 24 hours post-treatment (Fig. 2.10 B and C). Astonishingly, by 72 hours after treatment, we saw a near-complete recovery from G_2–M arrest with only a minor increase in the sub-G_1 population. We hypothesize that unrepaired DNA damage leads to G_2–M arrest but that this G_2–M arrest is not permanent. Eventually cells enter into M-phase and subsequently into G_1 phase where the presence of DNA DSBs triggers p53-mediated cell death. However, in the absence of p53, cells are either capable of tolerating unrepaired DNA crosslink damage or alternate repair mechanisms may exist that can at least partially compensate for loss of ERCC1.

2.3.5 p53 status may act as a confounding variable in clinical assessments of ERCC1 as a platinum biomarker

The potential for utilizing ERCC1 expression to predict clinical response to platinum-based chemotherapy has been extensively tested in multiple cancer types including lung and ovarian cancers with varying results (13, 163, 185, 186). We wanted to assess whether p53 status may be a confounding variable. Utilizing the TCGA lung adenocarcinoma data set, we split patients into two groups; those whose tumors had WT *TP53* and those whose tumors had any amino acid-changing mutation in *TP53*. Although we did not observe any significant difference in ERCC1 expression between groups ($p = 0.156$), when we stratified WT p53 tumors based upon ERCC1 high or low expression, we observed a significant 50% increase in median OS for patients with low ERCC1 (Fig.
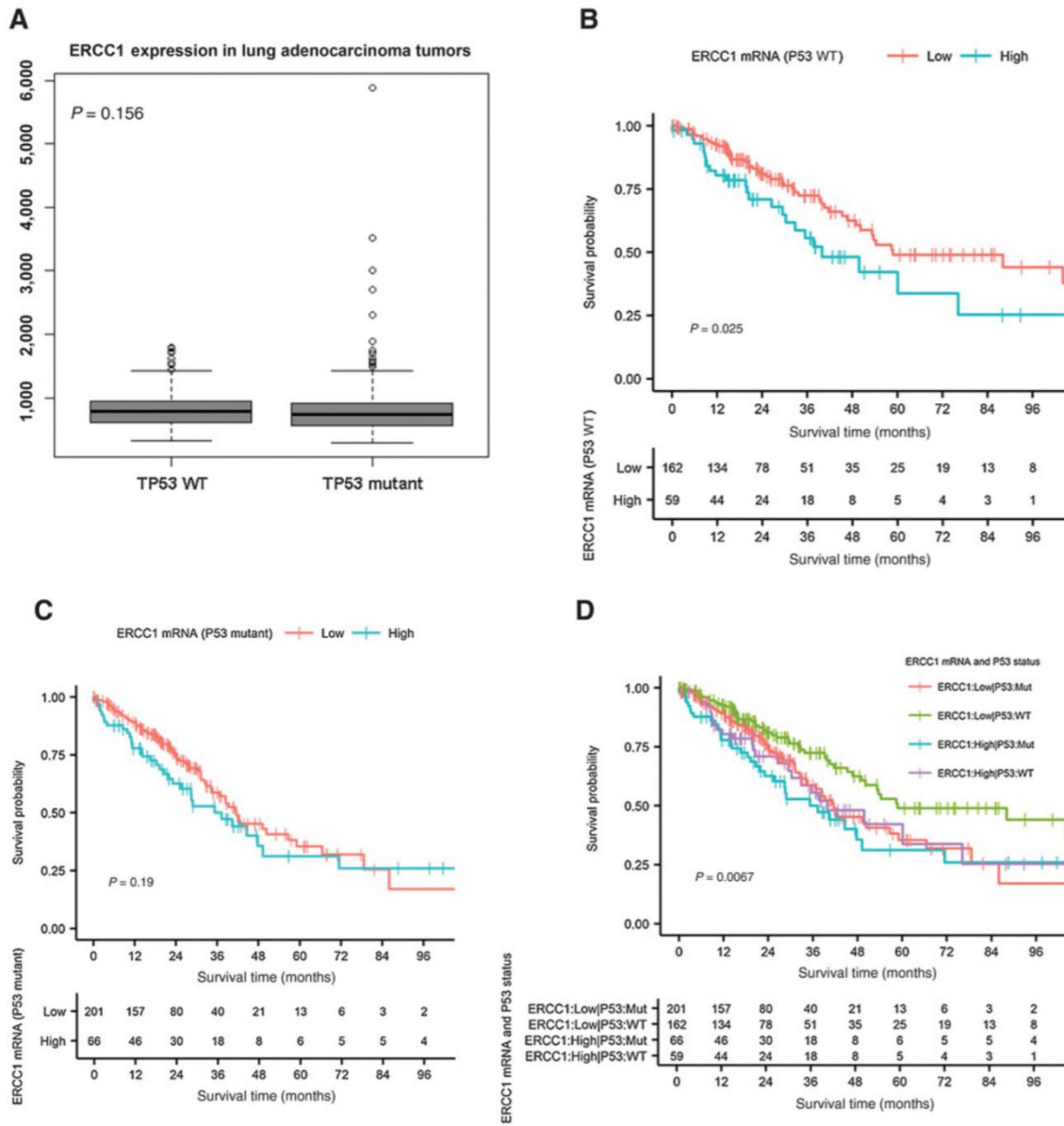
Figure 2.11 ERCC1 expression and p53 status in relation to OS in the TCGA lung adenocarcinoma data set. A. Expression of ERCC1 in lung adenocarcinoma tumors delineated by p53 status. Data compared by Student t test. OS of lung adenocarcinoma patients whose tumor harbored **B.** WT p53 and stratified by ERCC1 expression, or **C.** mutated p53 and stratified by ERCC1 expression. **D.** Combined model of OS of patients with lung adenocarcinoma accounting for p53 status and ERCC1 expression.

Figure 2.12 ERCC1 expression and p53 status in relation to OS in ovarian serous cystadenocarcinoma. Top: Progression Free Survival of Stage 3+4 ovarian cancer patients stratified by p53 status and ERCC1 expression who received a platinum agent. **Bottom:** Overall Survival of Stage 3+4 ovarian cancer patients stratified by p53 status and ERCC1 expression who received a platinum agent. Data obtained from the 2017 TCGA Ovarian Cancer Data Set from kmplot.com/ovca.

2.11 A, B, and D). However, in patients whose tumors had p53 mutations, no significant increase in median OS for patients with low compared with those with high ERCC1 was observed (Fig. 2.11 C and D). Although TCGA lung adenocarcinoma treatment data are not publicly available, nearly 100% of patients with lung adenocarcinoma receive a platinum agent during the course of treatment, and so we hypothesize that these data are contingent upon platinum treatment. We also corroborated these results in the TCGA ovarian cancer data set in terms of both progression-free and OS specifically in the context of platinum treatment (Fig. 2.12).

We also tested whether ERCC1 expression predicted OS in terms of response to platinum-based chemotherapy depending upon *KRAS* status (a common driver gene in non-small cell lung cancer) as there was a recent observation that *KRAS* status predicted platinum response in pancreatic cancer (187). *KRAS* status itself was not predictive in our TCGA lung adenocarcinoma data set (p = 0.46). Importantly, *KRAS* mutations were found to be mutually exclusive with *TP53* mutations (p < 0.001), demonstrating that in most cases *KRAS* mutations occur in *TP53* wildtype specimens and *vice versa TP53* mutations occur in *KRAS* wildtype specimens. In ovarian serous cystadenocarcinoma *TP53* mutations and *KRAS* mutations also had a tendency toward mutual exclusivity (p = 0.184) but a detailed study on this would need additional statistical power considering *TP53* mutations in ovarian cystadenocarcinoma occur in approximately 90% of tumors. These observations are directly opposed to pancreatic adenocarcinoma, where KRAS and TP53 mutations significantly co-occur (TCGA and QCMG; p < 0.001). This constitutes a major difference between these tumor types and has direct implications for our study assessing ERCC1 expression and *TP53* mutational status in lung adenocarcinoma and ovarian cystadenocarcinoma. ERCC1 did retain its

observed effects on prognosis when accounting for KRAS mutation status in the TCGA cohort (p = 0.0008). We observed a significant difference in survival in terms of ERCC1 expression in the *KRAS* mutant group, which happens to be overwhelmingly *TP53* wildtype. Thus, the *KRAS* and ERCC1 analysis is confounded by *TP53* status. Due to the mutual exclusivity of *TP53* mutations and *KRAS* mutations, stratification of the *KRAS* sample into ERCC1 high/low and *TP53* mutant and wildtype was not feasible with adequate statistical power. This data suggests that to investigate the effects of ERCC1 and *TP53* mutation status in the context of *KRAS* mutations at the population level, a separate study would need to target a substantial enrollment of *KRAS* mutant cancers due to the relative rarity of *TP53* mutations in these specific cancers. Additionally, we did not specifically test the effects of including BRCA1/2 mutation status in our analysis; however, BRCA1/2 mutations are generally observed in a p53 mutant context where we did not observe a significant benefit for patients with low ERCC1 in the context of OS.

2.3.6 Mechanistic characterization of ICL tolerance with ERCC1-deficiency

We hypothesized that in a p53 mutant/null background where apoptosis and G_1 checkpoint activation are diminished, alternate repair mechanisms may exist to deal with the damage from unrepaired ICLs that accumulate as result of loss of ERCC1. It is well documented that ERCC1/XPF activity is critical for ICL-R in G_1 phase, where replication-dependent processes are not available for dealing with ICLs, so we tested whether transient inhibition of entry into S phase could sensitize ICL-tolerant ERCC1Δ cells to cisplatin. Palbociclib alone inhibited growth of H1299 WT and ERCC1Δ cells and corresponded with an increase in the percentage of cells in G_1 phase compared with untreated cells (Fig. 2.14 C and D). For combination treatment experiments, we treated cells with cisplatin followed by 24-hour treatment with the CDK4/6 inhibitors, palbociclib
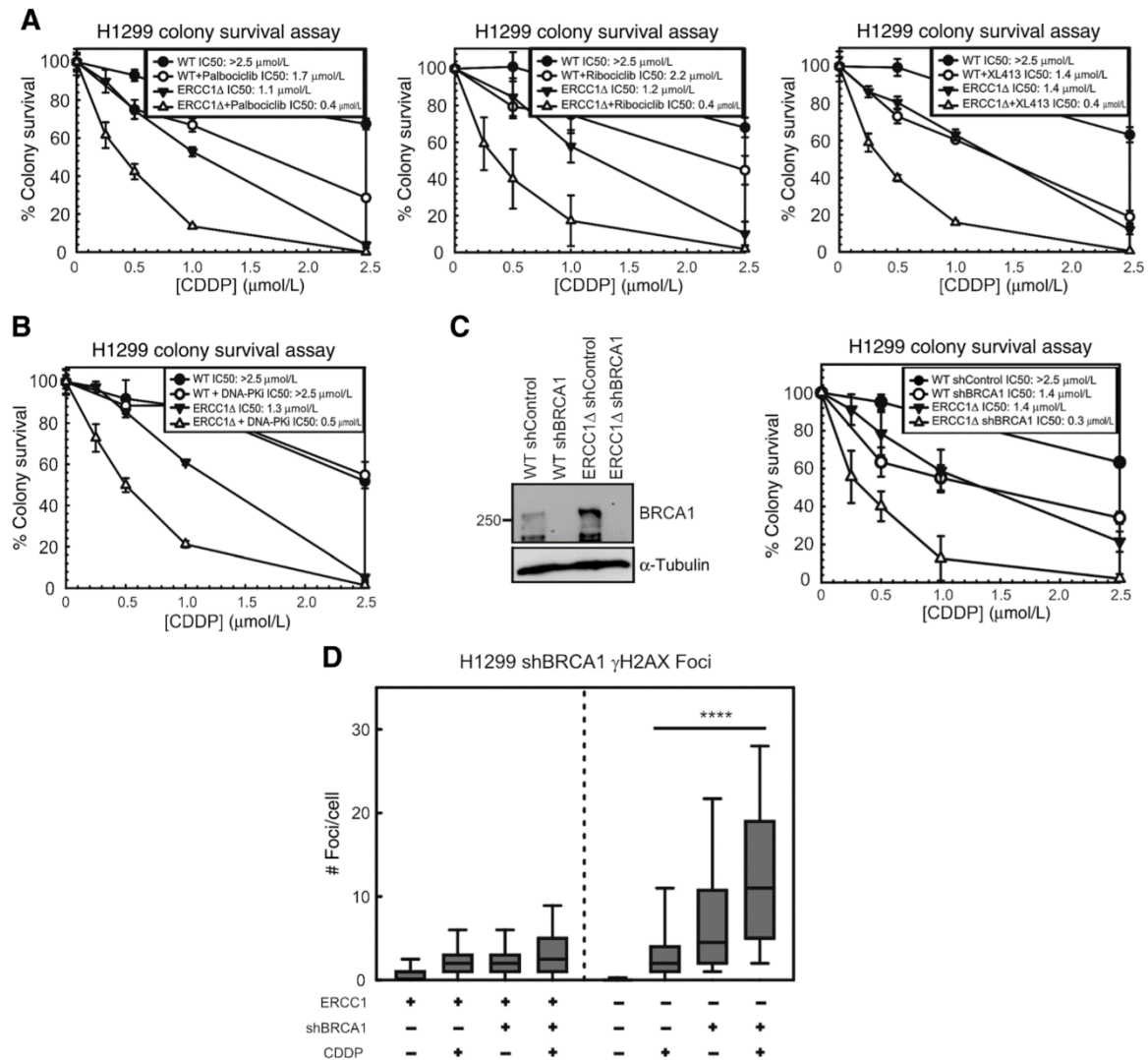
Figure 2.13 Molecular pathways contributing to cisplatin tolerance in p53-null cells with ERCC1 deficiency. **A.** Clonogenic survival assays of H1299 WT and ERCC1Δ cells treated with cisplatin and palbociclib, ribociclib, or DBF4-dependent kinase inhibitor. Left: Plot depicts one representative experiment (n = 3). Middle: Plot represents average of 3 independent experiments. Right: Plot represents 1 representative experiment (n = 3). **B.** Clonogenic survival of H1299 isogenic cells treated with cisplatin ± NU7441 (DNA-PKcs inhibitor; n = 3). **C.** Western blot analysis showing BRCA1 knockdown and clonogenic assays of H1299 WT and ERCC1Δ with shControl and shBRCA1 knockdown. **D.** Quantification of γH2AX foci formation 48 hours post-cisplatin treatment in H1299 WT and ERCC1Δ BRCA1 knockdown cells ± cisplatin treatment. Data are representative of 2 independent experiments. ****, P < 0.0001 as measured by Wilcoxon rank-sum test.

and ribociclib. We observed that H1299 WT and ERCC1Δ cells could be sensitized to cisplatin in clonogenic assays even with transient inhibition of CDK4/6 activity (Fig. 2.13 A; Fig. 2.14 B), which was very similar to what we observed with re-expression of p53 (Fig. 2.6 A). The addition of palbociclib to hypersensitive H460 or H522 ERCC1Δ cells did not further enhance cisplatin sensitivity, although there were small increases in sensitivity for the parental cell lines (Fig. 2.14 A and B). Furthermore, blocking replication initiation in H1299 ERCC1Δ cells via inhibiting the DBF4-dependent kinase (DDK) with the inhibitor, XL413, could also sensitize to cisplatin (Fig. 2.13 A). We take this to suggest that in hypersensitive ERCC1Δ cells, ICL-R is completely dependent upon ERCC1/XPF activity whether or not cells are in G_1 or S–G_2–M phases of the cell cycle. However, the increased sensitivity of H1299, H460, and H522 WT cells with CDK4/6 or DDK inhibition may indicate that timely entry into S-phase is also critical for supporting platinum resistance despite being DNA repair proficient. This requirement for S-phase entry appears to be exacerbated in p53-null H1299 ERCC1Δ cells where platinum sensitization by CDK4/6 or DDK inhibition indicates that ERCC1/XPF activity is critical for ICL-R in G_1 phase in ICL-tolerant cells, and that entry into S-phase may lead to ERCC1/XPF-independent mechanisms for tolerating or repairing ICL-DNA damage. Next, we tested whether factors involved in nonhomologous end joining (NHEJ) and HR supported the tolerance observed in H1299 ERCC1Δ cells. Inhibition of DNA-PKcs activity with the inhibitor, NU7441, selectively increased sensitivity of ERCC1Δ H1299 cells (1.3 μmol/L vs. 0.5 μmol/L), but not parental cells, to cisplatin (Fig. 2.13 B). In addition, we performed shRNA knockdown of BRCA1 in H1299 cells and assessed clonogenicity after cisplatin treatment. BRCA1 knockdown led to increased sensitivity in both H1299 WT and ERCC1Δ cells, consistent with critical roles for BRCA1 in regulating
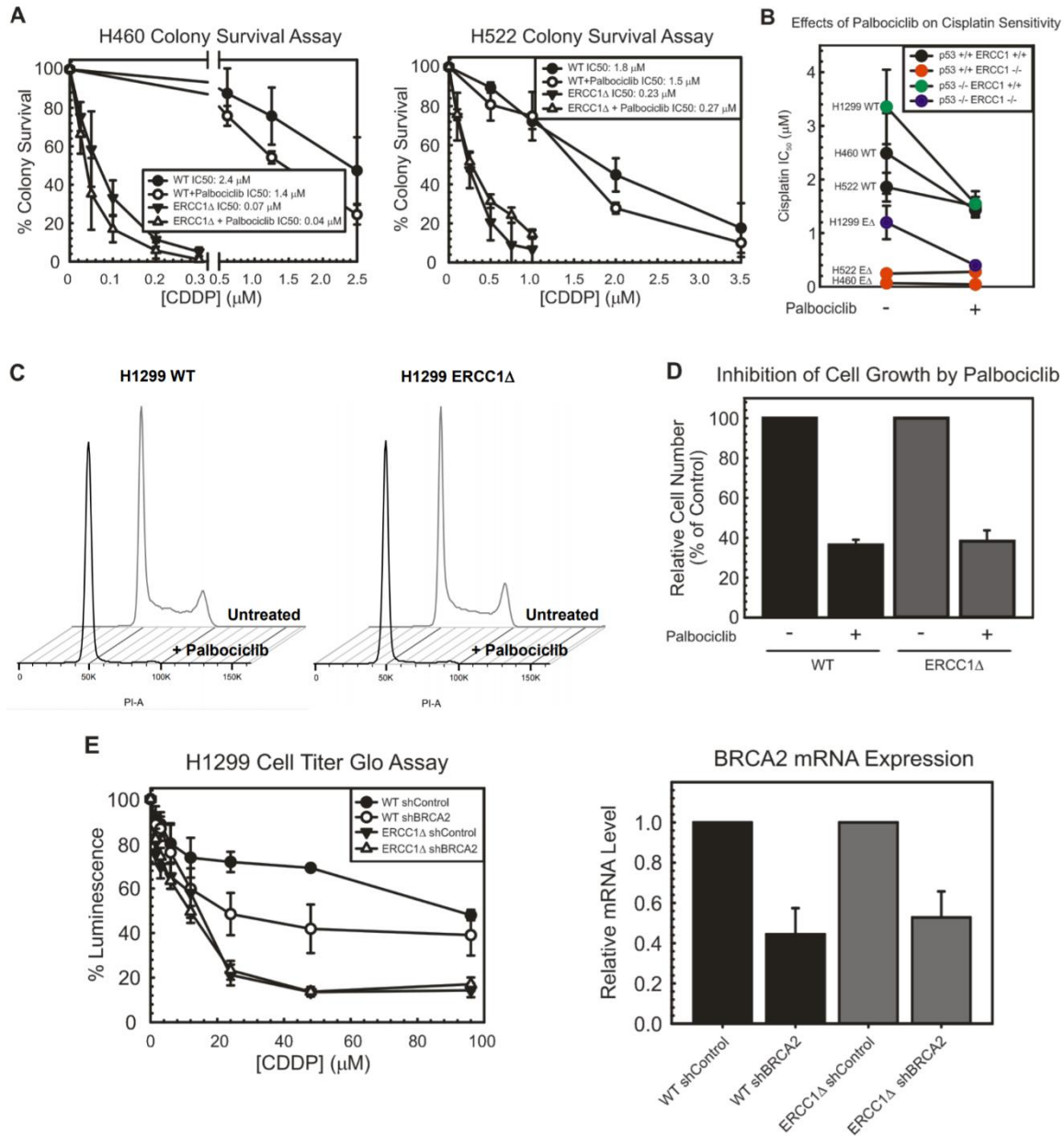
Figure 2.14 Sensitivity of ERCC1 knockout/p53 wildtype cells to CDK4/6 inhibition and effects of BRCA2 knockdown on H1299 sensitivity to cisplatin. A. Treatment of H460 and H522 cells with palbociclib in clonogenic survival assays. n=3, plated in triplicate for each cell line. Error bars represent ± SD. **B.** Effects of palbociclib treatment on sensitivity to cisplatin in H460, H522, and H1299 WT and ERCC1Δ cell lines. **C.** Cell cycle profiles of H1299 WT and ERCC1Δ cells with and without 48-hour treatment with palbociclib (representative from 2 independent experiments). **D.** Relative cell number of untreated and palbociclib treated H1299 WT and ERCC1Δ cells. **E.** Cell Titer Glo Assay with shControl and shBRCA2 H1299 WT and ERCC1Δ cells and transcript expression analysis via qRT-PCR showing knockdown of BRCA2 transcript levels. For all clonogenic survival assays: n=3, plated in triplicate for each cell line. Error bars represent ± SD.

DSB end-resection and contributing to HR, translesion synthesis, and microhomology-mediated end joining (Fig. 2.13 C). Interestingly, the effects of BRCA1 knockdown in sensitizing ICL-tolerant ERCC1Δ cells to cisplatin appear to be independent of BRCA2 as we only observed increased sensitivity in WT cells, but no increased sensitivity of ERCC1Δ cells to cisplatin (Fig. 2.14 E). Furthermore, BRCA1 knockdown led to a significant increase in the presence of γH2AX foci persisting 48 hours post-cisplatin treatment in the H1299 ERCC1Δ cells treated with cisplatin compared with ERCC1Δ alone (Fig. 2.13 D). Although the mechanism underlying ICL-tolerance in a subset of ERCC1Δ cells is not entirely parsed out, it appears that this tolerance is dependent upon DNA-PKcs and BRCA1 function, but likely independent of BRCA2.

2.4 Discussion

A recent international randomized phase III clinical trial utilizing ERCC1 expression to predict response to platinum-based chemotherapy did not show clinical benefit for patients with non–small cell lung cancer with low ERCC1 who received a platinum agent (163, 185). In addition, a preclinical study failed to show any correlation between pretreatment ERCC1 expression in ovarian cancers and response to platinum-based chemotherapy (186). Here, we showed that our *in vitro* data may have direct clinical implications where we observed a clinical benefit for patients with lung adenocarcinoma and ovarian carcinoma with low ERCC1 only when WT p53 was retained. These data may provide an additional explanation for conflicting results from clinical studies as to the benefit of using ERCC1 expression to predict responders to platinum-based chemotherapy. Our data may have the greatest impact in cancer types where the p53 mutation rate is markedly high, such as lung adenocarcinoma (50% p53

mutant) and ovarian serous carcinoma (90%), where ERCC1 has been investigated as a platinum biomarker.

In this study, we characterized a panel of ERCC1Δ lung cancer cell lines. We identified a differentially sensitive phenotype of ERCC1Δ lung cancer cell lines that appears to be at least partially associated with p53 status. If cells harbored WT p53, the ERCC1 deletion clones exhibited hypersensitivity to crosslinking agents, whereas the p53$^{mutant/null}$ cell lines exhibited mild sensitivity. Viability after cisplatin treatment of ERCC1Δ cells was dramatically increased by disrupting p53 by CRISPR-Cas9. However, clonogenicity of ERCC1Δ cells increased by disrupting p53 whereas sensitivity was increased in ERCC1Δ/p53^{null} cells following expression of TP53 cDNA. The modest increases in clonogenicity in isogenic ERCC1Δ cells with subsequent disruption of p53 compared with our panel of ERCC1Δ cells likely suggests additional factors, such as those involved in processing and stability of replication forks (RPA availability for example), may be critical for further enhancing clonogenicity in response to platinums with loss of ERCC1 (188). This would be most significant in terms of factors involved in response to intrastrand DNA damage which also theoretically requires ERCC1/XPF activity for resolution. A similar phenotype was observed by Feng and Jasin, where they observed a similar partial, but significant, rescue of clonogenicity of BRCA2-deficient cells with p53 loss, potentially suggesting that alterations in additional factors or pathways are critical for supporting clonogenic growth in tumors harboring a p53 mutation and loss of BRCA2 (189).

Interestingly, modified alkaline comet assays in H522 and H1299 cell lines showed differential repair of ICLs depending on p53 status. We also demonstrated that ERCC1Δ cells exhibit G$_2$–M arrest following cisplatin treatment. p53 disruption in H460

ERCC1Δ cells did not alter the initial G$_2$–M arrest observed in H460 ERCC1Δ cells, however, at 48 hours posttreatment there was a dramatic increase in a sub-G$_1$ population in H460 ERCC1Δ cells that corresponded with a decrease in the G$_2$–M population. This is opposed to the near complete abrogation of cell death and G$_2$–M arrest in the H460 ERCC1Δ/p53* cells.

Of importance, transient inhibition of entry into S-phase sensitized ICL-tolerant ERCC1Δ/p53* cells to cisplatin, suggesting ERCC1/XPF is indeed critical for ICL-R in G$_1$ phase and that the persistence of these unrepaired ICLs may trigger growth inhibition. This growth inhibition also suggests that entry into S-phase is critical for supporting ICL tolerance in these cells where there may be decreased dependence on ERCC1/XPF for ICL unhooking resulting in the accumulation of DNA DSBs. Based upon our data, it is likely that loss of downstream functions of ERCC1/XPF in ICL-R lead to persistent DSBs that are unresolved, at least initially, leading to G$_2$–M arrest. However, cells eventually escape this arrest and enter into M and subsequently into G$_1$ phase where p53 activity is critical for sensing persistent DNA damage from the previous round of the cell cycle and triggering apoptosis as well as activating the G$_1$ checkpoint. It is most likely that loss of p53 leads to a decrease in this apoptotic potential and loss of G$_1$ checkpoint activation which enables secondary, alternate repair pathways to at least partially contribute to ICL-R either in later stages of the cell cycle or in the subsequent G1 phase where a number of error-prone repair pathways, independent of BRCA2, may be available, including break-induced replication, microhomology-mediated end joining, and NHEJ. This hypothesis is supported by the observation that DNA-PKcs and BRCA1, but not BRCA2, are critical for supporting tolerance to ICLs in the absence of p53 and ERCC1. A similar phenotype with BRCA1 was recently reported in MMC-resistant, FANCC-

deficient cells where BRCA1 function was critical for supporting MMC resistance in the absence of USP48, despite loss of canonical ICL-R (172). Together, these data suggest that in both p53 and ICL-R deficient cells there is the potential uncovering of alternate DNA repair or tolerance mechanisms for dealing with unrepaired ICLs that specifically relies upon DNA-PKcs and BRCA1 as well as entry into S phase.

Several other groups have identified similar differential phenotypes *in vitro* and *in vivo* with loss of factors involved in ICL-R that appear to be correlated with p53 status including Mus81, BRCA2, and FANCD2 (171, 189, 190), although a mechanism for this differential phenotype has not been described. However, the role of p53 in inducing apoptosis does not appear to fully account for this differential phenotype as a recent report showed in FANCD2-deficient mice that p53 loss completely rescued mice from FA symptoms specifically in the context of aldehyde-DNA ICLs (171). Although the abrogation of FA symptoms was certainly related to a reduction in apoptosis, the authors also observed a dramatic increase in chromosomal aberrations including deletions and translocations suggesting that loss of p53 may uncover an alternate, error-prone ICL-R pathway and that WT p53 serves to suppress this error-prone repair likely through its roles in controlling apoptosis and mediating cell-cycle control. In conclusion, the work in this study characterizes a novel phenotype of ICL-tolerance in a subset of ERCC1-deficient cells and highlights the potential importance of p53 as a clinically relevant variable in studies evaluating ERCC1, and possibly other ICL-R factors, as a platinum biomarker. The surprising finding that DNA-PKcs and BRCA1 support this phenotype of tolerance suggests there are repair mechanisms in place which can at least partially overcome the ICL-R defects associated with loss of ERCC1. Furthermore, it will be important to fully characterize the molecular mechanisms underlying this process and to

expand the list of repair factors that are involved in supporting resistance to crosslinking agents despite loss of canonical ICL-R.

Better understanding mechanisms of resistance to DNA crosslinking agents in the context of DNA repair deficiencies may lead to the identification of novel targets for therapeutic intervention that could be developed to improve patient responses to platinum-based chemotherapy.

CHAPTER 3- ATR SUPPORTS PLATINUM TOLERANCE WITH ERCC1 DEFICIENCY BY SUPPRESSING REPLICATION CATASTROPHE

3.1 Introduction

DNA crosslinking agents, including the platinum-based analogues remain mainstay treatments for a variety of neoplasms. These crosslinking agents function by covalently binding to guanines in the DNA thereby blocking DNA replication and inhibiting tumor cell growth. These agents form a variety of DNA lesions including monoadducts, intrastrand crosslinks (ISAs), and interstrand crosslinks (ICLs) which ultimately require different pathways for ultimate resolution of the DNA damage including Nucleotide Excision Repair (NER), Homologous Recombination Repair (HR), and Interstrand Crosslink Repair (ICL-R).

Perhaps no DNA repair factor, excluding BRCA1 and BRCA2, has had more clinical interest in terms of biomarkers for response to cancer therapy than the NER factor, ERCC1 (13, 123, 154, 163). ERCC1 forms a constitutive heterodimer with the protein XPF which together constitutes a 5'-3' structure-specific endonuclease. ERCC1/XPF has critical roles in multiple DNA repair pathways including NER, ICL-R, HR and single strand annealing. In general, it is believed that ERCC1/XPF nuclease activity is essential for repair of platinum-induced DNA damage. ERCC1 was first identified as a potential biomarker for predicting response to platinum-based chemotherapy in the late 1990s and early 2000s and up to 60% of lung adenocarcinomas and up to 30% of lung squamous cell carcinomas harbor low to undetectable ERCC1 expression at the mRNA and protein levels (139, 151, 153, 191). However, the clinical utility of ERCC1 expression has been hampered by problems with antibody specificity, splice variant expression and inconsistent results in retrospective

clinical studies (13). Furthermore, a recent clinical trial in non-small cell lung cancer failed to show a survival benefit for patients with low ERCC1 who received a platinum agent (163, 185). Together, these observations suggest there remains an incomplete understanding of the biology of ERCC1 in human tumors.

Work from our lab recently identified a synthetic viable interaction between ERCC1 loss and p53 loss in a panel of ERCC1 knockout cell lines that we could recapitulate in two separate patient data sets (30). We observed that ERCC1-deficient cell lines harboring a mutation in or that were null for p53 were tolerant to crosslinking agents including cisplatin and mitomycin C (MMC) and that this tolerance was supported by DNA-PKcs and BRCA1 function as well as timely entry into S-phase following DNA damage (30). We hypothesized that p53 was critical for sensing persistent, replication-associated DNA damage in the subsequent G1 phase in platinum-treated ERCC1 knockout cells and that this function of p53 is what accounted for differential phenotypes in response to DNA crosslinking agents with loss of ERCC1. However, when we deleted wildtype p53 from hypersensitive ERCC1 knockout cells, we could nearly completely rescue viability after platinum treatment, but only mildly increase clonogenicity (30). This led us to hypothesize that functional loss of p53 may be necessary but insufficient to completely account for the differences in sensitivity between ERCC1 knockout cell lines and that additional processes during replication (e.g. RPA bioavailability) may be critical for promoting clonogenicity after platinum treatment with loss of ERCC1 by suppressing the accumulation of replication-associated DNA damage (188).

In the current study, we build upon our recent work identifying a novel subset of platinum-tolerant, ERCC1-deficient lung tumors by exploring the possibility of utilizing the ATR inhibitor M6620 as a means of overcoming platinum tolerance with ERCC1

deficiency. Utilizing previously established ERCC1 knockout cell line models of hypersensitivity and tolerance to DNA crosslinking agents, we show that synthetic lethality between ERCC1 loss and ATR inhibition depends upon cells being hypersensitive to crosslinking agents. These data potentially link the tolerance to DNA crosslinking agents in an ERCC1-deficient background to increased replication fork stability. On the other hand, we observe that tolerance to platinum and MMC with ERCC1 loss completely depends upon ATR function. Conversely, in an ERCC1 knockout cell line that is *de facto* hypersensitive to DNA crosslinking agents (i.e. ERCC1 knockout/p53 wildtype), there is no enhanced sensitivity to these agents with addition of an ATR inhibitor suggesting that even in the presence of ATR activity, there may be reduced capacity for fork protection in these cells. Treating platinum tolerant, ERCC1 knockout cells (i.e. ERCC1 knockout/p53 null) with platinum did not dramatically lead to increases in DNA double strand breaks following treatment. However, the addition of an ATR inhibitor promoted substantial increases in DNA double strand breaks following treatment. Finally, these increases in DNA double strand breaks were associated with substantial increases in replication catastrophe and subsequent micronuclei formation. Thus, in platinum tolerant, ERCC1 knockout cells, ATR promotes tolerance to DNA crosslinking agents by preventing the accumulation of aberrant DNA breaks and suppressing replication catastrophe. This work demonstrates the importance of ATR activity to promote tolerance to platinum-based chemotherapy in ERCC1 deficient cells and shows that chemical inhibition of ATR kinase activity by M6620 may represent a viable strategy for overcoming platinum tolerance in ERCC1 deficient tumors harboring a mutation in p53.

3.2 Materials and Methods

3.2.1 Cell Lines and Cell Culture

H460 and H1299 lung cancer cell lines were obtained from ATCC and were authenticated by the Karmanos Cancer Institute Biobanking and Correlative Sciences Core Facility. Cell lines were maintained in RPMI-1640 medium (Dharmacon) supplemented with 10% Fetal Bovine Serum (Atlanta Biologicals) and 1% Penicillin/Streptomycin (Dharmacon) and cells were grown in a humidified incubator with 5% CO_2. Cell lines were utilized for experiments for no greater than ~25 passages. *ERCC1* and *TP53* knockout cell lines have been previously validated and published (30, 135).

3.2.2 Western Blot

100 μg protein was loaded onto 10% Mini-PROTEAN TGX precast gels (Bio-Rad; 456-1043) and run at 150 V for ~40 minutes in Tris/Glycine/SDS buffer (Bio-Rad; 1610732). Proteins were transferred onto PVDF membrane at 100 V for ~35 minutes in transfer buffer (10 mmol/L CAPS, 10% Methanol, pH 10.5). Membrane was blocked for one hour with 5% non-fat milk in TBS-Tween. Proteins were probed overnight at 4 °C with anti-ERCC1 (Abcam; ab76236; 1:1,000), anti-XPF (Santa Cruz; sc-136153; 1:1,000), or for one hour at room temperature with anti-β-actin (Sigma-Aldrich; A5441; 1:100,000) in antibody dilution buffer (3% w/v bovine serum albumin (BSA), 0.2% v/v sodium azide in PBS-Tween). Excess antibody was removed by washing three times with PBS-Tween and the membrane was subsequently probed with goat anti-mouse or goat anti-rabbit secondary antibodies (Bio-Rad; 172-1011 and 172-1019; 1:2,000) for 45 minutes at room temperature. Excess secondary antibody was removed by washing three times with PBS-Tween.

3.2.3 Colony Survival Assay

Clonogenic survival assays were performed essentially as previously described (30). The day prior to treatment, 300 – 500 cells were seeded in complete medium in 60 mm plates. The day following seeding, cells were treated for varying times depending on the drug utilized in serum-free medium. Cisplatin (Sigma-Aldrich; 479306) was prepared daily as a fresh 1 mmol/L stock in PBS. All cisplatin treatments in clonogenic assays were performed for two hours. M6620 (Selleckchem; S7102), MK-1775 (Selleckchem; S1525), BMN 673 (Selleckchem; S7048), KU-55933 (Selleckchem; S1092) and CHIR-124 (Selleckchem; S2683) were prepared in DMSO, and treatments were performed for four hours. Mitomycin C (Selleckchem; S8146) was prepared in DMSO and treatments were performed for two hours. Once colonies reached a size of at least 50 or more cells, plates were washed once with PBS, and crystal violet was added (20% ethanol, 1% w/v crystal violet). For synergy studies, a constant cisplatin:M6620 ratio was utilized that was based upon the approximate IC_{50} value for each drug in each cell line (for H460 ERCC1Δ cells a ratio of 1:4 cisplatin:M6620 and for H1299 ERCC1Δ cells a ratio of 4:3 cisplatin:M6620 was used). Colony assay data were plotted and IC_{50}s estimated using Sigma Plot version 10.0.

3.2.4 Immunofluorescence

Cells were treated with the indicated concentrations of cisplatin (two hours), M6620 (four hours) or combination. For γH2AX foci experiments in Figure 4A, 10 μmol/L CDK1 inhibitor (RO-3306; Selleckchem; S7747) was added. For experiments presented in Figure 4A, immunofluorescence was performed ~16 hours after treatment. For experiments presented in Figure 5, no CDK1 inhibitor was added and immunofluorescence was performed ~40 hours after treatment. Cells were fixed with 4% paraformaldehyde for 20 minutes at room temperature, washed once with wash buffer

(0.1% Triton-X 100 in PBS), followed by permeabilization with 0.3% Triton-X 100 in PBS for 15 minutes. For micronuclei experiments, cells were stained with DAPI and coverslips sealed with nail polish. Cells were washed twice with wash buffer in PBS and blocked for one hour at room temperature using blocking buffer (0.02% Tween 20, 5% BSA in PBS). Cells were incubated with primary antibody (cGAS; Cell Signaling; D1D3G; 1:500 and/or H2AX-S139; EMD Millipore; JBW301; 1:1000) for 90 minutes at room temperature. Coverslips were washed with wash buffer and secondary antibody was added for one hour at room temperature in the dark (Alexa Fluor 488 goat anti-mouse IgG (H+L); Life Technologies; A11029; 1:2000 and Alexa Fluor 568 goat anti-rabbit IgG (H+L); Life Technologies; A11011; 1:1200). Coverslips were washed with wash buffer and with a final rinse with PBS. Cells were incubated with ProLong Gold antifade reagent with DAPI (Life Technologies; P36931) and coverslips were sealed with nail polish. Images were taken with a Nikon epifluorescent microscope using a 40x air objective. Micronuclei were quantified by visual inspection. Images were equally adjusted for presentation purposes.

3.2.5 Metaphase Spreads

For experiments utilizing chronic exposure to low dose cisplatin and M6620, cells were treated with 100 nmol/L cisplatin, 100 nmol/L M6620, or 100 nmol/L cisplatin + 100 nmol/L M6620 in complete medium daily for two days. For experiments utilizing a single concentration of cisplatin and M6620, cells were treated with 500 nmol/L cisplatin for two hours, followed by pulse labeling with 10 µmol/L EdU for 15 minutes, and subsequently treated with 750 nmol/L M6620 for four hours. 48 hours after chronic or single dose treatment, cells were incubated with Karyomax Colcemid (Life Technologies; 15212012) at 0.2 µg/mL for 90 minutes. Cells were subsequently suspended in ice cold 0.56% KCl

for 15 minutes at room temperature. Next, cells were fixed on ice in 3:1 methanol:acetic acid for approximately one hour. ~20 μL was added dropwise onto slides and allowed to air dry for 30 minutes followed by brief heat fixation. For EdU-incubated samples, slides were rehydrated with 3% BSA in PBS, followed by a 30-minute click chemistry reaction using an AF488 EdU Click It kit (Thermo Fisher; C10337). DNA was stained with anti-fade solution containing DAPI, a coverslip was added, and slides were sealed with nail polish. Spreads were counted on a Nikon epifluorescent microscope using a 40x oil objective. Images presented in this manuscript were taken on a Zeiss LSM 780 confocal microscope using a 63x oil objective. Images were cropped and entire images were equally sharpened or contrast adjusted for presentation purposes. For quantification of spreads, 50 or more spreads were counted for each condition. Experiments were performed three times.

3.2.6 Flow Cytometry

Cell Cycle: 5×10^5 cells were seeded on 10 cm plates. The following day, cells were incubated with 2 mmol/L thymidine overnight. Thymidine was removed and cells were allowed to grow for 8 hours followed by the addition of 2 mmol/L thymidine. For treatment, cells were treated with 1 μmol/L cisplatin in the presence of thymidine for two hours, and then released from the thymidine block into complete medium containing either no drug or 1 μmol/L M6620 for four hours. Samples were collected for Flow cytometry at the 4-hour, 22-hour, and 46-hour timepoints. Cells were fixed in 66% ethanol and stored at 4 °C for no greater than four days. Cells were prepared for detection of DNA content by flow cytometry using PI/RNase Staining Buffer (BD Biosciences; 550825) as per the manufacturer's instructions (with the exception that all spin steps were performed at 1,000 rpm for 3 minutes). Flow cytometry was performed

on a BD LSR II SORP Flow Cytometer (BD Biosciences). Data were analyzed using ModFit LT (Verity Software House) and FlowJo v10 (FlowJo, LLC). *Apoptosis:* On the day prior to treatment, cells were seeded onto 10 cm plates. Cells were treated with either 1 μmol/L cisplatin (two hours), 1 μmol/L M6620 (four hours) or combination. ~48 hours post-treatment, cells were processed for detection of 7-AAD and PE Annexin-V staining using the PE Annexin V Apoptosis Detection Kit I (BD Biosciences; 559763) as per the manufacturer's instructions. Flow cytometry was performed on a BD LSR II SORP Flow Cytometer (BD Biosciences). Data were analyzed using FlowJo v10 (FlowJo, LLC).

3.2.7 Senescence Assays

Cells were seeded in 6 well plates on the day prior to treatment. Cells were subsequently left untreated, treated with 500 nmol/L cisplatin for 2 hours, 500 nmol/L M6620 for 4 hours, or 500 nmol/L cisplatin + 500 nmol/L M6620. Cells were allowed to grow for six days after which cells were fixed and subsequently incubated with X-gal substrate overnight at 37 $^{\circ}$C as per the manufacturer's instructions using a β-galactosidase staining kit (Cell Signaling Technologies). Experiments were performed twice, and images taken on a Nikon epifluorescent microscope using a 20x air objective. Images were equally adjusted for presentation purposes.

3.2.8 Statistical Analyses for Cell Line Studies

All experiments were performed three times with the exception of flow cytometry and beta-galactosidase staining which were performed two times. IC_{50} values of drug sensitivity were estimated using Sigma Plot (v.10.0) from three independent experiments and values compared by two-sample t test. For comparisons of plating efficiency, normalized values were quantified from three independent experiments and compared

by two-sample t test. For metaphase spread experiments, data were compared by two-sample t test.

3.2.9 TCGA Analysis

Data were analyzed using cbioportal.org. Utilizing each data set indicated in Figure 3.2, mRNA expression (RNA Seq V2 RSEM) was compared between ERCC1 and ATR and ERCC1 and Chek1.

3.3 Results

3.3.1 Differential response of ERCC1Δ cell lines to cisplatin, mitomycin C, and ATR inhibition

We previously established a panel of ERCC1 knockout lung cancer cell lines and observed a differential phenotype in terms of response to cisplatin and MMC (30). We observed hypersensitivity to DNA crosslinks in ERCC1 deficient cells only when wildtype p53 was retained while those cell lines that were null for or harbored a mutation in p53 were significantly more tolerant to DNA crosslinks despite complete loss of ERCC1 (Figure 3.1 A). This led to the identification of two subsets of ERCC1-deficient tumors: platinum-hypersensitive and platinum-tolerant (Figure 3.1 A). Since our previous work identified DNA-PKcs, BRCA1, and timely progression into S-phase as being critical regulators of platinum-tolerance with ERCC1 deficiency, we focused our efforts on understanding whether inhibition of the DNA damage kinase, ATR, by the potent and highly selective small molecular inhibitor, M6620, could selectively sensitize platinum-tolerant, ERCC1-deficient cells and tumors to platinum-based chemotherapy. We utilized previously established lung cancer models of ERCC1-deficiency for our current studies, including the platinum hypersensitive model, H460, and the platinum-tolerant model, H1299 (Figure 3.1 A and 1B). We confirmed our previously reported observations of a

differential sensitivity to the DNA crosslinking agents, cisplatin and MMC, in our ERCC1-deficient cell line models. A clear hypersensitivity to cisplatin and MMC was observed in H460 ERCC1 knockout cells while the platinum-tolerant, ERCC1-deficient H1299 model was not dramatically more sensitive to cisplatin or MMC compared to H460 and H1299 ERCC1-wildtype cells (Figure 3.1 C and D).

There are mixed reports that ATR inhibition is synthetic lethal with loss of ERCC1, so we tested whether there were differences in response to the ATR inhibitor, M6620 and the Chk1 inhibitor, CHIR-124, between our platinum-hypersensitive and platinum-tolerant ERCC1 knockout cell line models (192-194). We observed that the platinum-hypersensitive H460 ERCC1 knockout cells were also sensitive to both ATR and Chk1 inhibition, however there was no synthetic lethality with ATR or Chk1 inhibition in the H1299 ERCC1 knockout platinum-tolerant cells, suggesting that there are compensatory processes occurring which not only render these cells tolerant to DNA crosslinking agents, but also to inhibitors of the ATR pathway (Figure 3.1 E and F). While there was a clear differential phenotype between ERCC1 knockout cell lines in terms of sensitivity to ATR inhibition, the sensitization of H460 ERCC1 knockout cells to Chk1 inhibition did not translate into a clear differential phenotype between H460 and H1299 ERCC1 knockout cells (Figure 3.1 E and F). Previous work looking at the synthetic lethal relationship between ATR inhibition and ERCC1-deficiency proposed that in the absence of ERCC1 there was increased reliance upon ATR-mediated signaling to respond to increased levels of damage associated with loss of ERCC1/XPF endonuclease activity (192). In support of this hypothesis, Mohni *et al.* identified enrichment of ERCC1 at replication forks (192). Along these lines, we asked whether there was any correlation between tumoral ERCC1 and ATR or Chek1 mRNA
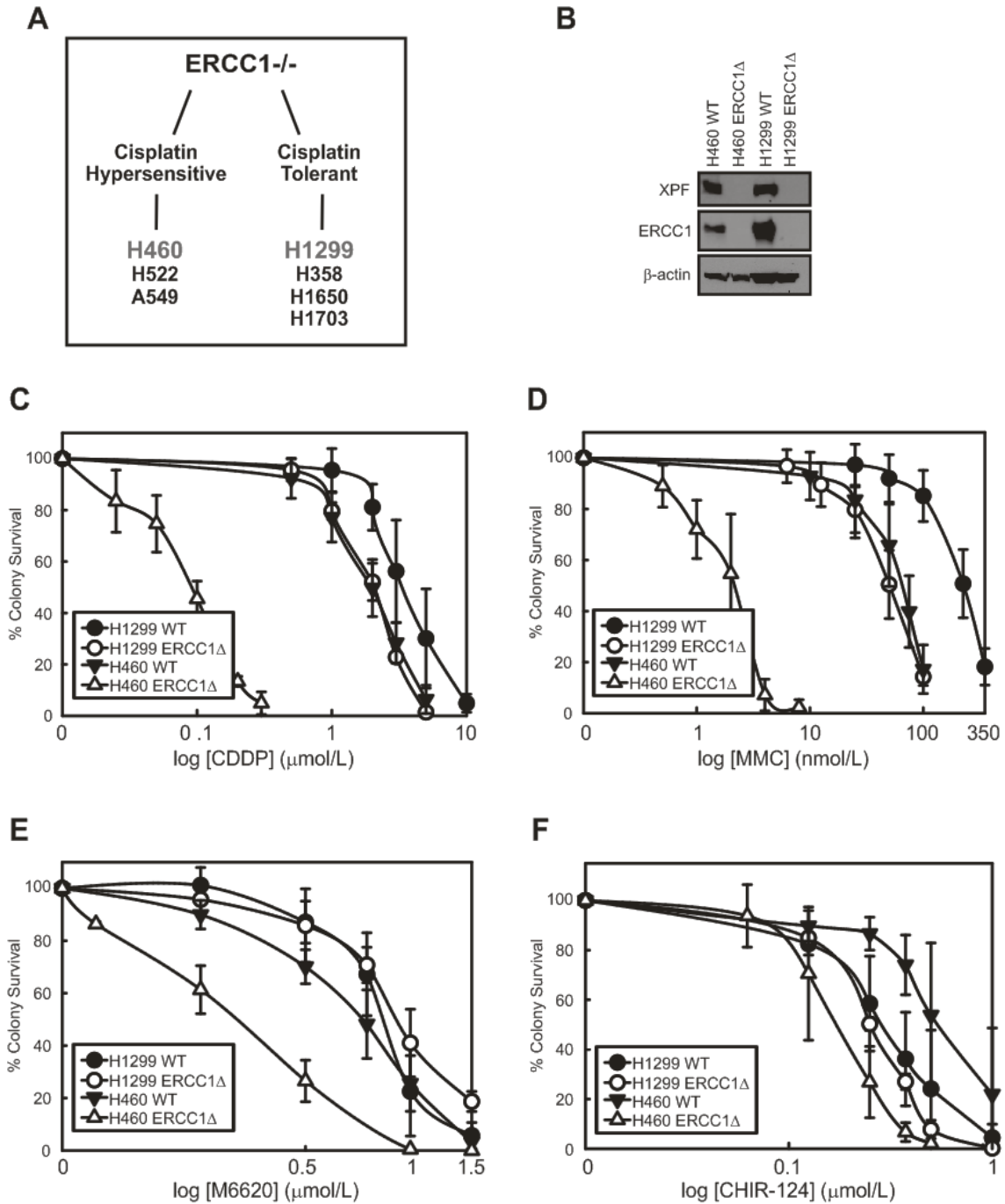
Figure 3.1 Differential sensitivity of ERCC1-knockout cells to cisplatin. **A,** Summary of previously established cell line models of ERCC1 deficiency. **B,** Western blot depicting ERCC1 and XPF expression in H460 and H1299 ERCC1 knockout cell lines. Sensitivity of H460 and H1299 isogenic cell lines to **C,** cisplatin, **D,** mitomycin C, **E,** the ATR inhibitor, M6620, and **F,** the Chk1 inhibitor, CHIR-124. All clonogenic assays are presented as the average of three independent experiments ± standard deviation.

Cancer Type	n	ATR vs ERCC1 mRNA		Chek1 vs ERCC1 mRNA	
		Spearman	p	Spearman	p
Head and Neck Squamous Cell Carcinoma	528	-0.38	1.38e-19	-0.05	0.301
Bladder Urothelial Carcinoma	412	-0.22	7.708e-6	0.06	0.250
Cervical Squamous Cell Carcinoma and Endocervical Adenocarcinoma	308	-0.33	5.60e-9	0.05	0.387
Esophageal Carcinoma	185	-0.20	5.872e-3	0.02	0.828
Lung Adenocarcinoma	584	-0.21	9.93e-7	-0.01	0.820
Lung Squamous Cell Carcinoma	511	-0.16	4.892e-4	0.04	0.376
Ovarian Serous Cystadenocarcinoma	594	-0.19	6.661e-4	-0.12	0.0415
Stomach Adenocarcinoma	478	-0.45	9.83e-22	-0.12	0.0174

Figure 3.2 Correlation between tumoral mRNA expression of ERCC1 and ATR or Chek1 in multiple TCGA data sets. Accessed from cBIOportal.org.

expression in tumors commonly treated with platinum-based chemotherapy. Utilizing eight TCGA patient data sets of tumor types commonly treated with platinum-based chemotherapy we observed moderate inverse correlations between tumoral ERCC1 mRNA and ATR mRNA suggesting that indeed ATR activity may be generally important for compensating for loss of ERCC1 (Figure 3.2). Interestingly, no notable correlations were observed between ERCC1 mRNA and Chk1 mRNA in the same data sets, suggesting that either Chk1 expression may not be strongly controlled at the mRNA level in the absence of ERCC1 or that Chk1 activity may not be as important as ATR for compensating for loss of ERCC1 (Figure 3.2). Together these data may indicate that certain compensatory mechanisms exist in platinum-tolerant, ERCC1 knockout cells to deal with endogenous damage that accumulates as a result of loss of ERCC1.

3.3.2 ATR inhibition selectively sensitizes platinum-tolerant, ERCC1-deficient cells to cisplatin

Because our previous work suggested that timely entry into S-phase was critical for platinum-tolerance with loss of ERCC1, we tested whether ATR inhibition could sensitize platinum tolerant, ERCC1-deficient cells to cisplatin. Utilizing a concentration of the ATR inhibitor, M6620, that was toxic on its own, we observed a striking, significant sensitization to cisplatin in H1299 ERCC1 knockout cells with ATR inhibition (1.50 μmol/L vs. 0.19 μmol/L) (Figure 3.3 A, C, & D). Conversely, in cells that were already hypersensitive to cisplatin, the addition of an IC_{50} concentration of ATR inhibitor did not further sensitize ERCC1-deficient cells to cisplatin (0.090 μmol/L vs. 0.085 μmol/L) (Figure 3.3 B-D). Consistent with this observation upon cisplatin treatment, we saw a similar pattern with MMC treatment, where ERCC1-deficient cells that were tolerant to MMC could be sensitized by ATR inhibition without further enhancing MMC sensitivity in
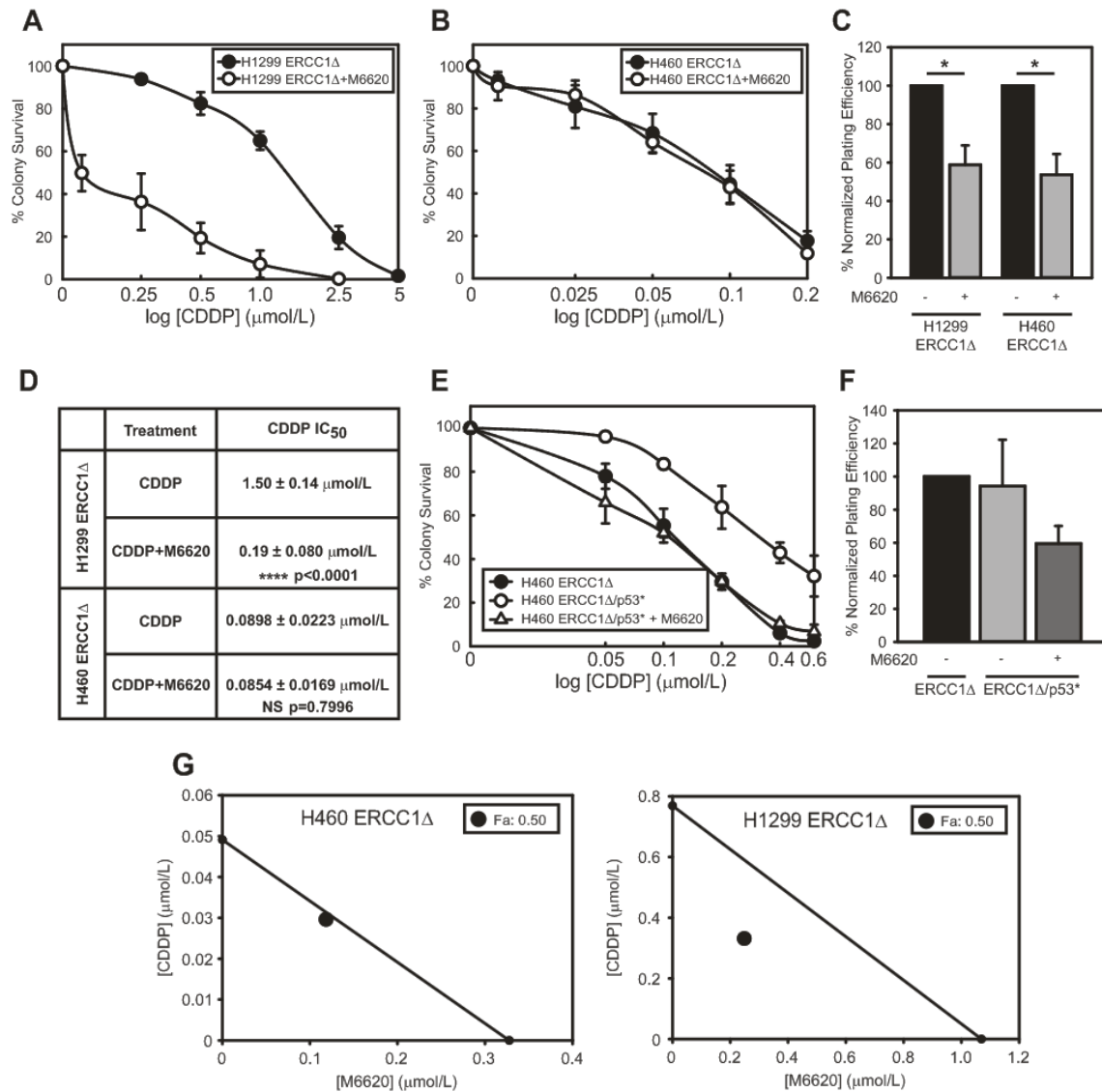
Figure 3.3 Platinum tolerance with ERCC1 deficiency is overcome by inhibition of ATR. **A,** Sensitization of H1299 ERCC1 knockout cells to cisplatin by M6620 treatment. **B,** Lack of sensitization of H460 ERCC1 knockout cells by M6620 treatment. **C,** Effect on plating efficiency of H1299 and H460 ERCC1 knockout with the concentration of M6620 utilized in sensitization experiments. **D,** Table depicting IC_{50} values from sensitization experiments depicted in Figure 2 A & B. IC_{50}s were estimated using Sigma Plot software and were compared by two-sided t test. **E,** Sensitization of H460 ERCC1 knockout/p53* cells to cisplatin by M6620 treatment. **F,** Effect on plating efficiency of H460 ERCC1 knockout/p53* cells with the concentration of M6620 utilized in sensitization experiments. **G,** Plots depicting synergy or lack of synergy between cisplatin and M6620 treatment in H460 and H1299 ERCC1 knockout cell lines. Data for all clonogenic assays are presented as the average of three independent experiments ± standard deviation. NS, not significant, * p<0.05, **** p<0.0001.
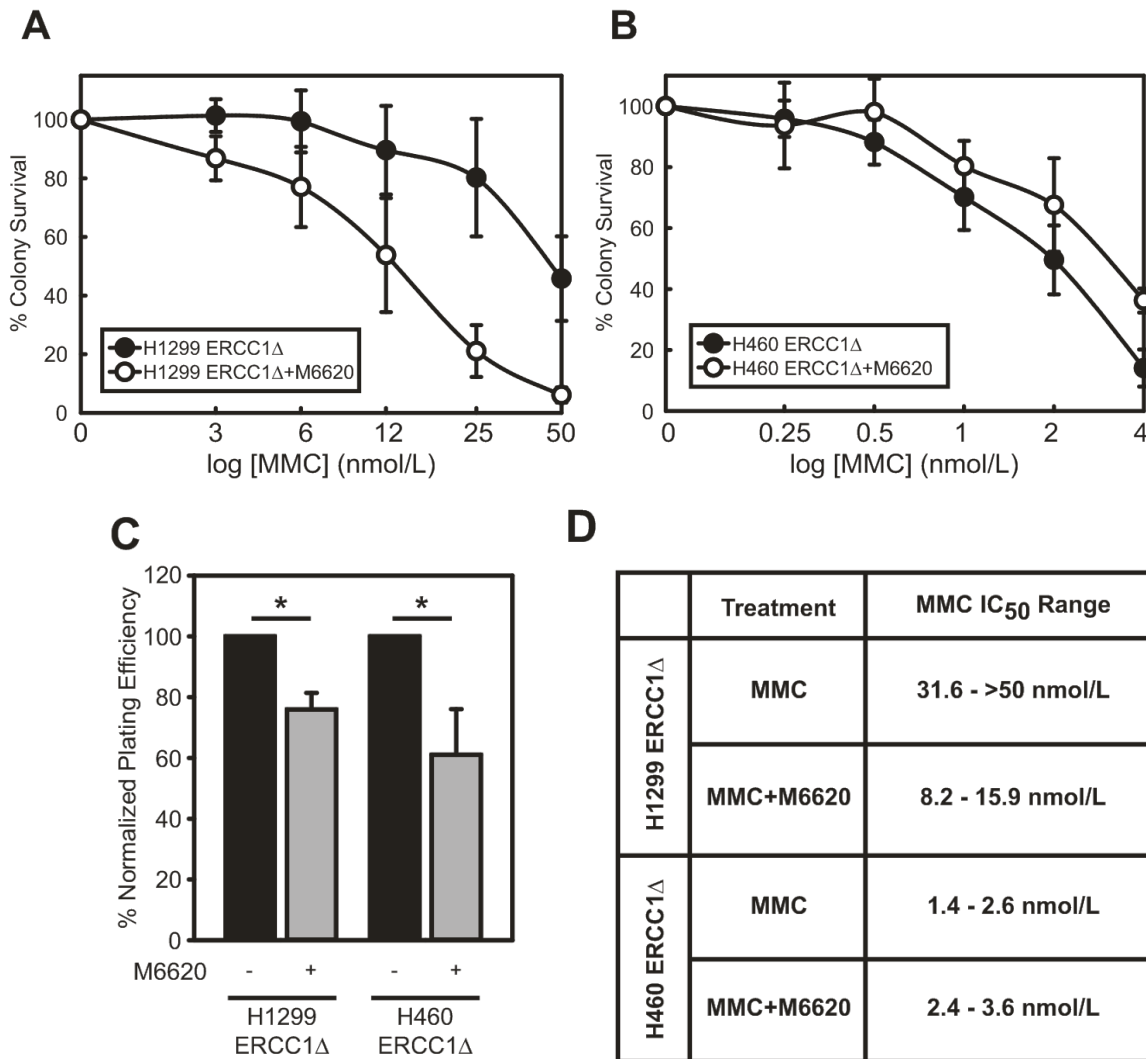
Figure 3.4 Effects of ATR inhibition on sensitivity to mitomycin C in H460 and H1299 ERCC1 knockout cell lines. Clonogenic survival of **A.** H1299 or **B.** H460 ERCC1 knockout cells treated with mitomycin C or mitomycin C + M6620. **C.** Effect of concentration of M6620 utilized for sensitization studies on plating efficiency relative to untreated control. **D.** Table depicting IC_{50} values estimated utilizing Sigma Plot software from experiments performed in A. and B. Data are presented as the average of three independent experiments ± S.D. * $p < 0.05$.

ERCC1 knockout cells that were already hypersensitive (Figure 3.4 A-D). We previously showed that knockout of p53 (p53*) in hypersensitive H460 ERCC1 knockout cells could partially increase tolerance to cisplatin (30). Next, we asked whether H460 ERCC1 knockout/p53* cells could be re-sensitized to cisplatin by ATR inhibition. Indeed, we observe that the increased tolerance to cisplatin in H460 ERCC1 knockout/p53* cells could be overcome by ATR inhibition and H460 ERCC1 knockout/p53* cells were re-sensitized to same level as H460 ERCC1 knockout/p53^{WT} cells (Figure 3.3 E and F).These data show that the partial relationship between ERCC1 loss and p53 in terms of platinum sensitivity may be related to levels of replication associated DNA damage and ultimately ATR function in suppressing extensive replication fork collapse and potentially replication catastrophe. We then asked whether the enhanced cisplatin sensitization we observed in H1299 ERCC1 knockout cells by ATR inhibition was synergistic. Combination cisplatin and ATR inhibition was synergistic in H1299 ERCC1 knockout cells, while combination treatment was only additive in H460 ERCC1 knockout cells (Figure 3.3 G). For this analysis, a point for combination treatment below the line connecting the IC$_{50}$ values for each drug represents a synergistic combination, while a point on the line is an additive drug-drug interaction, and a point above the line is an antagonistic drug-drug interaction.

As multiple protein targets have been studied in the context of sensitizing tumors to platinum-based chemotherapy, we tested whether the effects of ATR inhibition were independent of ATM inhibition. The addition of either 10 or 25 μmol/L KU-55933 did not enhance cisplatin sensitivity in H1299 ERCC1 knockout cells (Figure 3.5 A and B). These data confirm that platinum-tolerance with ERCC1 relies specifically upon ATR function and is not related to a more general inhibition of DNA damage kinase activity.
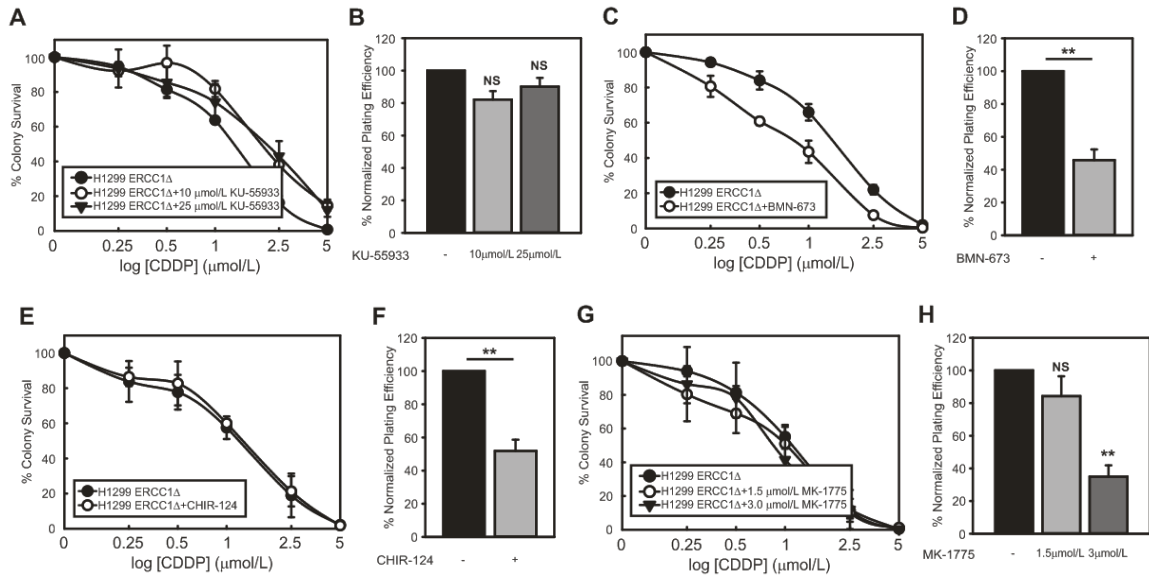
Figure 3.5 Lack of sensitization of H1299 ERCC1 knockout cells to cisplatin by ATM, PARP, Chk1, or Wee1 kinase inhibition. Clonogenic survival of H1299 ERCC1 knockout cells to cisplatin in combination with **A.** the ATM inhibitor KU-55933, **C.** the PARP inhibitor, BMN-673, **E.** the Chk1 inhibitor, CHIR-124, and **G.** the Wee1 kinase inhibitor, MK-1775. All results are presented as the average of three independent experiments ± S.D. **B, D, F, H.** Concentrations of each drug utilized for sensitization studies and the impact of each inhibitor on plating efficiency relative to untreated control. n=3 ± S.D. ** p<0.01.

Since PARP inhibitors have also entered clinical trials in combination with platinum-based chemotherapy, we asked whether ATR inhibition was a stronger sensitizer of platinum-tolerant, ERCC1-deficient cells to cisplatin than the PARP inhibitor, BMN-673. BMN-673 slightly enhanced sensitivity to cisplatin in H1299 ERCC1 knockout cells, but this effect was mild and did not approach the level of sensitization induced by ATR inhibition (Figure 3.5 C and D). Finally, we asked whether inhibiting the ATR target Chk1 or inhibiting the G_2/M checkpoint kinase Wee1 could also sensitize H1299 ERCC1 knockout cells to cisplatin treatment. We observed no increased sensitivity to cisplatin in H1299 ERCC1 knockout cells when we inhibited Chk1 or Wee1 kinase, suggesting that the effects of ATR-mediated platinum sensitization in this specific context are likely independent of Chk1- or Wee1k- related activity (Figure 3.5 E-H).

3.3.3 M6620 abrogates G2/M arrest following cisplatin treatment

It has been widely reported that ERCC1 deficient cells strongly arrest in G_2/M phase following treatment with DNA crosslinking agents. We next asked what effects M6620 had on cell cycle arrest and checkpoint activation in a model of platinum tolerance with ERCC1 deficiency. As we suspected that ATR inhibition in combination with cisplatin was leading to enhanced DNA damage compared to cisplatin alone, we hypothesized that combination treatment would lead to increased cell cycle arrest in G_2/M phase. To test this hypothesis, we treated H1299 wildtype and ERCC1 knockout cells with 1 μmol/L cisplatin, 1 μmol/L M6620, or combination and monitored cell cycle profiles by flow cytometry at ~20 hours post-treatment. In H1299 wildtype cells we observed mild increases in G_2/M arrest following treatment with cisplatin or combination ATRi and cisplatin (Figure 3.6 A). Consistent with previously reported observations,
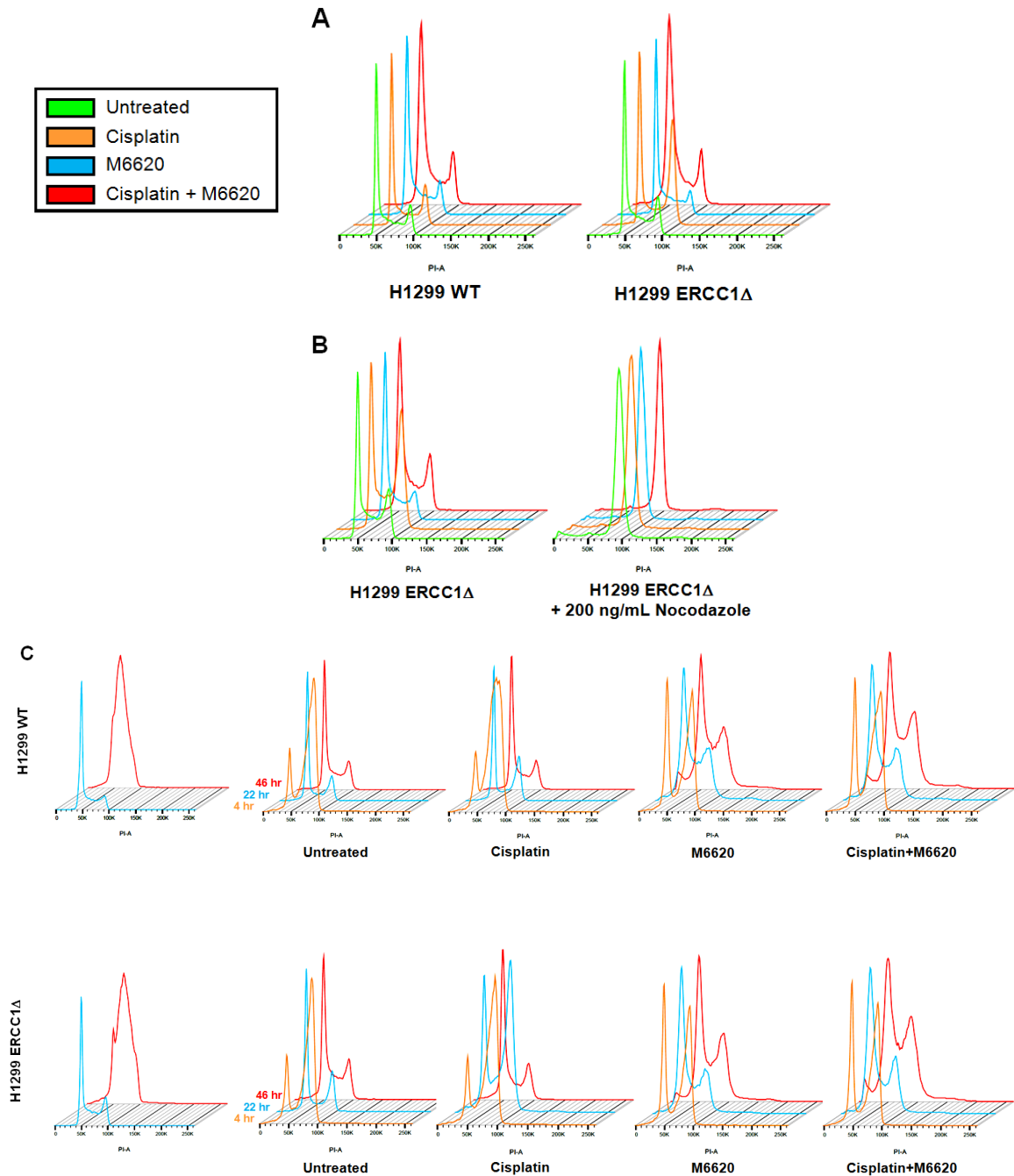
Figure 3.6 ATR inhibition abrogates G2/M arrest following platinum treatment. A, Cell cycle profiles following cisplatin and ATR inhibitor treatment in H1299 isogenic cells. **B,** Cell cycle profiles following cisplatin and ATR inhibitor treatment ± 200 ng/mL nocodazole. **C,** Cell cycle profiles over time after thymidine block in H1299 isogenic cells treated with cisplatin, ATR inhibitor, or combination. One experiment is presented. All cell cycle experiments were performed twice.

treatment of H1299 ERCC1 knockout cells with cisplatin led to G_2/M arrest, but strikingly, combination treatment led to fewer cells arresting at G_2/M (Figure 3.6 A).

While we observed fewer cells arresting in G2/M with combination treatment, we also observed that the G1 peak broadened and thought it possible that either ATR inhibition was leading to arrest in S-phase or that ATR inhibition was leading to bypass of the G2/M cell cycle checkpoint. To test which of these possibilities was the case, we performed the same treatments and monitored cell cycle profiles in the presence or absence of 200 ng/mL nocodazole. In the presence of nocodazole, all treatment groups strongly arrested at G2/M which indicated that ATR inhibition was not leading to S-phase arrest but was leading to bypass of the G2/M cell cycle checkpoint (Figure 3.6 B).

To further understand these events, we synchronized cells with a double thymidine block and monitored progression through the cell cycle following treatment at the 4-, 22-, and 46-hour time points (Figure 3.6 C). In H1299 ERCC1 knockout cells, we observed that cisplatin-treated cells arrested strongly at G2/M phase at the 4-hour and 22-hour time points, but that cells completely recovered from this G2/M arrest by 46 hours post-treatment. In the H1299 wildtype and ERCC1 knockout cells, we observed that treatment groups containing M6620 entered the subsequent G1 phase at a much faster rate than untreated and cisplatin-treated groups (Figure 3.6 C). We also observed that cells tended to accumulate and progress much more slowly through the subsequent S-phase possibly indicating that cells were requiring more time for DNA replication possibly due to the persistence of replication-associated damage from the previous round of the cell cycle. We detected increases in induction of apoptotic cell death in H1299 WT and ERCC1 knockout cells at 48 hours post-treatment by PE Annexin-V/7-AAD staining (Figure 3.7 A). Additionally, we saw increases in β-galactosidase staining
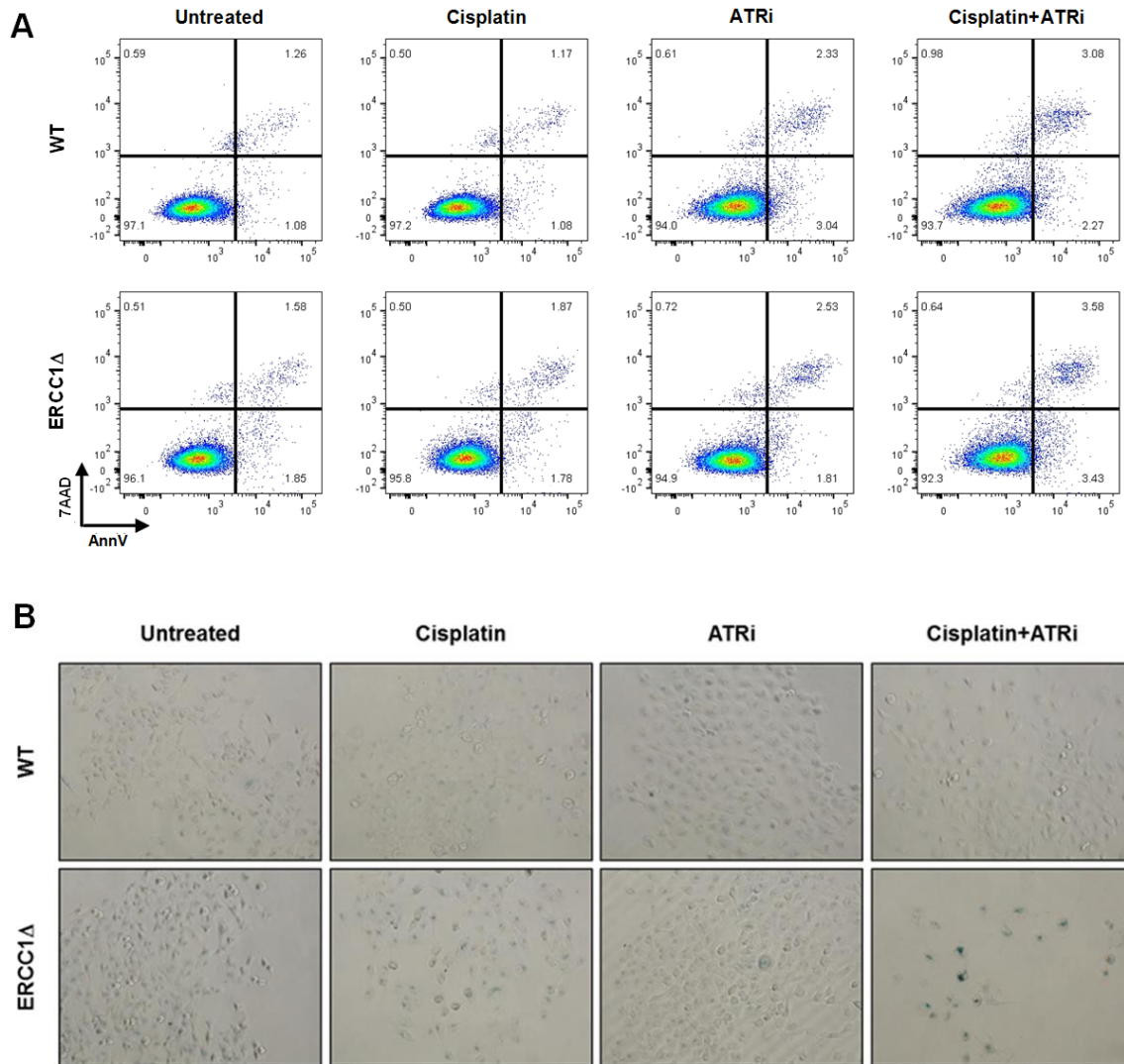
Figure 3.7 Induction of apoptosis and senescence following treatment in H1299 isogenic cell lines. A. Apoptotic cell death detected ~48 hours after treatment with 1 μmol/L cisplatin, 1 μmol/L M6620 or combination by 7AAD and PE-Annexin V staining and flow cytometry. Data is representative of two individual experiments. B. b-galactosidase staining in H1299 wildtype and knockout cells six days after treatment with 500 nmol/L cisplatin, 500 nmol/L M6620 or combination. Data is representative of two individual experiments.

in ERCC1 knockout cells following cisplatin and ATRi treatment 6 days following treatment consistent with induction of cellular senescence (Figure 3.7 B). We reason that cell fate after combination treatment is a cell-specific phenomenon that may depend upon the amount of DNA damage accumulated during the first round of DNA replication.

3.3.4 Dual treatment with cisplatin and M6620 enhances γH2AX formation and induces replication catastrophe

Next, we tested whether combination treatment induced DNA double-strand breaks in platinum tolerant, ERCC1-deficient cells. Approximately 16 hours post-treatment with cisplatin, M6620 or combination, cells were fixed and stained for γH2AX foci to monitor formation of DNA double-strand breaks. Cisplatin-treated cells had very few γH2AX foci above untreated cells consistent with our previously published data (30). Additionally, the addition of the ATR inhibitor alone did not dramatically increase formation of DNA double-strand breaks. Strikingly, the combination treatment led to substantial increases in γH2AX foci (Figure 3.8 A). Thus, ATR inhibition potentiated DNA double-strand break formation or persistence after cisplatin treatment in platinum-tolerant, ERCC1-deficient cells. As ATR activity has been shown to be critical for suppressing replication catastrophe after DNA damage by limiting depletion of available RPA pools, we asked whether combination treatment was inducing chromosome pulverization (195). We generated metaphase spreads following chronic treatment with cisplatin, ATRi, or cisplatin and ATRi and observed that platinum tolerant, ERCC1-deficient cells were more susceptible to chromosome pulverization than the parental ERCC1 wildtype cells with combination treatment (Figure 3.8 B & C). Next, we asked whether chromosome pulverization with combination treatment was specifically linked to defects associated with DNA replication. To answer this question, we treated cells with
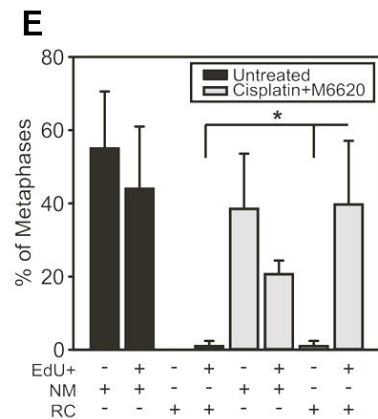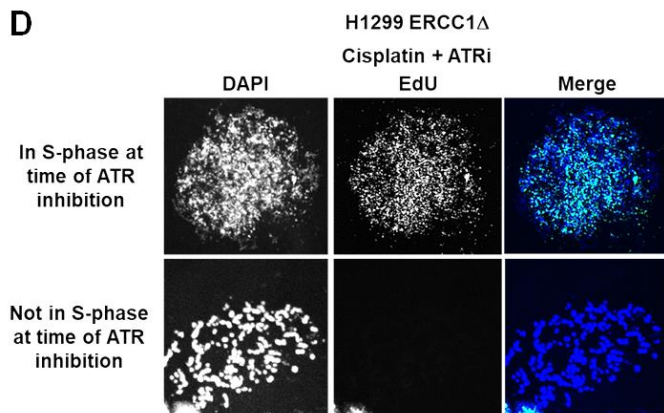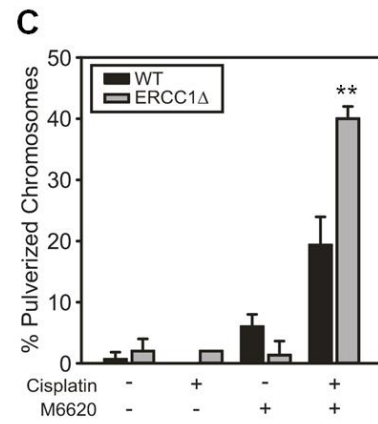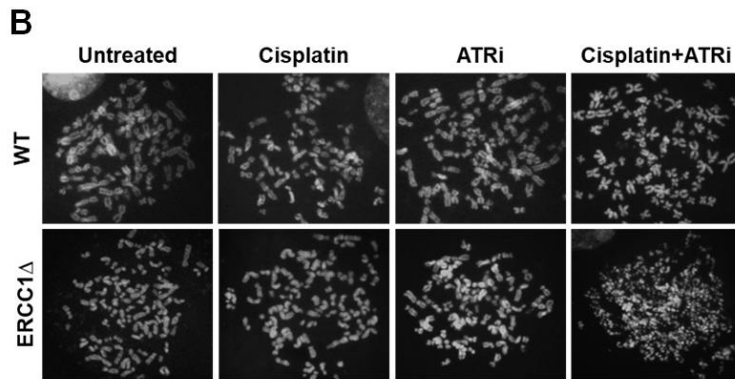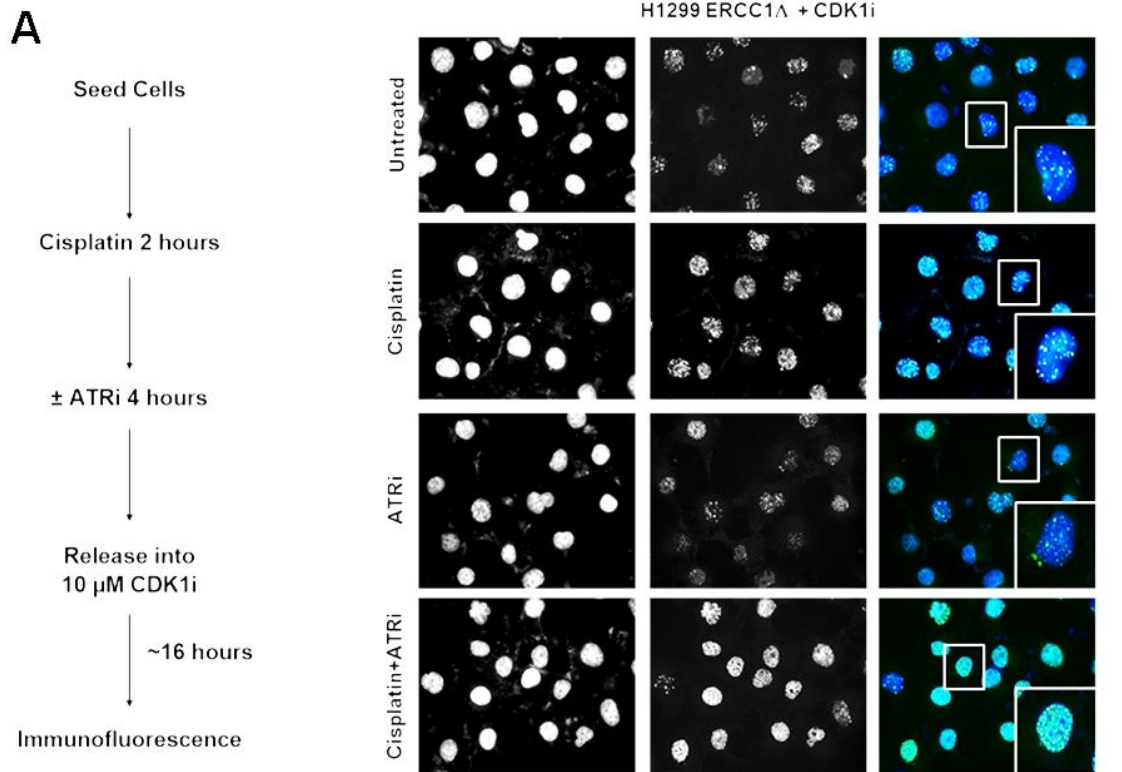
Figure 3.8 Effects of dual cisplatin and M6620 treatment on DNA double strand break formation and induction of chromosome pulverization. A. γH2AX staining by immunofluorescence ~22 hours after treatment in H1299 ERCC1 knockout cells. **B.** Representative metaphase spreads prepared from H1299 wildtype and ERCC1 knockout cells ~48 hours following treatment. **C.** Quantification of chromosome pulverization in H1299 wildtype and ERCC1 knockout cells following treatment. **D.** Representative images showing colocalization of EdU with pulverized chromosomes in H1299 ERCC1 knockout cells treated with cisplatin and M6620. **E.** Quantification of normal metaphases (NM) and chromosome pulverization (i.e. replication catstrophe (RC)) and colocalization with EdU staining in untreated and cisplatin + M6620 treated H1299 ERCC1 knockout cells. All experiments were performed three times. Error bars represent ± S.D. * p<0.05; ** p<0.01.

cisplatin for two hours, pulse labeled with EdU to label actively replicating cells, followed by ATR inhibition for four hours. 48 hours post-treatment metaphase spreads were generated and stained for EdU to identify whether chromosome pulverization was enriched for cells that were actively replicating DNA at the time of ATR inhibition. Compared to untreated cells, ERCC1 knockout cells that were positive for chromosome pulverization were significantly enriched for EdU positivity, indicating that chromosome pulverization (i.e. replication catastrophe) with combination treatment was specifically linked to inhibition of ATR during S-phase (Figure 3.8 D & E).

3.3.5 Combination treatment induces micronuclei formation associated with γH2AX and cGAS binding

Platinum in combination with immune checkpoint blockade inhibitors have become first-line treatment for the majority of non-small cell lung cancer patients. Next we asked whether combination treatment led to increased micronuclei formation in platinum tolerant, ERCC1 knockout cells and whether increased micronuclei were associated with DNA double-strand breaks and activation of the innate immune response. Activation of the innate immune response by cytosolic DNAs via cGAS-STING pathway has also been shown to influence response to immune checkpoint blockade inhibitors including anti-CTLA4 and anti-PD-L1 therapies (196, 197). To address this question, we monitored formation of micronuclei in H1299 wildtype and ERCC1 knockout cells following treatment with cisplatin, ATRi, or combination treatment. While we did not observe differences between wildtype and ERCC1 knockout cells in terms of the number of cells positive for micronuclei formation, we did see a significant difference between ERCC1 wildtype and knockout cells when we assessed the number of cells harboring greater than two micronuclei (Figure 3.9 A & B). In the context of DNA

A

B

C H1299 ERCC1Δ

DAPI | γH2AX | Merge

Cisplatin+M6620

D H1299 ERCC1Δ

DAPI | γH2AX | cGAS | Merge

Cisplatin+M6620
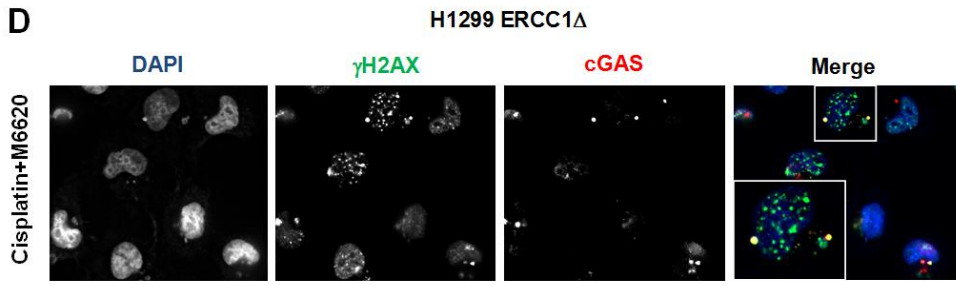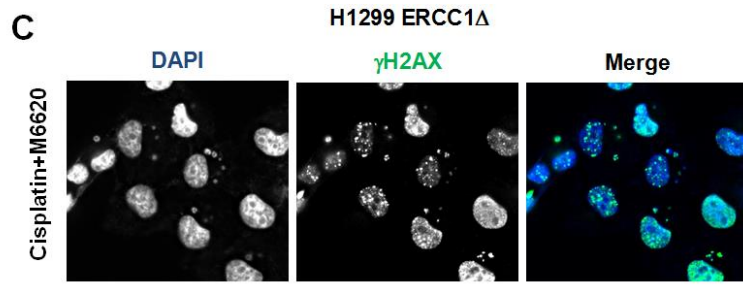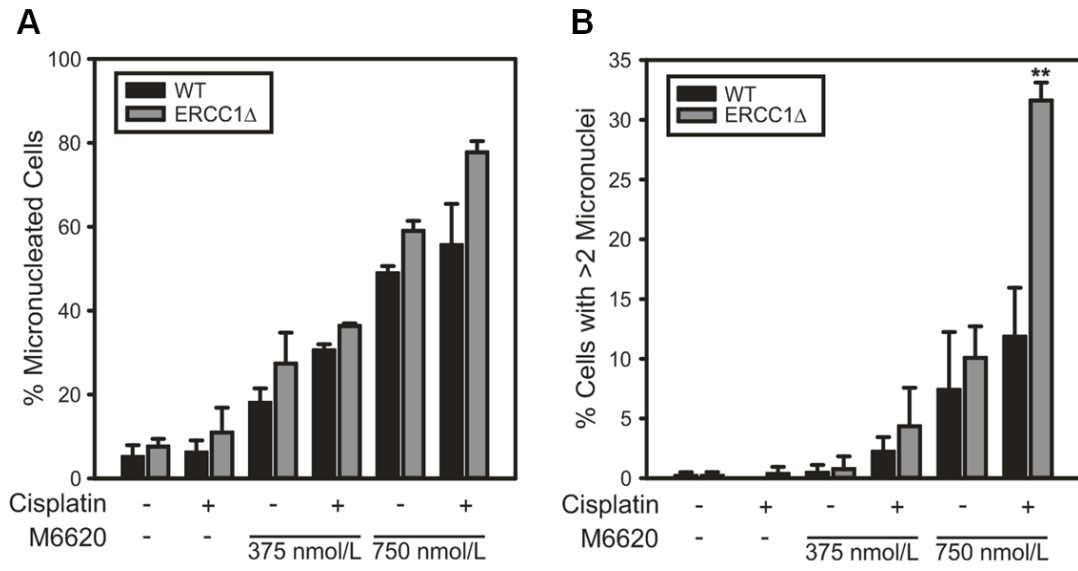
Figure 3.9 Detection of micronuclei following treatment in H1299 wildtype and ERCC1 knockout cell lines. A. Quantification of the total percent of micronucleated cells ~48 hours after treatment. Data presented as the average of three independent experiments ± S.D. **B.** Quantification of the number of cells positive for >2 micronuclei ~48 hours after treatment. Data presented as the average of three independent experiments ± S.D. **C.** Immunofluorescence reveals colocalization of micronuclei with gH2AX in H1299 ERCC1 knockout cells following combination treatment. Data are representative from two independent experiments. **D.** Detection of gH2AX and cGAS colocalization with micronuclei in H1299 ERCC1 knockout cells treated with cisplatin and M6620. Data are representative from two independent experiments.

damage, it was previously shown that micronuclei largely stain positive for γH2AX (196). Staining of micronuclei for γH2AX in H1299 ERCC1 knockout cells revealed that micronuclei are associated with DNA double-strand breaks (Figure 3.9 C). These micronuclei were also capable of being bound by the innate immunomodulatory factor cGAS, which could indicate that combination treatment may also have positive impacts in terms of modulating responses to immunotherapy (Figure 3.9 D).

3.4 Discussion

Setbacks in the clinical implementation of ERCC1 expression as a first-in-class biomarker for determining which lung cancer patients will benefit most from platinum-based chemotherapy suggest that our current understanding of its predictive power remain unclear. Our recent work identified p53 status as a partial confounding variable in clinical evaluations of ERCC1 as a platinum biomarker (30). Patients with lung tumors harboring low ERCC1 and wildtype p53 had a 50% increase in overall survival compared to those with ERCC1^{high}/p53^{WT} tumors. Conversely, there was no overall survival benefit for patients whose tumors had low ERCC1 compared to high ERCC1 when p53 was mutated. With these previous observations in mind, we show that ATR inhibition by M6620 represents a potential therapeutic strategy for overcoming tolerance to platinum-based chemotherapy in tumors harboring low ERCC1 and a functional deficiency in p53.

We identified that ATR activity was responsible for tolerance to DNA crosslinks induced by cisplatin in a cell line model of platinum tolerance with ERCC1 deficiency. While a model of cisplatin hypersensitivity could not be further sensitized to cisplatin by ATR inhibition, a model of cisplatin tolerance with ERCC1 deficiency could be sensitized to cisplatin by ATR inhibition in a synergistic manner (approximately ten-fold *in vitro*). These data appear to suggest that at least one reason for platinum tolerance with

ERCC1 deficiency is likely increased replication fork protection. Assessing cell cycle profiles after combination treatment revealed that ATR inhibition by M6620 leads to abrogation of the G_2/M cell cycle checkpoint after cisplatin treatment. Similar observations were recently made in BRCA mutant tumors when treated with the ATR inhibitor AZD6738 in combination with olaparib (198). Additionally, in cell synchronization studies, we observed that ATR inhibited cells enter the subsequent G_1 phase much faster than untreated control cells which could also be related to a deregulated S/G_2 checkpoint controlled by ATR which was recently described (199). After this bypass of the G_2/M checkpoint, we detected accumulation of cells in the subsequent S-phase, likely indicating the presence of persistent DNA damage from the previous round of DNA replication. In terms of sensitization of platinum-tolerant ERCC1 knockout cells to cisplatin by ATR inhibition, one possibility would be that G_2/M arrest following cisplatin treatment may be critical for promoting ERCC1-independent repair thus limiting the amount of persistent DNA damage detected in the subsequent G_1 phase and ultimately during the second round of DNA replication; thus, ATR inhibition may block this G_2/M arrest and sensitize these cells to cisplatin. Alternatively, ATR inhibition during S-phase may lead to enhanced replication-associated DNA damage associated with cisplatin and it is these effects in combination with bypass of the G_2/M checkpoint that is critical for promoting cisplatin sensitivity in the absence of ERCC1 and p53.

In platinum tolerant ERCC1-deficient cells, dual treatment coincided with substantial increases in DNA double-strand breaks as shown by γH2AX staining. Subsequent analysis revealed that dual treatment led to increased rates of replication catastrophe as shown by quantification of chromosome pulverization. Increased amounts of DNA double-strand breaks were also linked to increased micronuclei

formation, an activator of the innate immune response in H1299 ERCC1 knockout cells. These micronuclei were more numerous in ERCC1 knockout cells, were associated with DNA double strand breaks, and were capable of being bound by the innate immuno-modulatory factor, cGAS. Micronuclei formation has become a well-established marker for activation of the innate immune response that is associated with increased PD-L1 expression and may positively impact response of tumors to immunotherapy (196, 200, 201). Similar observations with micronuclei formation in the context of ERCC1 deficiency and PARP inhibition were recently published (202). In that context, increased micronuclei formation was associated with increased membranous PD-L1 expression, activation of IFN signaling mediated by cGAS-STING, and secretion of CCL5 (202). These observations have important implications for lung cancer therapy as first-line treatment for ~85% of advanced non-small cell lung cancer patients includes a platinum-based agent in combination with anti-PD-L1 therapy.

While three ATR inhibitors are currently in clinical trials, M6620 was the first to enter Phase II trials. This highly selective inhibitor of ATR kinase activity has shown promising activity in two Phase I studies. Results from a Phase I study combining topotecan with M6620 in 21 patients with advanced solid tumors who had failed at least one prior line of therapy showed two partial responses and eight patients with stable disease (203). Strikingly, three of five small cell lung cancer patients with platinum-refractory disease had durable clinical benefit from M6620 and topotecan combination therapy. Additionally, preliminary results from a Phase I study combining cisplatin and M6620 in triple negative breast cancers showed an objective response rate of nearly 39% and the disease control rate was approximately 72% (204).Preliminary clinical trial

data suggests promising activity of M6620 in combination with cytotoxic chemotherapy in a subset of patients, particularly those with deficiencies in DNA repair associated genes.

In summary, we recently identified p53 status as a confounding variable in clinical assessments of ERCC1 status as a first-in-class biomarker for predicting response to platinum-based chemotherapy. Building upon this work, we have identified ATR kinase activity as essential for tolerance to platinum-based chemotherapy in ERCC1-deficient/p53-deficient tumors and propose that these specific patients would benefit from combination treatment with M6620, a platinum analogue, and potentially anti-PD-L1 therapy.

CHAPTER 4- CONCLUSIONS

With its long history of being investigated as a biomarker for response to platinum-based chemotherapy, our understanding of the biology of ERCC1 in human tumors continues to evolve. Probably the best example of another set of factors that has had a similar trajectory in terms of scientific advances would be BRCA1 and BRCA2 in the context of PARP inhibition. While it was initially discovered that BRCA1 and BRCA2 mutant cancers respond exceptionally well to PARP inhibition, resistance to this therapy eventually occurs. Subsequent and ongoing research efforts have since identified multiple mechanisms of resistance to PARP inhibitors despite mutations in BRCA1 and BRCA2, including gene reversion, increased replication fork stability and restored homologous recombination. In a similar way, preclinical data showed that ERCC1 expression was strongly associated with response to platinum-based chemotherapy and a number of retrospective studies validated those *in vitro* observations. However, larger studies including an international, randomized Phase III clinical trial did not recapitulate those prior findings. These differences appeared to suggest that confounding variables related to either detection of ERCC1 or unknown resistance mechanisms may have influenced the ability of ERCC1 expression to predict patient response to platinum-based chemotherapy.

Chapter 2: Prior to the data described in this work, three main variables were thought to have influenced previous clinical studies of ERCC1: 1) Problems with antibody specificity for ERCC1 which impacted immunohistochemical detection of the protein; 2) Unoptimized cutoff for determining mRNA high vs. low ERCC1 tumors; and 3) ERCC1 splice variant expression of which only one of four splice variants is functional in DNA repair. In addition to these technical issues, our work described in Chapter 2 led to

the observation that ERCC1 deficiency does not always predispose to cisplatin hypersensitivity but is likely dependent upon the genetic background of the tumor, e.g. p53 status. Despite being thought to be absolutely required for repair of platinum-induced DNA damage, loss of ERCC1 does not appear to be strongly associated with platinum sensitivity when p53 function is impaired in both cell line and retrospective patient studies. Our general hypothesis for this phenomenon is that platinum treatment leads to DNA damage and that in the absence of ERCC1 this leads to repair refractory DNA double-strand breaks that trigger G_2/M arrest. However, we showed that G_2/M arrest is not permanent and cells eventually escape into the subsequent G_1 phase where wildtype p53 is critical for sensing persistent DNA damage, triggering growth arrest, and inducing apoptosis. In the absence of p53, there is loss of a functional G_1 cell cycle checkpoint, a reduction in apoptotic potential and the formation of an environment in which alternative DNA repair mechanisms (likely error prone) can partially compensate for loss of ERCC1/XPF activity. In support of these data, we observed that BRCA1 and DNA-PK function appear to be critical for supporting tolerance to platinum in the absence of ERCC1. Additionally, we found that timely entry into S-phase is also critical pointing to the importance of events during DNA replication for maintaining platinum tolerance in the absence of ERCC1.

Chapter 3: Because we found that events in S-phase were critical for supporting platinum tolerance in the absence of ERCC1, we asked whether pharmacological inhibition of the DNA damage kinase ATR could represent a viable strategy for resensitizing these cells to platinum. ATR is an important factor involved in orchestrating the processing of stalled replication forks, preserving replication fork stability, limiting origin firing, and promoting repair of DNA double-strand breaks induced in a replication-

dependent manner. Because of these critical functions, ATR has become an attractive therapeutic target in multiple tumor types and three ATR inhibitors have entered clinical trials. We found that platinum tolerant, ERCC1-deficient cells (p53 mutant/null) can be exquisitely sensitized to platinum-based chemotherapy by the ATR inhibitor M6620. This sensitization by M6620 was associated with increased DNA double-strand break formation and chromosome pulverization possibly suggesting that in the absence of ATR, stalled replication forks become unstable potentially mediated by RPA exhaustion and leading to global replication fork collapse. In addition, combination treatment induced micronuclei formation capable of being bound by the innate immunomodulatory factor cGAS which can trigger activation of the innate immune response. Thus, an ATR inhibitor not only could influence sensitivity of ERCC1 deficient tumors to cisplatin, but could also positively regulate response to immune checkpoint blockade inhibitors when given in combination with platinum-based chemotherapy in DNA repair deficient cells.

Remaining Questions: In conclusion, a number of subsequent scientific questions arising from our results warrant further investigation. First, it is unclear whether p53 status is sufficient for or whether it is only a necessary component of the phenotype of platinum tolerance in the absence of ERCC1. Our data utilizing isogenic cell lines appeared to suggest that other events beside loss of functional p53 likely play a role in this process, e.g. increased replication fork stability or increased alternative mechanisms of repair.

Second, it is also unclear whether loss of other DNA repair factors leads to a similar differential phenotype that depends upon p53, e.g. XPA, BRCA2, or FANCD2, although some evidence suggests that differential phenotypes exist with loss of various

Fanconi Anemia proteins and endonucleases involved in interstrand crosslink repair (171, 190).

Thirdly, the identification that timely entry into S-phase and ultimately ATR function are critical for supporting platinum tolerance in the absence of ERCC1 suggests that replication fork stability/protection likely play a role in facilitating these events. It will be important to clarify specifically whether this is the case as well as to examine in more detail whether p53 is associated with differences in basal capacity for replication fork protection between the cisplatin hypersensitive/tolerant ERCC1 deficient cell lines. It is possible that in the absence of ERCC1 replication forks approach an intrastrand platinum-DNA adduct and stall. This stalling leads to ATR recruitment which may facilitate recruitment of translesion polymerases to the stalled forks and allow for bypass past these adducts which represent up to ~90% of all platinum-DNA lesions. ATR would also support replication fork stability by limiting origin firing and suppressing RPA exhaustion which in turn would prevent accumulation of aberrant DNA double-strand breaks. However, in the absence of ATR, stalled forks accumulate which can lead to fork collapse and breakage induced by random endonucleases consistent with the pulverized chromosomes observed with combination cisplatin and ATRi treatment. Further clarifying these events will provide insight from a mechanistic perspective as to how ATR inhibition sensitizes platinum tolerant, ERCC1-deficient cells to cisplatin.

Fourth, key to identifying ways to sensitize these platinum tolerant tumors to cisplatin will be to identify what DNA structures are produced in the absence of ERCC1 and describe how alternative DNA repair occurs. One way to test this could be to look at global changes in the proteome with specific interest in DNA repair factors that may be upregulated after treatment in ERCC1 deficient cells. A second way to get at which DNA

repair pathways are involved in partially compensating for loss of ERCC1 after cisplatin treatment would be to look at mutation profiles in cell lines after treatment since patterns can be associated with particular DNA repair events, (e.g. deletions, specific types of mutation profiles, rearrangements, chromosome loss, etc.). A genome-wide CRISPR or RNAi screen could also be appropriate in this instance and could identify key factors for further study that may be necessary for promoting ERCC1-independent platinum-DNA adduct repair. These studies could be critical for further developing novel targets to sensitize platinum tolerant, ERCC1-deficient tumors to platinum-based chemotherapy.

Finally, when we combined an ATR inhibitor with cisplatin in ERCC1 deficient cells, we observed bypass of G_2/M cell cycle arrest. Subsequent studies revealed that combination treatment induced DNA double-strand breaks and ultimately led cells to undergo apoptosis or senescence. However, we also observed a large number of cells that entered another round of S-phase where a large number of cells accumulated as shown by cell cycle experiments. While cell fate is probably dependent upon the extent of DNA damage induced during the previous round of DNA replication, it is unclear what the consequences are of a second round of DNA replication in this context. For example, is a second round of DNA replication important for chromosome pulverization or is chromosome pulverization completely dependent upon the first round of DNA replication? Another question is what effects does persistent DNA damage from the first round of the cell cycle have once cells re-enter another S-phase: Is there processing that makes these persistent lesions especially toxic during a second round of S-phase? A complete characterization of the events during the second round of DNA replication could provide insight into the mechanism of sensitization to cisplatin by ATR inhibition in DNA repair deficient cells.

We have identified a novel phenotype of platinum resistance in ERCC1 deficient cells and patient tumors that may have important ramifications for the future clinical development of ERCC1 as a platinum biomarker or therapeutic target. The identification of ATR as a target for potent sensitization of platinum tolerant, ERCC1-deficient cells supports the idea that replication-dependent events are critical for platinum tolerance in this specific context and further clinical studies may be warranted.

APPENDIX-COPYRIGHT PERMISSIONS

1. Copyright permission for Figure 1.2 from Springer Nature.

Apr 09, 2019

This Agreement between Mr. Joshua Heyza ("You") and Springer Nature ("Springer Nature") consists of your license details and the terms and conditions provided by Springer Nature and Copyright Clearance Center.

License Number	4564530480223
License date	Apr 08, 2019
Licensed Content Publisher	Springer Nature
Licensed Content Publication	Nature Reviews Molecular Cell Biology
Licensed Content Title	Understanding nucleotide excision repair and its roles in cancer and ageing
Licensed Content Author	Jurgen A. Marteijn, Hannes Lans, Wim Vermeulen, Jan H. J. Hoeijmakers
Licensed Content Date	Jun 23, 2014
Licensed Content Volume	15
Licensed Content Issue	7
Type of Use	Thesis/Dissertation
Requestor type	academic/university or research institute
Format	print and electronic
Portion	figures/tables/illustrations
Number of figures/tables/illustrations	1
High-res required	no
Will you be translating?	no
Circulation/distribution	<501
Author of this Springer Nature content	no
Title	NOVEL INSIGHTS INTO THE USE OF ERCC1 AS A BIOMARKER FOR RESPONSE TO PLATINUM-BASED CHEMOTHERAPY IN LUNG CANCER
Institution name	Wayne State University
Expected presentation date	Jun 2019
Portions	Figure 1
Requestor Location	Mr. Joshua Heyza 1738 Kentucky Ave
	FLINT, MI 48506 United States Attn: Mr. Joshua Heyza

2. **Copyright permission for Figure 1.1. from the Massachusetts Medical Society.**

   (https://www.nejm.org/about-nejm/permissions)

Reuse of Content Within a Thesis or Dissertation

Content (full-text or portions thereof) may be used in print and electronic versions of a dissertation or thesis without formal permission from the Massachusetts Medical Society (MMS), Publisher of the *New England Journal of Medicine*.

The following credit line must be printed along with the copyrighted material:

Reproduced with permission from (scientific reference citation), Copyright Massachusetts Medical Society.

3. **Copyright permission for inclusion of Chapter 2 which was previously**

   published in Clinical Cancer Research by the American Association for Cancer

   Research. (http://aacrjournals.org/content/authors/copyright-permissions-and-

   access)

Article Reuse by Authors

Authors of articles published in AACR journals are permitted to use their article or parts of their article in the following ways without requesting permission from the AACR. All such uses must include appropriate attribution to the original AACR publication. Authors may do the following as applicable:

1. Reproduce parts of their article, including figures and tables, in books, reviews, or subsequent research articles they write;
2. Use parts of their article in presentations, including figures downloaded into PowerPoint, which can be done directly from the journal's website;
3. Post the accepted version of their article (after revisions resulting from peer review, but before editing and formatting) on their institutional website, if this is required by their institution. The version on the institutional repository must contain a link to the final, published version of the article on the AACR journal website so that any subsequent corrections to the published record will continue to be available to the broadest readership. The posted version may be released publicly (made open to anyone) 12 months after its publication in the journal;
4. Submit a copy of the article to a doctoral candidate's university in support of a doctoral thesis or dissertation.

4. **Copyright Permission for Figure 1.3 from Elsevier.**

This Agreement between Mr. Joshua Heyza ("You") and Elsevier ("Elsevier") consists of your license details and the terms and conditions provided by Elsevier and Copyright Clearance Center.

License Number	4565600047483
License date	Apr 10, 2019
Licensed Content Publisher	Elsevier
Licensed Content Publication	DNA Repair
Licensed Content Title	Mechanism and regulation of incisions during DNA interstrand cross-link repair
Licensed Content Author	Jieqiong Zhang,Johannes C. Walter
Licensed Content Date	Jul 1, 2014
Licensed Content Volume	19
Licensed Content Issue	n/a
Licensed Content Pages	8
Start Page	135
End Page	142
Type of Use	reuse in a thesis/dissertation
Intended publisher of new work	other
Portion	figures/tables/illustrations
Number of figures/tables/illustrations	1
Format	both print and electronic
Are you the author of this Elsevier article?	No
Will you be translating?	No
Original figure numbers	Figure 1
Title of your thesis/dissertation	NOVEL INSIGHTS INTO THE USE OF ERCC1 AS A BIOMARKER FOR RESPONSE TO PLATINUM-BASED CHEMOTHERAPY IN LUNG CANCER
Publisher of new work	Wayne State University
Expected completion date	Jun 2019
Estimated size (number of pages)	1

5. **Copyright permission for Figure 1.4 and 1.5 from Royal Society of Chemistry.**

Customer Information

Customer: Joshua Heyza
Account Number: 3001427260
Organization: Joshua Heyza
Email: jrheyza@med.wayne.edu
Phone: +1 (810) 730-5093

Search order details by: [Choose One ▼] [   ] [Go]

This is not an invoice

Order Details

Metallomics : integrated biometal science

Billing Status:
N/A

Order detail ID:	71876092
ISSN:	1756-591X
Publication Type:	e-Journal
Volume:	
Issue:	
Start page:	
Publisher:	RSC Pub
Author/Editor:	Royal Society of Chemistry (Great Britain)

Permission Status: ✅ Granted

Permission type: Republish or display content
Type of use: Thesis/Dissertation
Order License Id: 4566641375223

⊞ View details

REFERENCES

1. Lehmann AR, McGibbon D, Stefanini M. Xeroderma pigmentosum. Orphanet journal of rare diseases. 2011;6:70. Epub 2011/11/03. doi: 10.1186/1750-1172-6-70. PubMed PMID: 22044607; PMCID: PMC3221642.

2. Rothblum-Oviatt C, Wright J, Lefton-Greif MA, McGrath-Morrow SA, Crawford TO, Lederman HM. Ataxia telangiectasia: a review. Orphanet journal of rare diseases. 2016;11(1):159. Epub 2016/11/26. doi: 10.1186/s13023-016-0543-7. PubMed PMID: 27884168; PMCID: PMC5123280.

3. Nalepa G, Clapp DW. Fanconi anaemia and cancer: an intricate relationship. Nature reviews Cancer. 2018;18(3):168-85. Epub 2018/01/30. doi: 10.1038/nrc.2017.116. PubMed PMID: 29376519.

4. Ferri D, Orioli D, Botta E. Heterogeneity and overlaps in nucleotide excision repair (NER) disorders. Clinical genetics. 2019. Epub 2019/03/29. doi: 10.1111/cge.13545. PubMed PMID: 30919937.

5. de Renty C, Ellis NA. Bloom's syndrome: Why not premature aging?: A comparison of the BLM and WRN helicases. Ageing research reviews. 2017;33:36-51. Epub 2016/05/31. doi: 10.1016/j.arr.2016.05.010. PubMed PMID: 27238185; PMCID: PMC5124422.

6. Hanahan D, Weinberg RA. Hallmarks of cancer: the next generation. Cell. 2011;144(5):646-74. Epub 2011/03/08. doi: 10.1016/j.cell.2011.02.013. PubMed PMID: 21376230.

7. Waqar SN, Devarakonda SHK, Michel LS, Maggi LB, Watson M, Guebert K, Carpenter D, Sleckman BP, Govindan R, Morgensztern D. BRCAness in non-

small cell lung cancer (NSCLC). Journal of Clinical Oncology. 2014;32(15_suppl):11033-. doi: 10.1200/jco.2014.32.15_suppl.11033.

8.   Park CH, Bessho T, Matsunaga T, Sancar A. Purification and characterization of the XPF-ERCC1 complex of human DNA repair excision nuclease. The Journal of biological chemistry. 1995;270(39):22657-60. Epub 1995/09/29. PubMed PMID: 7559382.

9.   Sargent RG, Meservy JL, Perkins BD, Kilburn AE, Intody Z, Adair GM, Nairn RS, Wilson JH. Role of the nucleotide excision repair gene ERCC1 in formation of recombination-dependent rearrangements in mammalian cells. Nucleic acids research. 2000;28(19):3771-8. Epub 2000/09/23. PubMed PMID: 11000269; PMCID: PMC110761.

10. Kuraoka I, Kobertz WR, Ariza RR, Biggerstaff M, Essigmann JM, Wood RD. Repair of an interstrand DNA cross-link initiated by ERCC1-XPF repair/recombination nuclease. The Journal of biological chemistry. 2000;275(34):26632-6. Epub 2000/07/07. doi: 10.1074/jbc.C000337200. PubMed PMID: 10882712.

11. Niedernhofer LJ, Essers J, Weeda G, Beverloo B, de Wit J, Muijtjens M, Odijk H, Hoeijmakers JH, Kanaar R. The structure-specific endonuclease Ercc1-Xpf is required for targeted gene replacement in embryonic stem cells. The EMBO journal. 2001;20(22):6540-9. Epub 2001/11/15. doi: 10.1093/emboj/20.22.6540. PubMed PMID: 11707424; PMCID: PMC125716.

12. Westerveld A, Hoeijmakers JH, van Duin M, de Wit J, Odijk H, Pastink A, Wood RD, Bootsma D. Molecular cloning of a human DNA repair gene. Nature. 1984;310(5976):425-9. Epub 1984/08/02. PubMed PMID: 6462228.

13. Friboulet L, Olaussen KA, Pignon JP, Shepherd FA, Tsao MS, Graziano S, Kratzke R, Douillard JY, Seymour L, Pirker R, Filipits M, Andre F, Solary E, Ponsonnailles F, Robin A, Stoclin A, Dorvault N, Commo F, Adam J, Vanhecke E, Saulnier P, Thomale J, Le Chevalier T, Dunant A, Rousseau V, Le Teuff G, Brambilla E, Soria JC. ERCC1 isoform expression and DNA repair in non-small-cell lung cancer. The New England journal of medicine. 2013;368(12):1101-10. Epub 2013/03/22. doi: 10.1056/NEJMoa1214271. PubMed PMID: 23514287; PMCID: PMC4054818.

14. McNeil EM, Melton DW. DNA repair endonuclease ERCC1-XPF as a novel therapeutic target to overcome chemoresistance in cancer therapy. Nucleic acids research. 2012;40(20):9990-10004. Epub 2012/09/04. doi: 10.1093/nar/gks818. PubMed PMID: 22941649; PMCID: PMC3488251.

15. Tsodikov OV, Enzlin JH, Scharer OD, Ellenberger T. Crystal structure and DNA binding functions of ERCC1, a subunit of the DNA structure-specific endonuclease XPF-ERCC1. Proceedings of the National Academy of Sciences of the United States of America. 2005;102(32):11236-41. Epub 2005/08/04. doi: 10.1073/pnas.0504341102. PubMed PMID: 16076955; PMCID: PMC1183572.

16. Dabholkar M, Vionnet J, Parker R, Bostickbruton F, Dobbins A, Reed E. Expression of an alternatively spliced ercc1 messenger-RNA species, is related to reduced DNA-repair efficiency in human T-lymphocytes. Oncology reports. 1995;2(2):209-14. Epub 1995/03/01. PubMed PMID: 21597714.

17. Solier S, Barb J, Zeeberg BR, Varma S, Ryan MC, Kohn KW, Weinstein JN, Munson PJ, Pommier Y. Genome-wide analysis of novel splice variants induced by topoisomerase I poisoning shows preferential occurrence in genes encoding

splicing factors. Cancer research. 2010;70(20):8055-65. Epub 2010/09/08. doi: 10.1158/0008-5472.can-10-2491. PubMed PMID: 20817775; PMCID: PMC2992871.

18. Friboulet L, Postel-Vinay S, Sourisseau T, Adam J, Stoclin A, Ponsonnailles F, Dorvault N, Commo F, Saulnier P, Salome-Desmoulez S, Pottier G, Andre F, Kroemer G, Soria JC, Olaussen KA. ERCC1 function in nuclear excision and interstrand crosslink repair pathways is mediated exclusively by the ERCC1-202 isoform. Cell cycle (Georgetown, Tex). 2013;12(20):3298-306. Epub 2013/09/17. doi: 10.4161/cc.26309. PubMed PMID: 24036546; PMCID: PMC3885640.

19. Kuo MS, Adam J, Dorvault N, Robin A, Friboulet L, Soria JC, Olaussen KA. A novel antibody-based approach to detect the functional ERCC1-202 isoform. DNA repair. 2018;64:34-44. Epub 2018/02/27. doi: 10.1016/j.dnarep.2018.02.002. PubMed PMID: 29482102.

20. Zhao J, Wang G, Del Mundo IM, McKinney JA, Lu X, Bacolla A, Boulware SB, Zhang C, Zhang H, Ren P, Freudenreich CH, Vasquez KM. Distinct Mechanisms of Nuclease-Directed DNA-Structure-Induced Genetic Instability in Cancer Genomes. Cell reports. 2018;22(5):1200-10. Epub 2018/02/02. doi: 10.1016/j.celrep.2018.01.014. PubMed PMID: 29386108; PMCID: PMC6011834.

21. van Vuuren AJ, Appeldoorn E, Odijk H, Yasui A, Jaspers NG, Bootsma D, Hoeijmakers JH. Evidence for a repair enzyme complex involving ERCC1 and complementing activities of ERCC4, ERCC11 and xeroderma pigmentosum group F. The EMBO journal. 1993;12(9):3693-701. Epub 1993/09/01. PubMed PMID: 8253091; PMCID: PMC413646.

22.   Biggerstaff M, Szymkowski DE, Wood RD. Co-correction of the ERCC1, ERCC4 and xeroderma pigmentosum group F DNA repair defects in vitro. The EMBO journal. 1993;12(9):3685-92. Epub 1993/09/01. PubMed PMID: 8253090; PMCID: PMC413645.

23.   Tomkinson AE, Bardwell AJ, Bardwell L, Tappe NJ, Friedberg EC. Yeast DNA repair and recombination proteins Rad1 and Rad10 constitute a single-stranded-DNA endonuclease. Nature. 1993;362(6423):860-2. Epub 1993/04/29. doi: 10.1038/362860a0. PubMed PMID: 8479526.

24.   de Laat WL, Appeldoorn E, Jaspers NG, Hoeijmakers JH. DNA structural elements required for ERCC1-XPF endonuclease activity. The Journal of biological chemistry. 1998;273(14):7835-42. Epub 1998/05/09. PubMed PMID: 9525876.

25.   Bardwell AJ, Bardwell L, Tomkinson AE, Friedberg EC. Specific cleavage of model recombination and repair intermediates by the yeast Rad1-Rad10 DNA endonuclease. Science (New York, NY). 1994;265(5181):2082-5. Epub 1994/09/30. PubMed PMID: 8091230.

26.   Tomkinson AE, Bardwell AJ, Tappe N, Ramos W, Friedberg EC. Purification of Rad1 protein from Saccharomyces cerevisiae and further characterization of the Rad1/Rad10 endonuclease complex. Biochemistry. 1994;33(17):5305-11. Epub 1994/05/03. PubMed PMID: 8172904.

27.   Siede W, Friedberg AS, Friedberg EC. Evidence that the Rad1 and Rad10 proteins of Saccharomyces cerevisiae participate as a complex in nucleotide excision repair of UV radiation damage. Journal of bacteriology.

1993;175(19):6345-7. Epub 1993/10/01. PubMed PMID: 8407807; PMCID: PMC206733.

28.   van Vuuren AJ, Appeldoorn E, Odijk H, Humbert S, Moncollin V, Eker AP, Jaspers NG, Egly JM, Hoeijmakers JH. Partial characterization of the DNA repair protein complex, containing the ERCC1, ERCC4, ERCC11 and XPF correcting activities. Mutation research. 1995;337(1):25-39. Epub 1995/07/01. PubMed PMID: 7596355.

29.   Tripsianes K, Folkers G, Ab E, Das D, Odijk H, Jaspers NG, Hoeijmakers JH, Kaptein R, Boelens R. The structure of the human ERCC1/XPF interaction domains reveals a complementary role for the two proteins in nucleotide excision repair. Structure (London, England : 1993). 2005;13(12):1849-58. Epub 2005/12/13. doi: 10.1016/j.str.2005.08.014. PubMed PMID: 16338413.

30.   Heyza JR, Lei W, Watza D, Zhang H, Chen W, Back JB, Schwartz AG, Bepler G, Patrick SM. Identification and Characterization of Synthetic Viability with ERCC1 Deficiency in Response to Interstrand Crosslinks in Lung Cancer. Clinical cancer research : an official journal of the American Association for Cancer Research. 2019;25(8):2523-36. Epub 2018/12/13. doi: 10.1158/1078-0432.ccr-18-3094. PubMed PMID: 30538112.

31.   Arora S, Kothandapani A, Tillison K, Kalman-Maltese V, Patrick SM. Downregulation of XPF-ERCC1 enhances cisplatin efficacy in cancer cells. DNA repair. 2010;9(7):745-53. Epub 2010/04/27. doi: 10.1016/j.dnarep.2010.03.010. PubMed PMID: 20418188; PMCID: PMC4331052.

32.   Lehmann J, Seebode C, Smolorz S, Schubert S, Emmert S. XPF knockout via CRISPR/Cas9 reveals that ERCC1 is retained in the cytoplasm without its

heterodimer partner XPF. Cellular and molecular life sciences : CMLS. 2017;74(11):2081-94. Epub 2017/01/29. doi: 10.1007/s00018-017-2455-7. PubMed PMID: 28130555.

33.   Das D, Tripsianes K, Jaspers NG, Hoeijmakers JH, Kaptein R, Boelens R, Folkers GE. The HhH domain of the human DNA repair protein XPF forms stable homodimers. Proteins. 2008;70(4):1551-63. Epub 2007/10/04. doi: 10.1002/prot.21635. PubMed PMID: 17912758.

34.   Marteijn JA, Lans H, Vermeulen W, Hoeijmakers JH. Understanding nucleotide excision repair and its roles in cancer and ageing. Nature reviews Molecular cell biology. 2014;15(7):465-81. Epub 2014/06/24. doi: 10.1038/nrm3822. PubMed PMID: 24954209.

35.   Kisker C, Kuper J, Van Houten B. Prokaryotic nucleotide excision repair. Cold Spring Harbor perspectives in biology. 2013;5(3):a012591. Epub 2013/03/05. doi: 10.1101/cshperspect.a012591. PubMed PMID: 23457260; PMCID: PMC3578354.

36.   Masutani C, Sugasawa K, Yanagisawa J, Sonoyama T, Ui M, Enomoto T, Takio K, Tanaka K, van der Spek PJ, Bootsma D, et al. Purification and cloning of a nucleotide excision repair complex involving the xeroderma pigmentosum group C protein and a human homologue of yeast RAD23. The EMBO journal. 1994;13(8):1831-43. Epub 1994/04/15. PubMed PMID: 8168482; PMCID: PMC395023.

37.   Nishi R, Okuda Y, Watanabe E, Mori T, Iwai S, Masutani C, Sugasawa K, Hanaoka F. Centrin 2 stimulates nucleotide excision repair by interacting with xeroderma pigmentosum group C protein. Molecular and cellular biology.

2005;25(13):5664-74. Epub 2005/06/21. doi: 10.1128/mcb.25.13.5664-5674.2005. PubMed PMID: 15964821; PMCID: PMC1156980.

38. Wakasugi M, Kawashima A, Morioka H, Linn S, Sancar A, Mori T, Nikaido O, Matsunaga T. DDB accumulates at DNA damage sites immediately after UV irradiation and directly stimulates nucleotide excision repair. The Journal of biological chemistry. 2002;277(3):1637-40. Epub 2001/11/14. doi: 10.1074/jbc.C100610200. PubMed PMID: 11705987.

39. Scrima A, Konickova R, Czyzewski BK, Kawasaki Y, Jeffrey PD, Groisman R, Nakatani Y, Iwai S, Pavletich NP, Thoma NH. Structural basis of UV DNA-damage recognition by the DDB1-DDB2 complex. Cell. 2008;135(7):1213-23. Epub 2008/12/27. doi: 10.1016/j.cell.2008.10.045. PubMed PMID: 19109893; PMCID: PMC2676164.

40. Yokoi M, Masutani C, Maekawa T, Sugasawa K, Ohkuma Y, Hanaoka F. The xeroderma pigmentosum group C protein complex XPC-HR23B plays an important role in the recruitment of transcription factor IIH to damaged DNA. The Journal of biological chemistry. 2000;275(13):9870-5. Epub 2000/03/29. PubMed PMID: 10734143.

41. Volker M, Mone MJ, Karmakar P, van Hoffen A, Schul W, Vermeulen W, Hoeijmakers JH, van Driel R, van Zeeland AA, Mullenders LH. Sequential assembly of the nucleotide excision repair factors in vivo. Molecular cell. 2001;8(1):213-24. Epub 2001/08/21. PubMed PMID: 11511374.

42. de Laat WL, Appeldoorn E, Sugasawa K, Weterings E, Jaspers NG, Hoeijmakers JH. DNA-binding polarity of human replication protein A positions nucleases in

nucleotide excision repair. Genes & development. 1998;12(16):2598-609. Epub 1998/08/26. PubMed PMID: 9716411; PMCID: PMC317078.

43. Orelli B, McClendon TB, Tsodikov OV, Ellenberger T, Niedernhofer LJ, Scharer OD. The XPA-binding domain of ERCC1 is required for nucleotide excision repair but not other DNA repair pathways. The Journal of biological chemistry. 2010;285(6):3705-12. Epub 2009/11/27. doi: 10.1074/jbc.M109.067538. PubMed PMID: 19940136; PMCID: PMC2823511.

44. He Z, Henricksen LA, Wold MS, Ingles CJ. RPA involvement in the damage-recognition and incision steps of nucleotide excision repair. Nature. 1995;374(6522):566-9. Epub 1995/04/06. doi: 10.1038/374566a0. PubMed PMID: 7700386.

45. Matsunaga T, Park CH, Bessho T, Mu D, Sancar A. Replication protein A confers structure-specific endonuclease activities to the XPF-ERCC1 and XPG subunits of human DNA repair excision nuclease. The Journal of biological chemistry. 1996;271(19):11047-50. Epub 1996/05/10. PubMed PMID: 8626644.

46. de Laat WL, Jaspers NG, Hoeijmakers JH. Molecular mechanism of nucleotide excision repair. Genes & development. 1999;13(7):768-85. Epub 1999/04/10. PubMed PMID: 10197977.

47. Brueckner F, Hennecke U, Carell T, Cramer P. CPD damage recognition by transcribing RNA polymerase II. Science (New York, NY). 2007;315(5813):859-62. Epub 2007/02/10. doi: 10.1126/science.1135400. PubMed PMID: 17290000.

48. Tantin D, Kansal A, Carey M. Recruitment of the putative transcription-repair coupling factor CSB/ERCC6 to RNA polymerase II elongation complexes.

Molecular and cellular biology. 1997;17(12):6803-14. Epub 1997/12/31. doi: 10.1128/mcb.17.12.6803. PubMed PMID: 9372911; PMCID: PMC232536.

49. Saijo M. The role of Cockayne syndrome group A (CSA) protein in transcription-coupled nucleotide excision repair. Mechanisms of ageing and development. 2013;134(5-6):196-201. Epub 2013/04/11. doi: 10.1016/j.mad.2013.03.008. PubMed PMID: 23571135.

50. Sigurdsson S, Dirac-Svejstrup AB, Svejstrup JQ. Evidence that transcript cleavage is essential for RNA polymerase II transcription and cell viability. Molecular cell. 2010;38(2):202-10. Epub 2010/04/27. doi: 10.1016/j.molcel.2010.02.026. PubMed PMID: 20417599; PMCID: PMC2994637.

51. Muniandy PA, Liu J, Majumdar A, Liu ST, Seidman MM. DNA interstrand crosslink repair in mammalian cells: step by step. Critical reviews in biochemistry and molecular biology. 2010;45(1):23-49. Epub 2009/12/31. doi: 10.3109/10409230903501819. PubMed PMID: 20039786; PMCID: PMC2824768.

52. Kelland L. The resurgence of platinum-based cancer chemotherapy. Nature reviews Cancer. 2007;7(8):573-84. Epub 2007/07/13. doi: 10.1038/nrc2167. PubMed PMID: 17625587.

53. Kato N, Kawasoe Y, Williams H, Coates E, Roy U, Shi Y, Beese LS, Scharer OD, Yan H, Gottesman ME, Takahashi TS, Gautier J. Sensing and Processing of DNA Interstrand Crosslinks by the Mismatch Repair Pathway. Cell reports. 2017;21(5):1375-85. Epub 2017/11/02. doi: 10.1016/j.celrep.2017.10.032. PubMed PMID: 29091773; PMCID: PMC5806701.

54. Hashimoto S, Anai H, Hanada K. Mechanisms of interstrand DNA crosslink repair and human disorders. Genes and environment : the official journal of the Japanese Environmental Mutagen Society. 2016;38:9. Epub 2016/06/29. doi: 10.1186/s41021-016-0037-9. PubMed PMID: 27350828; PMCID: PMC4918140.

55. Niedernhofer LJ, Odijk H, Budzowska M, van Drunen E, Maas A, Theil AF, de Wit J, Jaspers NG, Beverloo HB, Hoeijmakers JH, Kanaar R. The structure-specific endonuclease Ercc1-Xpf is required to resolve DNA interstrand cross-link-induced double-strand breaks. Molecular and cellular biology. 2004;24(13):5776-87. Epub 2004/06/17. doi: 10.1128/mcb.24.13.5776-5787.2004. PubMed PMID: 15199134; PMCID: PMC480908.

56. Deans AJ, West SC. DNA interstrand crosslink repair and cancer. Nature reviews Cancer. 2011;11(7):467-80. Epub 2011/06/28. doi: 10.1038/nrc3088. PubMed PMID: 21701511; PMCID: PMC3560328.

57. Zhang J, Walter JC. Mechanism and regulation of incisions during DNA interstrand cross-link repair. DNA repair. 2014;19:135-42. Epub 2014/04/29. doi: 10.1016/j.dnarep.2014.03.018. PubMed PMID: 24768452; PMCID: PMC4076290.

58. Huang J, Liu S, Bellani MA, Thazhathveetil AK, Ling C, de Winter JP, Wang Y, Wang W, Seidman MM. The DNA translocase FANCM/MHF promotes replication traverse of DNA interstrand crosslinks. Molecular cell. 2013;52(3):434-46. Epub 2013/11/12. doi: 10.1016/j.molcel.2013.09.021. PubMed PMID: 24207054; PMCID: PMC3880019.

59. Klein Douwel D, Boonen RA, Long DT, Szypowska AA, Raschle M, Walter JC, Knipscheer P. XPF-ERCC1 acts in Unhooking DNA interstrand crosslinks in

cooperation with FANCD2 and FANCP/SLX4. Molecular cell. 2014;54(3):460-71. Epub 2014/04/15. doi: 10.1016/j.molcel.2014.03.015. PubMed PMID: 24726325; PMCID: PMC5067070.

60. Abdullah UB, McGouran JF, Brolih S, Ptchelkine D, El-Sagheer AH, Brown T, McHugh PJ. RPA activates the XPF-ERCC1 endonuclease to initiate processing of DNA interstrand crosslinks. The EMBO journal. 2017;36(14):2047-60. Epub 2017/06/14. doi: 10.15252/embj.201796664. PubMed PMID: 28607004; PMCID: PMC5510000.

61. Niedernhofer LJ, Garinis GA, Raams A, Lalai AS, Robinson AR, Appeldoorn E, Odijk H, Oostendorp R, Ahmad A, van Leeuwen W, Theil AF, Vermeulen W, van der Horst GT, Meinecke P, Kleijer WJ, Vijg J, Jaspers NG, Hoeijmakers JH. A new progeroid syndrome reveals that genotoxic stress suppresses the somatotroph axis. Nature. 2006;444(7122):1038-43. Epub 2006/12/22. doi: 10.1038/nature05456. PubMed PMID: 17183314.

62. De Silva IU, McHugh PJ, Clingen PH, Hartley JA. Defining the roles of nucleotide excision repair and recombination in the repair of DNA interstrand cross-links in mammalian cells. Molecular and cellular biology. 2000;20(21):7980-90. Epub 2000/10/12. PubMed PMID: 11027268; PMCID: PMC86408.

63. Andersson BS, Sadeghi T, Siciliano MJ, Legerski R, Murray D. Nucleotide excision repair genes as determinants of cellular sensitivity to cyclophosphamide analogs. Cancer chemotherapy and pharmacology. 1996;38(5):406-16. Epub 1996/01/01. doi: 10.1007/s002800050504. PubMed PMID: 8765433.

64.   Li S, Lu H, Wang Z, Hu Q, Wang H, Xiang R, Chiba T, Wu X. ERCC1/XPF is important for repair of DNA double-strand breaks containing secondary structures. iScience. doi: 10.1016/j.isci.2019.05.017.

65.   Bergstralh DT, Sekelsky J. Interstrand crosslink repair: can XPF-ERCC1 be let off the hook? Trends in genetics : TIG. 2008;24(2):70-6. Epub 2008/01/15. doi: 10.1016/j.tig.2007.11.003. PubMed PMID: 18192062.

66.   Jasin M, Rothstein R. Repair of strand breaks by homologous recombination. Cold Spring Harbor perspectives in biology. 2013;5(11):a012740. Epub 2013/10/08. doi: 10.1101/cshperspect.a012740. PubMed PMID: 24097900; PMCID: PMC3809576.

67.   Al-Minawi AZ, Lee YF, Hakansson D, Johansson F, Lundin C, Saleh-Gohari N, Schultz N, Jenssen D, Bryant HE, Meuth M, Hinz JM, Helleday T. The ERCC1/XPF endonuclease is required for completion of homologous recombination at DNA replication forks stalled by inter-strand cross-links. Nucleic acids research. 2009;37(19):6400-13. Epub 2009/08/29. doi: 10.1093/nar/gkp705. PubMed PMID: 19713438; PMCID: PMC2770670.

68.   Bennardo N, Cheng A, Huang N, Stark JM. Alternative-NHEJ is a mechanistically distinct pathway of mammalian chromosome break repair. PLoS genetics. 2008;4(6):e1000110. Epub 2008/06/28. doi: 10.1371/journal.pgen.1000110. PubMed PMID: 18584027; PMCID: PMC2430616.

69.   Adair GM, Rolig RL, Moore-Faver D, Zabelshansky M, Wilson JH, Nairn RS. Role of ERCC1 in removal of long non-homologous tails during targeted homologous recombination. The EMBO journal. 2000;19(20):5552-61. Epub

2000/10/18. doi: 10.1093/emboj/19.20.5552. PubMed PMID: 11032822; PMCID: PMC313999.

70. Bhargava R, Onyango DO, Stark JM. Regulation of Single-Strand Annealing and its Role in Genome Maintenance. Trends in genetics : TIG. 2016;32(9):566-75. Epub 2016/07/28. doi: 10.1016/j.tig.2016.06.007. PubMed PMID: 27450436; PMCID: PMC4992407.

71. Munoz MC, Laulier C, Gunn A, Cheng A, Robbiani DF, Nussenzweig A, Stark JM. RING finger nuclear factor RNF168 is important for defects in homologous recombination caused by loss of the breast cancer susceptibility factor BRCA1. The Journal of biological chemistry. 2012;287(48):40618-28. Epub 2012/10/12. doi: 10.1074/jbc.M112.410951. PubMed PMID: 23055523; PMCID: PMC3504775.

72. Escribano-Diaz C, Orthwein A, Fradet-Turcotte A, Xing M, Young JT, Tkac J, Cook MA, Rosebrock AP, Munro M, Canny MD, Xu D, Durocher D. A cell cycle-dependent regulatory circuit composed of 53BP1-RIF1 and BRCA1-CtIP controls DNA repair pathway choice. Molecular cell. 2013;49(5):872-83. Epub 2013/01/22. doi: 10.1016/j.molcel.2013.01.001. PubMed PMID: 23333306.

73. Sartori AA, Lukas C, Coates J, Mistrik M, Fu S, Bartek J, Baer R, Lukas J, Jackson SP. Human CtIP promotes DNA end resection. Nature. 2007;450(7169):509-14. Epub 2007/10/30. doi: 10.1038/nature06337. PubMed PMID: 17965729; PMCID: PMC2409435.

74. Chen L, Nievera CJ, Lee AY, Wu X. Cell cycle-dependent complex formation of BRCA1.CtIP.MRN is important for DNA double-strand break repair. The Journal

of biological chemistry. 2008;283(12):7713-20. Epub 2008/01/04. doi: 10.1074/jbc.M710245200. PubMed PMID: 18171670.

75. Huertas P, Jackson SP. Human CtIP mediates cell cycle control of DNA end resection and double strand break repair. The Journal of biological chemistry. 2009;284(14):9558-65. Epub 2009/02/10. doi: 10.1074/jbc.M808906200. PubMed PMID: 19202191; PMCID: PMC2666608.

76. Rothenberg E, Grimme JM, Spies M, Ha T. Human Rad52-mediated homology search and annealing occurs by continuous interactions between overlapping nucleoprotein complexes. Proceedings of the National Academy of Sciences of the United States of America. 2008;105(51):20274-9. Epub 2008/12/17. doi: 10.1073/pnas.0810317106. PubMed PMID: 19074292; PMCID: PMC2629295.

77. Motycka TA, Bessho T, Post SM, Sung P, Tomkinson AE. Physical and functional interaction between the XPF/ERCC1 endonuclease and hRad52. The Journal of biological chemistry. 2004;279(14):13634-9. Epub 2004/01/22. doi: 10.1074/jbc.M313779200. PubMed PMID: 14734547.

78. Ivanov EL, Sugawara N, Fishman-Lobell J, Haber JE. Genetic requirements for the single-strand annealing pathway of double-strand break repair in Saccharomyces cerevisiae. Genetics. 1996;142(3):693-704. Epub 1996/03/01. PubMed PMID: 8849880; PMCID: PMC1207011.

79. Sfeir A, Symington LS. Microhomology-Mediated End Joining: A Back-up Survival Mechanism or Dedicated Pathway? Trends in biochemical sciences. 2015;40(11):701-14. Epub 2015/10/07. doi: 10.1016/j.tibs.2015.08.006. PubMed PMID: 26439531; PMCID: PMC4638128.

80.   Howard SM, Yanez DA, Stark JM. DNA damage response factors from diverse pathways, including DNA crosslink repair, mediate alternative end joining. PLoS genetics. 2015;11(1):e1004943. Epub 2015/01/30. doi: 10.1371/journal.pgen.1004943. PubMed PMID: 25629353; PMCID: PMC4309583.

81.   Wang M, Wu W, Wu W, Rosidi B, Zhang L, Wang H, Iliakis G. PARP-1 and Ku compete for repair of DNA double strand breaks by distinct NHEJ pathways. Nucleic acids research. 2006;34(21):6170-82. Epub 2006/11/08. doi: 10.1093/nar/gkl840. PubMed PMID: 17088286; PMCID: PMC1693894.

82.   Mateos-Gomez PA, Kent T, Deng SK, McDevitt S, Kashkina E, Hoang TM, Pomerantz RT, Sfeir A. The helicase domain of Poltheta counteracts RPA to promote alt-NHEJ. Nature structural & molecular biology. 2017;24(12):1116-23. Epub 2017/10/24. doi: 10.1038/nsmb.3494. PubMed PMID: 29058711; PMCID: PMC6047744.

83.   Mateos-Gomez PA, Gong F, Nair N, Miller KM, Lazzerini-Denchi E, Sfeir A. Mammalian polymerase theta promotes alternative NHEJ and suppresses recombination. Nature. 2015;518(7538):254-7. Epub 2015/02/03. doi: 10.1038/nature14157. PubMed PMID: 25642960; PMCID: PMC4718306.

84.   Ceccaldi R, Liu JC, Amunugama R, Hajdu I, Primack B, Petalcorin MI, O'Connor KW, Konstantinopoulos PA, Elledge SJ, Boulton SJ, Yusufzai T, D'Andrea AD. Homologous-recombination-deficient tumours are dependent on Poltheta-mediated repair. Nature. 2015;518(7538):258-62. Epub 2015/02/03. doi: 10.1038/nature14184. PubMed PMID: 25642963; PMCID: PMC4415602.

85. Wyatt DW, Feng W, Conlin MP, Yousefzadeh MJ, Roberts SA, Mieczkowski P, Wood RD, Gupta GP, Ramsden DA. Essential Roles for Polymerase theta-Mediated End Joining in the Repair of Chromosome Breaks. Molecular cell. 2016;63(4):662-73. Epub 2016/07/28. doi: 10.1016/j.molcel.2016.06.020. PubMed PMID: 27453047; PMCID: PMC4992412.

86. Rosenberg B, Vancamp L, Krigas T. INHIBITION OF CELL DIVISION IN ESCHERICHIA COLI BY ELECTROLYSIS PRODUCTS FROM A PLATINUM ELECTRODE. Nature. 1965;205:698-9. Epub 1965/02/13. PubMed PMID: 14287410.

87. Rosenberg B, Van Camp L, Grimley EB, Thomson AJ. The inhibition of growth or cell division in Escherichia coli by different ionic species of platinum(IV) complexes. The Journal of biological chemistry. 1967;242(6):1347-52. Epub 1967/03/25. PubMed PMID: 5337590.

88. Rosenberg B, VanCamp L, Trosko JE, Mansour VH. Platinum compounds: a new class of potent antitumour agents. Nature. 1969;222(5191):385-6. Epub 1969/04/26. PubMed PMID: 5782119.

89. Galanski M, Jakupec MA, Keppler BK. Update of the preclinical situation of anticancer platinum complexes: novel design strategies and innovative analytical approaches. Current medicinal chemistry. 2005;12(18):2075-94. Epub 2005/08/17. PubMed PMID: 16101495.

90. Williams SD, Birch R, Einhorn LH, Irwin L, Greco FA, Loehrer PJ. Treatment of disseminated germ-cell tumors with cisplatin, bleomycin, and either vinblastine or etoposide. The New England journal of medicine. 1987;316(23):1435-40. Epub 1987/06/04. doi: 10.1056/nejm198706043162302. PubMed PMID: 2437455.

91.   Todd RC, Lippard SJ. Inhibition of transcription by platinum antitumor compounds. Metallomics : integrated biometal science. 2009;1(4):280-91. Epub 2010/01/05. doi: 10.1039/b907567d. PubMed PMID: 20046924; PMCID: PMC2752884.

92.   Rocha CRR, Silva MM, Quinet A, Cabral-Neto JB, Menck CFM. DNA repair pathways and cisplatin resistance: an intimate relationship. Clinics (Sao Paulo, Brazil).   2018;73(suppl   1):e478s.   Epub   2018/09/13.   doi: 10.6061/clinics/2018/e478s. PubMed PMID: 30208165; PMCID: PMC6113849.

93.   Siddik ZH. Cisplatin: mode of cytotoxic action and molecular basis of resistance. Oncogene.   2003;22(47):7265-79.   Epub   2003/10/25.   doi: 10.1038/sj.onc.1206933. PubMed PMID: 14576837.

94.   Knox RJ, Friedlos F, Lydall DA, Roberts JJ. Mechanism of cytotoxicity of anticancer platinum drugs: evidence that cis-diamminedichloroplatinum(II) and cis-diammine-(1,1-cyclobutanedicarboxylato)platinum(II) differ only in the kinetics of their interaction with DNA. Cancer research. 1986;46(4 Pt 2):1972-9. Epub 1986/04/01. PubMed PMID: 3512077.

95.   Pinato O, Musetti C, Farrell NP, Sissi C. Platinum-based drugs and proteins: reactivity and relevance to DNA adduct formation. Journal of inorganic biochemistry.   2013;122:27-37.   Epub   2013/02/26.   doi: 10.1016/j.jinorgbio.2013.01.007.   PubMed   PMID: 23435290;   PMCID: PMC3602126.

96.   Hostetter AA, Osborn MF, DeRose VJ. RNA-Pt adducts following cisplatin treatment of Saccharomyces cerevisiae. ACS chemical biology. 2012;7(1):218-

25. Epub 2011/10/19. doi: 10.1021/cb200279p. PubMed PMID: 22004017; PMCID: PMC3262962.

97. Baik MH, Friesner RA, Lippard SJ. Theoretical study of cisplatin binding to purine bases: why does cisplatin prefer guanine over adenine? Journal of the American Chemical Society. 2003;125(46):14082-92. Epub 2003/11/13. doi: 10.1021/ja036960d. PubMed PMID: 14611245.

98. Pinto AL, Lippard SJ. Sequence-dependent termination of in vitro DNA synthesis by cis- and trans-diamminedichloroplatinum (II). Proceedings of the National Academy of Sciences of the United States of America. 1985;82(14):4616-9. Epub 1985/07/01. PubMed PMID: 3895221; PMCID: PMC390436.

99. Ye J, Farrington CR, Millard JT. Polymerase bypass of N7-guanine monoadducts of cisplatin, diepoxybutane, and epichlorohydrin. Mutation research. 2018;809:6-12. Epub 2018/03/27. doi: 10.1016/j.mrfmmm.2018.03.002. PubMed PMID: 29579534; PMCID: PMC5962418.

100. Lopez-Martinez D, Liang CC, Cohn MA. Cellular response to DNA interstrand crosslinks: the Fanconi anemia pathway. Cellular and molecular life sciences : CMLS. 2016;73(16):3097-114. Epub 2016/04/21. doi: 10.1007/s00018-016-2218-x. PubMed PMID: 27094386; PMCID: PMC4951507.

101. Fichtinger-Schepman AM, van der Veer JL, den Hartog JH, Lohman PH, Reedijk J. Adducts of the antitumor drug cis-diamminedichloroplatinum(II) with DNA: formation, identification, and quantitation. Biochemistry. 1985;24(3):707-13. Epub 1985/01/29. PubMed PMID: 4039603.

102. Tornaletti S, Patrick SM, Turchi JJ, Hanawalt PC. Behavior of T7 RNA polymerase and mammalian RNA polymerase II at site-specific cisplatin adducts

in the template DNA. The Journal of biological chemistry. 2003;278(37):35791-7. Epub 2003/06/28. doi: 10.1074/jbc.M305394200. PubMed PMID: 12829693.

103.   Malinge JM, Giraud-Panis MJ, Leng M. Interstrand cross-links of cisplatin induce striking distortions in DNA. Journal of inorganic biochemistry. 1999;77(1-2):23-9. Epub 2000/01/08. PubMed PMID: 10626349.

104.   Coste F, Malinge JM, Serre L, Shepard W, Roth M, Leng M, Zelwer C. Crystal structure of a double-stranded DNA containing a cisplatin interstrand cross-link at 1.63 A resolution: hydration at the platinated site. Nucleic acids research. 1999;27(8):1837-46. Epub 1999/04/02. PubMed PMID: 10101191; PMCID: PMC148391.

105.   Huang H, Zhu L, Reid BR, Drobny GP, Hopkins PB. Solution structure of a cisplatin-induced DNA interstrand cross-link. Science (New York, NY). 1995;270(5243):1842-5. Epub 1995/12/15. PubMed PMID: 8525382.

106.   Bernal-Mendez E, Boudvillain M, Gonzalez-Vilchez F, Leng M. Chemical versatility of transplatin monofunctional adducts within multiple site-specifically platinated DNA. Biochemistry. 1997;36(24):7281-7. Epub 1997/06/17. doi: 10.1021/bi9703148. PubMed PMID: 9200676.

107.   Aris SM, Farrell NP. Towards Antitumor Active trans-Platinum Compounds. European journal of inorganic chemistry. 2009;2009(10):1293. Epub 2010/02/18. doi: 10.1002/ejic.200801118. PubMed PMID: 20161688; PMCID: PMC2821104.

108.   Yu J, Xiao J, Yang Y, Cao B. Oxaliplatin-Based Doublets Versus Cisplatin or Carboplatin-Based Doublets in the First-Line Treatment of Advanced Nonsmall Cell Lung Cancer. Medicine. 2015;94(27):e1072. Epub 2015/07/15. doi:

10.1097/md.0000000000001072. PubMed PMID: 26166081; PMCID: PMC4504603.

109. Atmaca A, Al-Batran SE, Werner D, Pauligk C, Guner T, Koepke A, Bernhard H, Wenzel T, Banat AG, Brueck P, Caca K, Prasnikar N, Kullmann F, Gunther Derigs H, Koenigsmann M, Dingeldein G, Neuhaus T, Jager E. A randomised multicentre phase II study with cisplatin/docetaxel vs oxaliplatin/docetaxel as first-line therapy in patients with advanced or metastatic non-small cell lung cancer. British journal of cancer. 2013;108(2):265-70. Epub 2013/01/19. doi: 10.1038/bjc.2012.555. PubMed PMID: 23329236; PMCID: PMC3566804.

110. Scagliotti GV, Kortsik C, Dark GG, Price A, Manegold C, Rosell R, O'Brien M, Peterson PM, Castellano D, Selvaggi G, Novello S, Blatter J, Kayitalire L, Crino L, Paz-Ares L. Pemetrexed combined with oxaliplatin or carboplatin as first-line treatment in advanced non-small cell lung cancer: a multicenter, randomized, phase II trial. Clinical cancer research : an official journal of the American Association for Cancer Research. 2005;11(2 Pt 1):690-6. Epub 2005/02/11. PubMed PMID: 15701857.

111. Gramont Ad, Figer A, Seymour M, Homerin M, Hmissi A, Cassidy J, Boni C, Cortes-Funes H, Cervantes A, Freyer G, Papamichael D, Bail NL, Louvet C, Hendler D, Braud Fd, Wilson C, Morvan F, Bonetti A. Leucovorin and Fluorouracil With or Without Oxaliplatin as First-Line Treatment in Advanced Colorectal Cancer. Journal of Clinical Oncology. 2000;18(16):2938-47. doi: 10.1200/jco.2000.18.16.2938. PubMed PMID: 10944126.

112. Giacchetti S, Perpoint B, Zidani R, Bail NL, Faggiuolo R, Focan C, Chollet P, Llory JF, Letourneau Y, Coudert B, Bertheaut-Cvitkovic F, Larregain-Fournier D,

Rol AL, Walter S, Adam R, Misset JL, Lévi F. Phase III Multicenter Randomized Trial of Oxaliplatin Added to Chronomodulated Fluorouracil–Leucovorin as First-Line Treatment of Metastatic Colorectal Cancer. Journal of Clinical Oncology. 2000;18(1):136-. doi: 10.1200/jco.2000.18.1.136. PubMed PMID: 10623704.

113.　Woynarowski JM, Faivre S, Herzig MC, Arnett B, Chapman WG, Trevino AV, Raymond E, Chaney SG, Vaisman A, Varchenko M, Juniewicz PE. Oxaliplatin-induced damage of cellular DNA. Molecular pharmacology. 2000;58(5):920-7. Epub 2000/10/20. PubMed PMID: 11040038.

114.　Wheate NJ, Walker S, Craig GE, Oun R. The status of platinum anticancer drugs in the clinic and in clinical trials. Dalton transactions (Cambridge, England : 2003). 2010;39(35):8113-27. Epub 2010/07/02. doi: 10.1039/c0dt00292e. PubMed PMID: 20593091.

115.　Bhargava A, Vaishampayan UN. Satraplatin: leading the new generation of oral platinum agents. Expert opinion on investigational drugs. 2009;18(11):1787-97. Epub 2009/11/06. doi: 10.1517/13543780903362437. PubMed PMID: 19888874; PMCID: PMC3856359.

116.　Kelland LR, Abel G, McKeage MJ, Jones M, Goddard PM, Valenti M, Murrer BA, Harrap KR. Preclinical antitumor evaluation of bis-acetato-ammine-dichloro-cyclohexylamine platinum(IV): an orally active platinum drug. Cancer research. 1993;53(11):2581-6. Epub 1993/06/01. PubMed PMID: 8388318.

117.　Raynaud FI, Boxall FE, Goddard PM, Valenti M, Jones M, Murrer BA, Abrams M, Kelland LR. cis-Amminedichloro(2-methylpyridine) platinum(II) (AMD473), a novel sterically hindered platinum complex: in vivo activity, toxicology, and pharmacokinetics in mice. Clinical cancer research : an official journal of the

American Association for Cancer Research. 1997;3(11):2063-74. Epub 1998/11/17. PubMed PMID: 9815598.

118.   Holford J, Sharp SY, Murrer BA, Abrams M, Kelland LR. In vitro circumvention of cisplatin resistance by the novel sterically hindered platinum complex AMD473. British journal of cancer. 1998;77(3):366-73. Epub 1998/02/24. PubMed PMID: 9472630; PMCID: PMC2151285.

119.   Sharp SY, O'Neill CF, Rogers P, Boxall FE, Kelland LR. Retention of activity by the new generation platinum agent AMD0473 in four human tumour cell lines possessing acquired resistance to oxaliplatin. European journal of cancer (Oxford, England : 1990). 2002;38(17):2309-15. Epub 2002/11/21. PubMed PMID: 12441268.

120.   Treat J, Schiller J, Quoix E, Mauer A, Edelman M, Modiano M, Bonomi P, Ramlau R, Lemarie E. ZD0473 treatment in lung cancer: an overview of the clinical trial results. European journal of cancer (Oxford, England : 1990). 2002;38 Suppl 8:S13-8. Epub 2003/03/21. PubMed PMID: 12645908.

121.   Damia G, Broggini M. Platinum Resistance in Ovarian Cancer: Role of DNA Repair. Cancers. 2019;11(1). Epub 2019/01/24. doi: 10.3390/cancers11010119. PubMed PMID: 30669514; PMCID: PMC6357127.

122.   Galluzzi L, Senovilla L, Vitale I, Michels J, Martins I, Kepp O, Castedo M, Kroemer G. Molecular mechanisms of cisplatin resistance. Oncogene. 2012;31(15):1869-83. Epub 2011/09/06. doi: 10.1038/onc.2011.384. PubMed PMID: 21892204.

123.   Olaussen KA, Dunant A, Fouret P, Brambilla E, Andre F, Haddad V, Taranchon E, Filipits M, Pirker R, Popper HH, Stahel R, Sabatier L, Pignon JP, Tursz T, Le

Chevalier T, Soria JC. DNA repair by ERCC1 in non-small-cell lung cancer and cisplatin-based adjuvant chemotherapy. The New England journal of medicine. 2006;355(10):983-91. Epub 2006/09/08. doi: 10.1056/NEJMoa060570. PubMed PMID: 16957145.

124. Usanova S, Piee-Staffa A, Sied U, Thomale J, Schneider A, Kaina B, Koberle B. Cisplatin sensitivity of testis tumour cells is due to deficiency in interstrand-crosslink repair and low ERCC1-XPF expression. Molecular cancer. 2010;9:248. Epub 2010/09/18. doi: 10.1186/1476-4598-9-248. PubMed PMID: 20846399; PMCID: PMC3098011.

125. Hoffmann AC, Wild P, Leicht C, Bertz S, Danenberg KD, Danenberg PV, Stohr R, Stockle M, Lehmann J, Schuler M, Hartmann A. MDR1 and ERCC1 expression predict outcome of patients with locally advanced bladder cancer receiving adjuvant chemotherapy. Neoplasia (New York, NY). 2010;12(8):628-36. Epub 2010/08/07. PubMed PMID: 20689757; PMCID: PMC2915407.

126. Fareed KR, Al-Attar A, Soomro IN, Kaye PV, Patel J, Lobo DN, Parsons SL, Madhusudan S. Tumour regression and ERCC1 nuclear protein expression predict clinical outcome in patients with gastro-oesophageal cancer treated with neoadjuvant chemotherapy. British journal of cancer. 2010;102(11):1600-7. Epub 2010/05/13. doi: 10.1038/sj.bjc.6605686. PubMed PMID: 20461087; PMCID: PMC2883154.

127. Mesquita KA, Alabdullah M, Griffin M, Toss MS, Fatah T, Alblihy A, Moseley P, Chan SYT, Rakha EA, Madhusudan S. ERCC1-XPF deficiency is a predictor of olaparib induced synthetic lethality and platinum sensitivity in epithelial ovarian

cancers. Gynecologic oncology. 2019. Epub 2019/02/25. doi: 10.1016/j.ygyno.2019.02.014. PubMed PMID: 30797591.

128. Steffensen KD, Waldstrom M, Jakobsen A. The relationship of platinum resistance and ERCC1 protein expression in epithelial ovarian cancer. International journal of gynecological cancer : official journal of the International Gynecological Cancer Society. 2009;19(5):820-5. Epub 2009/07/04. doi: 10.1111/IGC.0b013e3181a12e09. PubMed PMID: 19574766.

129. Simon GR, Sharma S, Cantor A, Smith P, Bepler G. ERCC1 expression is a predictor of survival in resected patients with non-small cell lung cancer. Chest. 2005;127(3):978-83. Epub 2005/03/15. doi: 10.1378/chest.127.3.978. PubMed PMID: 15764785.

130. Zheng Z, Chen T, Li X, Haura E, Sharma A, Bepler G. DNA synthesis and repair genes RRM1 and ERCC1 in lung cancer. The New England journal of medicine. 2007;356(8):800-8. Epub 2007/02/23. doi: 10.1056/NEJMoa065411. PubMed PMID: 17314339.

131. Shuck SC, Turchi JJ. Targeted inhibition of Replication Protein A reveals cytotoxic activity, synergy with chemotherapeutic DNA-damaging agents, and insight into cellular function. Cancer research. 2010;70(8):3189-98. Epub 2010/04/17. doi: 10.1158/0008-5472.can-09-3422. PubMed PMID: 20395205; PMCID: PMC2882864.

132. Gavande NS, VanderVere-Carozza P, Mishra AK, Vernon TL, Pawelczak KS, Turchi JJ. Design and Structure-Guided Development of Novel Inhibitors of the Xeroderma Pigmentosum Group A (XPA) Protein-DNA Interaction. Journal of

medicinal chemistry. 2017;60(19):8055-70. Epub 2017/09/22. doi: 10.1021/acs.jmedchem.7b00780. PubMed PMID: 28933851.

133. Neher TM, Shuck SC, Liu JY, Zhang JT, Turchi JJ. Identification of novel small molecule inhibitors of the XPA protein using in silico based screening. ACS chemical biology. 2010;5(10):953-65. Epub 2010/07/29. doi: 10.1021/cb1000444. PubMed PMID: 20662484; PMCID: PMC2955790.

134. Heyza JR, Arora S, Zhang H, Conner KL, Lei W, Floyd AM, Deshmukh RR, Sarver J, Trabbic CJ, Erhardt P, Chan TH, Dou QP, Patrick SM. Targeting the DNA Repair Endonuclease ERCC1-XPF with Green Tea Polyphenol Epigallocatechin-3-Gallate (EGCG) and Its Prodrug to Enhance Cisplatin Efficacy in Human Cancer Cells. Nutrients. 2018;10(11). Epub 2018/11/08. doi: 10.3390/nu10111644. PubMed PMID: 30400270; PMCID: PMC6267282.

135. Arora S, Heyza J, Zhang H, Kalman-Maltese V, Tillison K, Floyd AM, Chalfin EM, Bepler G, Patrick SM. Identification of small molecule inhibitors of ERCC1-XPF that inhibit DNA repair and potentiate cisplatin efficacy in cancer cells. Oncotarget. 2016;7(46):75104-17. Epub 2016/09/22. doi: 10.18632/oncotarget.12072. PubMed PMID: 27650543; PMCID: PMC5342726.

136. Chapman TM, Wallace C, Gillen KJ, Bakrania P, Khurana P, Coombs PJ, Fox S, Bureau EA, Brownlees J, Melton DW, Saxty B. N-Hydroxyimides and hydroxypyrimidinones as inhibitors of the DNA repair complex ERCC1-XPF. Bioorganic & medicinal chemistry letters. 2015;25(19):4104-8. Epub 2015/09/01. doi: 10.1016/j.bmcl.2015.08.024. PubMed PMID: 26321360.

137. McNeil EM, Astell KR, Ritchie AM, Shave S, Houston DR, Bakrania P, Jones HM, Khurana P, Wallace C, Chapman T, Wear MA, Walkinshaw MD, Saxty B,

Melton DW. Inhibition of the ERCC1-XPF structure-specific endonuclease to overcome cancer chemoresistance. DNA repair. 2015;31:19-28. Epub 2015/05/10. doi: 10.1016/j.dnarep.2015.04.002. PubMed PMID: 25956741.

138. Dabholkar M, Bostick-Bruton F, Weber C, Bohr VA, Egwuagu C, Reed E. ERCC1 and ERCC2 expression in malignant tissues from ovarian cancer patients. Journal of the National Cancer Institute. 1992;84(19):1512-7. Epub 1992/10/07. PubMed PMID: 1433335.

139. Dabholkar M, Vionnet J, Bostick-Bruton F, Yu JJ, Reed E. Messenger RNA levels of XPAC and ERCC1 in ovarian cancer tissue correlate with response to platinum-based chemotherapy. The Journal of clinical investigation. 1994;94(2):703-8. Epub 1994/08/01. doi: 10.1172/jci117388. PubMed PMID: 8040325; PMCID: PMC296149.

140. Geleziunas R, McQuillan A, Malapetsa A, Hutchinson M, Kopriva D, Wainberg MA, Hiscott J, Bramson J, Panasci L. Increased DNA synthesis and repair-enzyme expression in lymphocytes from patients with chronic lymphocytic leukemia resistant to nitrogen mustards. Journal of the National Cancer Institute. 1991;83(8):557-64. Epub 1991/04/17. PubMed PMID: 2005641.

141. Yagi T, Katsuya A, Koyano A, Takebe H. Sensitivity of group F xeroderma pigmentosum cells to UV and mitomycin C relative to levels of XPF and ERCC1 overexpression. Mutagenesis. 1998;13(6):595-9. Epub 1998/12/23. PubMed PMID: 9862190.

142. Warren AJ, Ihnat MA, Ogdon SE, Rowell EE, Hamilton JW. Binding of nuclear proteins associated with mammalian DNA repair to the mitomycin C-DNA

interstrand crosslink. Environmental and molecular mutagenesis. 1998;31(1):70-81. Epub 1998/02/17. PubMed PMID: 9464318.

143. Lee KB, Parker RJ, Bohr V, Cornelison T, Reed E. Cisplatin sensitivity/resistance in UV repair-deficient Chinese hamster ovary cells of complementation groups 1 and 3. Carcinogenesis. 1993;14(10):2177-80. Epub 1993/10/01. PubMed PMID: 8222071.

144. Larminat F, Bohr VA. Role of the human ERCC-1 gene in gene-specific repair of cisplatin-induced DNA damage. Nucleic acids research. 1994;22(15):3005-10. Epub 1994/08/11. PubMed PMID: 8065913; PMCID: PMC310268.

145. Moggs JG, Yarema KJ, Essigmann JM, Wood RD. Analysis of incision sites produced by human cell extracts and purified proteins during nucleotide excision repair of a 1,3-intrastrand d(GpTpG)-cisplatin adduct. The Journal of biological chemistry. 1996;271(12):7177-86. Epub 1996/03/22. PubMed PMID: 8636155.

146. Huang JC, Zamble DB, Reardon JT, Lippard SJ, Sancar A. HMG-domain proteins specifically inhibit the repair of the major DNA adduct of the anticancer drug cisplatin by human excision nuclease. Proceedings of the National Academy of Sciences of the United States of America. 1994;91(22):10394-8. Epub 1994/10/25. PubMed PMID: 7937961; PMCID: PMC45026.

147. Li Q, Gardner K, Zhang L, Tsang B, Bostick-Bruton F, Reed E. Cisplatin induction of ERCC-1 mRNA expression in A2780/CP70 human ovarian cancer cells. The Journal of biological chemistry. 1998;273(36):23419-25. Epub 1998/08/29. PubMed PMID: 9722577.

148. Li W, Melton DW. Cisplatin regulates the MAPK kinase pathway to induce increased expression of DNA repair gene ERCC1 and increase melanoma

chemoresistance. Oncogene. 2012;31(19):2412-22. Epub 2011/10/15. doi: 10.1038/onc.2011.426. PubMed PMID: 21996734.

149.   Planchard D, Camara-Clayette V, Dorvault N, Soria JC, Fouret P. p38 Mitogen-activated protein kinase signaling, ERCC1 expression, and viability of lung cancer cells from never or light smoker patients. Cancer. 2012;118(20):5015-25. Epub 2012/03/15. doi: 10.1002/cncr.27510. PubMed PMID: 22415779.

150.   Youn CK, Kim MH, Cho HJ, Kim HB, Chang IY, Chung MH, You HJ. Oncogenic H-Ras up-regulates expression of ERCC1 to protect cells from platinum-based anticancer agents. Cancer research. 2004;64(14):4849-57. Epub 2004/07/17. doi: 10.1158/0008-5472.can-04-0348. PubMed PMID: 15256455.

151.   Metzger R, Leichman CG, Danenberg KD, Danenberg PV, Lenz HJ, Hayashi K, Groshen S, Salonga D, Cohen H, Laine L, Crookes P, Silberman H, Baranda J, Konda B, Leichman L. ERCC1 mRNA levels complement thymidylate synthase mRNA levels in predicting response and survival for gastric cancer patients receiving combination cisplatin and fluorouracil chemotherapy. Journal of clinical oncology : official journal of the American Society of Clinical Oncology. 1998;16(1):309-16. Epub 1998/01/24. doi: 10.1200/jco.1998.16.1.309. PubMed PMID: 9440758.

152.   Shirota Y, Stoehlmacher J, Brabender J, Xiong YP, Uetake H, Danenberg KD, Groshen S, Tsao-Wei DD, Danenberg PV, Lenz HJ. ERCC1 and thymidylate synthase mRNA levels predict survival for colorectal cancer patients receiving combination oxaliplatin and fluorouracil chemotherapy. Journal of clinical oncology : official journal of the American Society of Clinical Oncology.

2001;19(23):4298-304. Epub 2001/12/04. doi: 10.1200/jco.2001.19.23.4298. PubMed PMID: 11731512.

153. Lord RV, Brabender J, Gandara D, Alberola V, Camps C, Domine M, Cardenal F, Sanchez JM, Gumerlock PH, Taron M, Sanchez JJ, Danenberg KD, Danenberg PV, Rosell R. Low ERCC1 expression correlates with prolonged survival after cisplatin plus gemcitabine chemotherapy in non-small cell lung cancer. Clinical cancer research : an official journal of the American Association for Cancer Research. 2002;8(7):2286-91. Epub 2002/07/13. PubMed PMID: 12114432.

154. Bepler G, Kusmartseva I, Sharma S, Gautam A, Cantor A, Sharma A, Simon G. RRM1 modulated in vitro and in vivo efficacy of gemcitabine and platinum in non-small-cell lung cancer. Journal of clinical oncology : official journal of the American Society of Clinical Oncology. 2006;24(29):4731-7. Epub 2006/09/13. doi: 10.1200/jco.2006.06.1101. PubMed PMID: 16966686.

155. Ceppi P, Volante M, Novello S, Rapa I, Danenberg KD, Danenberg PV, Cambieri A, Selvaggi G, Saviozzi S, Calogero R, Papotti M, Scagliotti GV. ERCC1 and RRM1 gene expressions but not EGFR are predictive of shorter survival in advanced non-small-cell lung cancer treated with cisplatin and gemcitabine. Annals of oncology : official journal of the European Society for Medical Oncology. 2006;17(12):1818-25. Epub 2006/09/19. doi: 10.1093/annonc/mdl300. PubMed PMID: 16980606.

156. Azuma K, Komohara Y, Sasada T, Terazaki Y, Ikeda J, Hoshino T, Itoh K, Yamada A, Aizawa H. Excision repair cross-complementation group 1 predicts progression-free and overall survival in non-small cell lung cancer patients treated with platinum-based chemotherapy. Cancer science. 2007;98(9):1336-43.

Epub 2007/07/21. doi: 10.1111/j.1349-7006.2007.00557.x. PubMed PMID: 17640298.

157. Fujii T, Toyooka S, Ichimura K, Fujiwara Y, Hotta K, Soh J, Suehisa H, Kobayashi N, Aoe M, Yoshino T, Kiura K, Date H. ERCC1 protein expression predicts the response of cisplatin-based neoadjuvant chemotherapy in non-small-cell lung cancer. Lung cancer (Amsterdam, Netherlands). 2008;59(3):377-84. Epub 2007/10/02. doi: 10.1016/j.lungcan.2007.08.025. PubMed PMID: 17905465.

158. Booton R, Ward T, Ashcroft L, Morris J, Heighway J, Thatcher N. ERCC1 mRNA expression is not associated with response and survival after platinum-based chemotherapy regimens in advanced non-small cell lung cancer. Journal of thoracic oncology : official publication of the International Association for the Study of Lung Cancer. 2007;2(10):902-6. Epub 2007/10/03. doi: 10.1097/JTO.0b013e318155a637. PubMed PMID: 17909351.

159. Bhagwat NR, Roginskaya VY, Acquafondata MB, Dhir R, Wood RD, Niedernhofer LJ. Immunodetection of DNA repair endonuclease ERCC1-XPF in human tissue. Cancer research. 2009;69(17):6831-8. Epub 2009/09/03. doi: 10.1158/0008-5472.can-09-1237. PubMed PMID: 19723666; PMCID: PMC2739111.

160. Vaezi AE, Bepler G, Bhagwat NR, Malysa A, Rubatt JM, Chen W, Hood BL, Conrads TP, Wang L, Kemp CE, Niedernhofer LJ. Choline phosphate cytidylyltransferase-alpha is a novel antigen detected by the anti-ERCC1 antibody 8F1 with biomarker value in patients with lung and head and neck

squamous cell carcinomas. Cancer. 2014;120(12):1898-907. Epub 2014/04/03. doi: 10.1002/cncr.28643. PubMed PMID: 24692084; PMCID: PMC4047200.

161. Rosell R, Lord RV, Taron M, Reguart N. DNA repair and cisplatin resistance in non-small-cell lung cancer. Lung cancer (Amsterdam, Netherlands). 2002;38(3):217-27. Epub 2002/11/26. PubMed PMID: 12445742.

162. Santarpia M, Altavilla G, Salazar F, Taron M, Rosell R. From the bench to the bed: individualizing treatment in non-small-cell lung cancer. Clinical & translational oncology : official publication of the Federation of Spanish Oncology Societies and of the National Cancer Institute of Mexico. 2006;8(2):71-6. Epub 2006/04/25. PubMed PMID: 16632419.

163. Bepler G, Williams C, Schell MJ, Chen W, Zheng Z, Simon G, Gadgeel S, Zhao X, Schreiber F, Brahmer J, Chiappori A, Tanvetyanon T, Pinder-Schenck M, Gray J, Haura E, Antonia S, Fischer JR. Randomized international phase III trial of ERCC1 and RRM1 expression-based chemotherapy versus gemcitabine/carboplatin in advanced non-small-cell lung cancer. Journal of clinical oncology : official journal of the American Society of Clinical Oncology. 2013;31(19):2404-12. Epub 2013/05/22. doi: 10.1200/jco.2012.46.9783. PubMed PMID: 23690416; PMCID: PMC3691357.

164. Scharer OD. ERCC1-XPF endonuclease-positioned to cut. The EMBO journal. 2017;36(14):1993-5. Epub 2017/07/01. doi: 10.15252/embj.201797489. PubMed PMID: 28659377; PMCID: PMC5509994.

165. Zhang N, Liu X, Li L, Legerski R. Double-strand breaks induce homologous recombinational repair of interstrand cross-links via cooperation of MSH2, ERCC1-XPF, REV3, and the Fanconi anemia pathway. DNA repair.

2007;6(11):1670-8. Epub 2007/08/03. doi: 10.1016/j.dnarep.2007.06.002. PubMed PMID: 17669695; PMCID: PMC2586762.

166. Kothandapani A, Sawant A, Dangeti VS, Sobol RW, Patrick SM. Epistatic role of base excision repair and mismatch repair pathways in mediating cisplatin cytotoxicity. Nucleic acids research. 2013;41(15):7332-43. Epub 2013/06/14. doi: 10.1093/nar/gkt479. PubMed PMID: 23761438; PMCID: PMC3753620.

167. Loh SY, Mistry P, Kelland LR, Abel G, Harrap KR. Reduced drug accumulation as a major mechanism of acquired resistance to cisplatin in a human ovarian carcinoma cell line: circumvention studies using novel platinum (II) and (IV) ammine/amine complexes. British journal of cancer. 1992;66(6):1109-15. Epub 1992/12/01. PubMed PMID: 1457352; PMCID: PMC1978040.

168. Ferry KV, Hamilton TC, Johnson SW. Increased nucleotide excision repair in cisplatin-resistant ovarian cancer cells: role of ERCC1-XPF. Biochemical pharmacology. 2000;60(9):1305-13. Epub 2000/09/29. PubMed PMID: 11008124.

169. Britten RA, Liu D, Tessier A, Hutchison MJ, Murray D. ERCC1 expression as a molecular marker of cisplatin resistance in human cervical tumor cells. International journal of cancer. 2000;89(5):453-7. Epub 2000/09/29. PubMed PMID: 11008208.

170. Bellmunt J, Paz-Ares L, Cuello M, Cecere FL, Albiol S, Guillem V, Gallardo E, Carles J, Mendez P, de la Cruz JJ, Taron M, Rosell R, Baselga J. Gene expression of ERCC1 as a novel prognostic marker in advanced bladder cancer patients receiving cisplatin-based chemotherapy. Annals of oncology : official

journal of the European Society for Medical Oncology. 2007;18(3):522-8. Epub 2007/01/19. doi: 10.1093/annonc/mdl435. PubMed PMID: 17229776.

171. Garaycoechea JI, Crossan GP, Langevin F, Mulderrig L, Louzada S, Yang F, Guilbaud G, Park N, Roerink S, Nik-Zainal S, Stratton MR, Patel KJ. Alcohol and endogenous aldehydes damage chromosomes and mutate stem cells. Nature. 2018;553(7687):171-7. Epub 2018/01/13. doi: 10.1038/nature25154. PubMed PMID: 29323295.

172. Velimezi G, Robinson-Garcia L, Munoz-Martinez F, Wiegant WW, Ferreira da Silva J, Owusu M, Moder M, Wiedner M, Rosenthal SB, Fisch KM, Moffat J, Menche J, van Attikum H, Jackson SP, Loizou JI. Map of synthetic rescue interactions for the Fanconi anemia DNA repair pathway identifies USP48. Nature communications. 2018;9(1):2280. Epub 2018/06/13. doi: 10.1038/s41467-018-04649-z. PubMed PMID: 29891926; PMCID: PMC5996029.

173. Moder M, Velimezi G, Owusu M, Mazouzi A, Wiedner M, Ferreira da Silva J, Robinson-Garcia L, Schischlik F, Slavkovsky R, Kralovics R, Schuster M, Bock C, Ideker T, Jackson SP, Menche J, Loizou JI. Parallel genome-wide screens identify synthetic viable interactions between the BLM helicase complex and Fanconi anemia. Nature communications. 2017;8(1):1238. Epub 2017/11/02. doi: 10.1038/s41467-017-01439-x. PubMed PMID: 29089570; PMCID: PMC5663702.

174. Sawant A, Floyd AM, Dangeti M, Lei W, Sobol RW, Patrick SM. Differential role of base excision repair proteins in mediating cisplatin cytotoxicity. DNA repair. 2017;51:46-59. Epub 2017/01/24. doi: 10.1016/j.dnarep.2017.01.002. PubMed PMID: 28110804; PMCID: PMC5328804.

175. Campbell JD, Alexandrov A, Kim J, Wala J, Berger AH, Pedamallu CS, Shukla SA, Guo G, Brooks AN, Murray BA, Imielinski M, Hu X, Ling S, Akbani R, Rosenberg M, Cibulskis C, Ramachandran A, Collisson EA, Kwiatkowski DJ, Lawrence MS, Weinstein JN, Verhaak RG, Wu CJ, Hammerman PS, Cherniack AD, Getz G, Artyomov MN, Schreiber R, Govindan R, Meyerson M. Distinct patterns of somatic genome alterations in lung adenocarcinomas and squamous cell carcinomas. Nature genetics. 2016;48(6):607-16. Epub 2016/05/10. doi: 10.1038/ng.3564. PubMed PMID: 27158780; PMCID: PMC4884143.

176. Comprehensive molecular profiling of lung adenocarcinoma. Nature. 2014;511(7511):543-50. Epub 2014/08/01. doi: 10.1038/nature13385. PubMed PMID: 25079552; PMCID: PMC4231481.

177. Gao J, Aksoy BA, Dogrusoz U, Dresdner G, Gross B, Sumer SO, Sun Y, Jacobsen A, Sinha R, Larsson E, Cerami E, Sander C, Schultz N. Integrative analysis of complex cancer genomics and clinical profiles using the cBioPortal. Science signaling. 2013;6(269):pl1. Epub 2013/04/04. doi: 10.1126/scisignal.2004088. PubMed PMID: 23550210; PMCID: PMC4160307.

178. Gyorffy B, Lanczky A, Szallasi Z. Implementing an online tool for genome-wide validation of survival-associated biomarkers in ovarian-cancer using microarray data from 1287 patients. Endocrine-related cancer. 2012;19(2):197-208. Epub 2012/01/27. doi: 10.1530/erc-11-0329. PubMed PMID: 22277193.

179. Sawant A, Kothandapani A, Zhitkovich A, Sobol RW, Patrick SM. Role of mismatch repair proteins in the processing of cisplatin interstrand cross-links. DNA repair. 2015;35:126-36. Epub 2015/11/01. doi:

10.1016/j.dnarep.2015.10.003.   PubMed   PMID: 26519826;   PMCID: PMC4651805.

180.   Fraser M, Chan SL, Chan SS, Fiscus RR, Tsang BK. Regulation of p53 and suppression of apoptosis by the soluble guanylyl cyclase/cGMP pathway in human ovarian cancer cells. Oncogene. 2006;25(15):2203-12. Epub 2005/11/17. doi: 10.1038/sj.onc.1209251. PubMed PMID: 16288207.

181.   Fraser M, Leung BM, Yan X, Dan HC, Cheng JQ, Tsang BK. p53 is a determinant of X-linked inhibitor of apoptosis protein/Akt-mediated chemoresistance in human ovarian cancer cells. Cancer research. 2003;63(21):7081-8. Epub 2003/11/13. PubMed PMID: 14612499.

182.   Celeste A, Difilippantonio S, Difilippantonio MJ, Fernandez-Capetillo O, Pilch DR, Sedelnikova OA, Eckhaus M, Ried T, Bonner WM, Nussenzweig A. H2AX haploinsufficiency modifies genomic stability and tumor susceptibility. Cell. 2003;114(3):371-83. Epub 2003/08/14. PubMed PMID: 12914701; PMCID: PMC4737479.

183.   Bassing CH, Chua KF, Sekiguchi J, Suh H, Whitlow SR, Fleming JC, Monroe BC, Ciccone DN, Yan C, Vlasakova K, Livingston DM, Ferguson DO, Scully R, Alt FW. Increased ionizing radiation sensitivity and genomic instability in the absence of histone H2AX. Proceedings of the National Academy of Sciences of the United States of America. 2002;99(12):8173-8. Epub 2002/05/30. doi: 10.1073/pnas.122228699. PubMed PMID: 12034884; PMCID: PMC123040.

184.   Kao J, Milano MT, Javaheri A, Garofalo MC, Chmura SJ, Weichselbaum RR, Kron SJ. gamma-H2AX as a therapeutic target for improving the efficacy of

radiation therapy. Current cancer drug targets. 2006;6(3):197-205. Epub 2006/05/23. PubMed PMID: 16712457.

185. Lee SM, Falzon M, Blackhall F, Spicer J, Nicolson M, Chaudhuri A, Middleton G, Ahmed S, Hicks J, Crosse B, Napier M, Singer JM, Ferry D, Lewanski C, Forster M, Rolls SA, Capitanio A, Rudd R, Iles N, Ngai Y, Gandy M, Lillywhite R, Hackshaw A. Randomized Prospective Biomarker Trial of ERCC1 for Comparing Platinum and Nonplatinum Therapy in Advanced Non-Small-Cell Lung Cancer: ERCC1 Trial (ET). Journal of clinical oncology : official journal of the American Society of Clinical Oncology. 2017;35(4):402-11. Epub 2016/11/29. doi: 10.1200/jco.2016.68.1841. PubMed PMID: 27893326.

186. Rubatt JM, Darcy KM, Tian C, Muggia F, Dhir R, Armstrong DK, Bookman MA, Niedernhofer LJ, Deloia J, Birrer M, Krivak TC. Pre-treatment tumor expression of ERCC1 in women with advanced stage epithelial ovarian cancer is not predictive of clinical outcomes: a Gynecologic Oncology Group study. Gynecologic oncology. 2012;125(2):421-6. Epub 2012/01/21. doi: 10.1016/j.ygyno.2012.01.008. PubMed PMID: 22261301; PMCID: PMC3490188.

187. Hijioka S, Hosoda W, Matsuo K, Ueno M, Furukawa M, Yoshitomi H, Kobayashi N, Ikeda M, Ito T, Nakamori S, Ishii H, Kodama Y, Morizane C, Okusaka T, Yanagimoto H, Notohara K, Taguchi H, Kitano M, Yane K, Maguchi H, Tsuchiya Y, Komoto I, Tanaka H, Tsuji A, Hashigo S, Kawaguchi Y, Mine T, Kanno A, Murohisa G, Miyabe K, Takagi T, Matayoshi N, Yoshida T, Hara K, Imamura M, Furuse J, Yatabe Y, Mizuno N. Rb Loss and KRAS Mutation Are Predictors of the Response to Platinum-Based Chemotherapy in Pancreatic Neuroendocrine Neoplasm with Grade 3: A Japanese Multicenter Pancreatic NEN-G3 Study.

Clinical cancer research : an official journal of the American Association for Cancer Research. 2017;23(16):4625-32. Epub 2017/04/30. doi: 10.1158/1078-0432.ccr-16-3135. PubMed PMID: 28455360.

188.   Belanger F, Fortier E, Dube M, Lemay JF, Buisson R, Masson JY, Elsherbiny A, Costantino S, Carmona E, Mes-Masson AM, Wurtele H, Drobetsky E. Replication Protein A Availability during DNA Replication Stress Is a Major Determinant of Cisplatin Resistance in Ovarian Cancer Cells. Cancer research. 2018;78(19):5561-73. Epub 2018/08/04. doi: 10.1158/0008-5472.can-18-0618. PubMed PMID: 30072396.

189.   Feng W, Jasin M. BRCA2 suppresses replication stress-induced mitotic and G1 abnormalities through homologous recombination. Nature communications. 2017;8(1):525. Epub 2017/09/15. doi: 10.1038/s41467-017-00634-0. PubMed PMID: 28904335; PMCID: PMC5597640.

190.   Pamidi A, Cardoso R, Hakem A, Matysiak-Zablocki E, Poonepalli A, Tamblyn L, Perez-Ordonez B, Hande MP, Sanchez O, Hakem R. Functional interplay of p53 and Mus81 in DNA damage responses and cancer. Cancer research. 2007;67(18):8527-35. Epub 2007/09/19. doi: 10.1158/0008-5472.can-07-1161. PubMed PMID: 17875692.

191.   Friboulet L, Barrios-Gonzales D, Commo F, Olaussen KA, Vagner S, Adam J, Goubar A, Dorvault N, Lazar V, Job B, Besse B, Validire P, Girard P, Lacroix L, Hasmats J, Dufour F, Andre F, Soria JC. Molecular Characteristics of ERCC1-Negative versus ERCC1-Positive Tumors in Resected NSCLC. Clinical cancer research : an official journal of the American Association for Cancer Research.

2011;17(17):5562-72. Epub 2011/07/14. doi: 10.1158/1078-0432.ccr-11-0790. PubMed PMID: 21750204.

192. Mohni KN, Kavanaugh GM, Cortez D. ATR pathway inhibition is synthetically lethal in cancer cells with ERCC1 deficiency. Cancer research. 2014;74(10):2835-45. Epub 2014/03/26. doi: 10.1158/0008-5472.can-13-3229. PubMed PMID: 24662920; PMCID: PMC4043842.

193. Mohni KN, Thompson PS, Luzwick JW, Glick GG, Pendleton CS, Lehmann BD, Pietenpol JA, Cortez D. A Synthetic Lethal Screen Identifies DNA Repair Pathways that Sensitize Cancer Cells to Combined ATR Inhibition and Cisplatin Treatments. PloS one. 2015;10(5):e0125482. Epub 2015/05/13. doi: 10.1371/journal.pone.0125482. PubMed PMID: 25965342; PMCID: PMC4428765.

194. Hustedt N, Álvarez-Quilón A, McEwan A, Yuan JY, Cho T, Koob L, Hart T, Durocher D. A consensus set of genetic vulnerabilities to ATR inhibition. bioRxiv. 2019:574533. doi: 10.1101/574533.

195. Toledo LI, Altmeyer M, Rask MB, Lukas C, Larsen DH, Povlsen LK, Bekker-Jensen S, Mailand N, Bartek J, Lukas J. ATR prohibits replication catastrophe by preventing global exhaustion of RPA. Cell. 2013;155(5):1088-103. Epub 2013/11/26. doi: 10.1016/j.cell.2013.10.043. PubMed PMID: 24267891.

196. Harding SM, Benci JL, Irianto J, Discher DE, Minn AJ, Greenberg RA. Mitotic progression following DNA damage enables pattern recognition within micronuclei. Nature. 2017;548(7668):466-70. Epub 2017/08/02. doi: 10.1038/nature23470. PubMed PMID: 28759889; PMCID: PMC5857357.

197. Wang H, Hu S, Chen X, Shi H, Chen C, Sun L, Chen ZJ. cGAS is essential for the antitumor effect of immune checkpoint blockade. Proceedings of the National Academy of Sciences of the United States of America. 2017;114(7):1637-42. Epub 2017/02/01. doi: 10.1073/pnas.1621363114. PubMed PMID: 28137885; PMCID: PMC5320994.

198. Kim H, George E, Ragland R, Rafial S, Zhang R, Krepler C, Morgan M, Herlyn M, Brown E, Simpkins F. Targeting the ATR/CHK1 Axis with PARP Inhibition Results in Tumor Regression in BRCA-Mutant Ovarian Cancer Models. Clinical cancer research : an official journal of the American Association for Cancer Research. 2017;23(12):3097-108. Epub 2016/12/21. doi: 10.1158/1078-0432.ccr-16-2273. PubMed PMID: 27993965; PMCID: PMC5474193.

199. Saldivar JC, Hamperl S, Bocek MJ, Chung M, Bass TE, Cisneros-Soberanis F, Samejima K, Xie L, Paulson JR, Earnshaw WC, Cortez D, Meyer T, Cimprich KA. An intrinsic S/G2 checkpoint enforced by ATR. Science (New York, NY). 2018;361(6404):806-10. Epub 2018/08/25. doi: 10.1126/science.aap9346. PubMed PMID: 30139873; PMCID: PMC6365305.

200. Sen T, Rodriguez BL, Chen L, Della Corte C, Morikawa N, Fujimoto J, Cristea S, Nguyen T, Diao L, Li L, Fan Y, Yang Y, Wang J, Glisson BS, Wistuba II, Sage J, Heymach JV, Gibbons DL, Byers LA. Targeting DNA damage response promotes anti-tumor immunity through STING-mediated T-cell activation in small cell lung cancer. Cancer Discovery. 2019:CD-18-1020. doi: 10.1158/2159-8290.cd-18-1020.

201. Mackenzie KJ, Carroll P, Martin CA, Murina O, Fluteau A, Simpson DJ, Olova N, Sutcliffe H, Rainger JK, Leitch A, Osborn RT, Wheeler AP, Nowotny M, Gilbert N,

Chandra T, Reijns MAM, Jackson AP. cGAS surveillance of micronuclei links genome instability to innate immunity. Nature. 2017;548(7668):461-5. Epub 2017/07/25. doi: 10.1038/nature23449. PubMed PMID: 28738408; PMCID: PMC5870830.

202. Chabanon RM, Muirhead G, Krastev DB, Adam J, Morel D, Garrido M, Lamb A, Henon C, Dorvault N, Rouanne M, Marlow R, Bajrami I, Cardenosa ML, Konde A, Besse B, Ashworth A, Pettitt SJ, Haider S, Marabelle A, Tutt AN, Soria JC, Lord CJ, Postel-Vinay S. PARP inhibition enhances tumor cell-intrinsic immunity in ERCC1-deficient non-small cell lung cancer. The Journal of clinical investigation. 2019;129(3):1211-28. Epub 2018/12/28. doi: 10.1172/jci123319. PubMed PMID: 30589644; PMCID: PMC6391116.

203. Thomas A, Redon CE, Sciuto L, Padiernos E, Ji J, Lee MJ, Yuno A, Lee S, Zhang Y, Tran L, Yutzy W, Rajan A, Guha U, Chen H, Hassan R, Alewine CC, Szabo E, Bates SE, Kinders RJ, Steinberg SM, Doroshow JH, Aladjem MI, Trepel JB, Pommier Y. Phase I Study of ATR Inhibitor M6620 in Combination With Topotecan in Patients With Advanced Solid Tumors. Journal of clinical oncology : official journal of the American Society of Clinical Oncology. 2018;36(16):1594-602. Epub 2017/12/19. doi: 10.1200/jco.2017.76.6915. PubMed PMID: 29252124; PMCID: PMC5978471.

204. Telli ML, Lord S, Dean E, Abramson V, Arkenau H-T, Becerra C, Tolaney SM, Tang R, Penney MS, Pollard J, Conboy G, Fields SZ, Shapiro G. 242PDInitial results of a phase 1 dose expansion cohort of M6620 (formerly VX-970), an ATR inhibitor, in combination with cisplatin in patients with advanced triple-negative

breast cancer NCT02157792). Annals of Oncology. 2017;28(suppl_5). doi: 10.1093/annonc/mdx365.005.

ABSTRACT

NOVEL INSIGHTS INTO THE USE OF ERCC1 AS A BIOMARKER FOR RESPONSE TO PLATINUM-BASED CHEMOTHERAPY IN LUNG CANCER

by

JOSHUA R. HEYZA

August 2019

Advisor: Steve M. Patrick, Ph.D.

Major: Cancer Biology

Degree: Doctor of Philosophy

ERCC1/XPF is a DNA endonuclease with variable expression in primary tumor specimens, and has been investigated as a predictive biomarker for efficacy of platinum-based chemotherapy in non-small cell lung cancers where up to 30-60% of tumors harbor low to undetectable ERCC1 expression. The failure of an international, randomized Phase III clinical trial utilizing ERCC1 expression to predict response to platinum-based chemotherapy suggests additional mechanisms underlying the basic biology of ERCC1 in the response to platinum-DNA damage remain unknown. In this work, we aimed to characterize a panel of ERCC1 knockout cell lines generated via CRISPR-Cas9 where we identified a synthetic viable phenotype in response to intestrand crosslinks (ICLs) with ERCC1 deficiency. Characterization of these ERCC1 knockout cell lines revealed loss of ERCC1 hypersensitized cells to cisplatin when wildtype (WT) p53 is retained, while there was only modest sensitivity in cell lines that were p53$^{mutant/null}$. Additionally, when p53 was disrupted by CRISPR-Cas9 (p53*) in ERCC1 knockout/p53^{WT} cells, there was reduced apoptosis and increased viability after platinum treatment. These results were recapitulated in two patient data sets utilizing p53 mutation analysis and ERCC1 expression to assess Overall Survival. We also show

that kinetics of ICL-repair differed between ERCC1 knockout/p53^{WT} and ERCC1 knockout/p53* cells. Finally, we provide evidence that cisplatin tolerance in the context of ERCC1 deficiency relies on DNA-PKcs and BRCA1 function as well as timely entry into S phase suggesting that replication dependent mechanisms are likely involved in promoting platinum tolerance.

Building upon these observations, we utilized our established lung cancer cell line models of ERCC1 deficiency to find that platinum tolerance with ERCC1 deficiency relies upon ATR signaling. ATR inhibition by M6620 selectively and synergistically enhanced platinum sensitivity of platinum tolerant ERCC1-deficient cells. Interestingly, this increased sensitivity was independent of Chk1 and Wee1 kinase inhibition, suggesting that ATR may support platinum-tolerance in the absence of ERCC1 by suppressing global replication fork collapse independent of activating the G_2/M cell cycle checkpoint. Additionally, dual treatment led to increased formation of DNA double strand breaks and was associated with increased levels of pulverized chromosomes. Combination treatment was also associated with increased micronuclei formation which were capable of being bound by the innate immunomodulatory factor, cGAS, suggesting that combination platinum and ATRi treatment may also enhance response to immunotherapy in ERCC1-deficient tumors harboring a p53 mutation.

Our findings implicate p53 as a potential confounding variable in clinical assessments of ERCC1 as a platinum biomarker via promoting an environment in which error-prone mechanisms of ICL-repair may be able to partially compensate for loss of ERCC1. Additionally, results of this study have led to the identification of a feasible therapeutic strategy combining M6620 with cisplatin to overcome platinum tolerance in ERCC1-deficient, p53-mutant lung cancers.

AUTOBIOGRAPHICAL STATEMENT

EDUCATION
Wayne State University 2019
Doctor of Philosophy in Cancer Biology
University of Michigan-Flint 2014
Bachelor of Science in Biology

FUNDING
Graduate Research Assistantship 2014-2016
Wayne State University School of Medicine
T32CA009531 2016-2018
National Institutes of Health/National Cancer Institute
Competitive Graduate Research Assistantship 2018-2019
Wayne State University

SELECTED PUBLICATIONS

1. **J. Heyza**, W. Lei, L. Polin, E. Van Buren, J. Back, W. Chen, D. Watza, N. Snyder, H. Mamdani, A. Schwartz, G. Bepler, S. Patrick. ATR supports platinum tolerance with ERCC1 deficiency by suppressing replication catastrophe. *In Preparation*

2. **J. Heyza**, W. Lei, D. Watza, H. Zhang, W. Chen, J. Back, A. Schwartz, G. Bepler, S. Patrick. Identification and characterization of synthetic viability with ERCC1 deficiency in response to interstrand crosslinks. *Clinical Cancer Research.* 2019. (Published with commentary by Friboulet *et al. Clinical Cancer Research. 2019).*

3. **J. Heyza***, S. Arora*, H. Zhang, K. Conner, W. Lei, A. Floyd, R. Deshmukh, J. Sarver, C. Trabbic, P. Erhardt, T.-H. Chan, Q.P. Dou, S. Patrick. Targeting the DNA Repair Endonuclease ERCC1-XPF with Green Tea Polyphenol Epigallocatechin-3-Gallate (EGCG) and Its Prodrug to Enhance Cisplatin Efficacy in Human Cancer Cells. *Nutrients* 2018, *10*, 1644. * Co-first author

4. S. Arora, **J. Heyza**, E. Chalfin, G. Westphal, E. Cook, R. Ruch, and S. Patrick. Gap Junction Intercellular Communication Positively Regulates Cisplatin Toxicity by Inducing DNA Damage through Bystander Signaling. *Cancers.* 2018, *10*, 368.

5. S. Arora, **J. Heyza**, H. Zhang, V. Kalman-Maltese, K. Tillison, A. Floyd, E. Chalfin, G. Bepler, S. Patrick. Identification of small molecule inhibitors of ERCC1-XPF that inhibit DNA repair and potentiate cisplatin efficacy in cancer cells. *Oncotarget.* 2016 Nov 15;7 (46):75104-75117.

6. K. Ji, **J. Heyza**, D. Cavallo-Medved, B. Sloane. Pathomimetic Cancer Avatars for Live-Cell Imaging of Protease Activity. *Biochimie.* 2016 Mar; 122:68-76.